

**The development of symmetrical 3,3'-diindolylmethane
analogues (c-DIMs) and their potential cytotoxic
effects towards glioblastoma**

by

Emily Jones

A thesis submitted in partial fulfilment for the requirements for the degree of
MSc (by Research) at the University of Central Lancashire

September 2020

STUDENT DECLARATION FORM

Concurrent registration for two or more academic awards

*I declare that while registered as a candidate for the research degree, I have not been a registered candidate or enrolled student for another award of the University or other academic or professional institution

Material submitted for another award

*I declare that no material contained in the thesis has been used in any other submission for an academic award and is solely my own work

Collaboration

Where a candidate's research programme is part of a collaborative project, the thesis must indicate in addition clearly the candidate's individual contribution and the extent of the collaboration. Please state below:

Signature of Candidate

E. Jones

Type of Award

MSc By Research

School

School of Pharmacy and Biomedical Sciences

Abstract

Glioblastoma is a World Health Organisation (WHO) grade IV tumour which remains the most aggressive and common malignant brain tumour in adults.^[1] The average 2-year survival of glioblastoma patients is sadly only around 25%.^[2] Glioblastoma tumours arise in the glial cells of the brain; these tumours have protruding fibres that infiltrate into other areas of the brain creating a support network for the tumour.^{[3][4]} Glioblastoma is associated with poor prognosis and survival rates, which have not increased significantly enough in recent years, especially when compared to other cancers, such as breast and colon cancer.^{[5][6]} Although the available interventions are effective and offer improved prognosis, they cannot eradicate all glioblastoma tumour cells, giving reasons for the extremely high re-occurrence rates. Therefore, a more effective pharmaceutical agent is necessary for the treatment of glioblastoma.

In the search for new chemotherapeutic agents, the dietary phytochemicals found in cruciferous vegetables have gained considerable attention. In particular, the dimeric product of indole-3-carbinol (I3C); 3,3'-diindolylmethane (DIM, Figure 1).

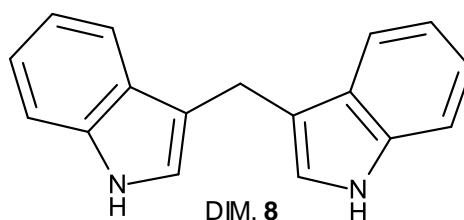


Figure 1- The structure of the lead compound, 3,3'-diindolylmethane (**8**).

The anti-cancer effects of DIM and its c-substituted derivatives, known as c-DIMs, have been established against a number of different cancer cell types.^{[7][8][9][10]} c-DIMs are characterised by substitution at the methylene carbon bridge of DIM, and their effects towards glioblastoma are currently unknown. Therefore, using DIM as a basic scaffold, a series of symmetrical functionalised DIM derivatives have been synthesised.

DIM and the synthesised compounds underwent *in vitro* screening studies, using the MTS assay, to identify their anti-proliferative effects towards the human glioblastoma cell line U-87 MG. Compounds **19**, **17** and **65** (Figure 2) exhibited the highest activity, with IC₅₀ values of 31.6 μM, 38 μM and 33.1 μM respectively.

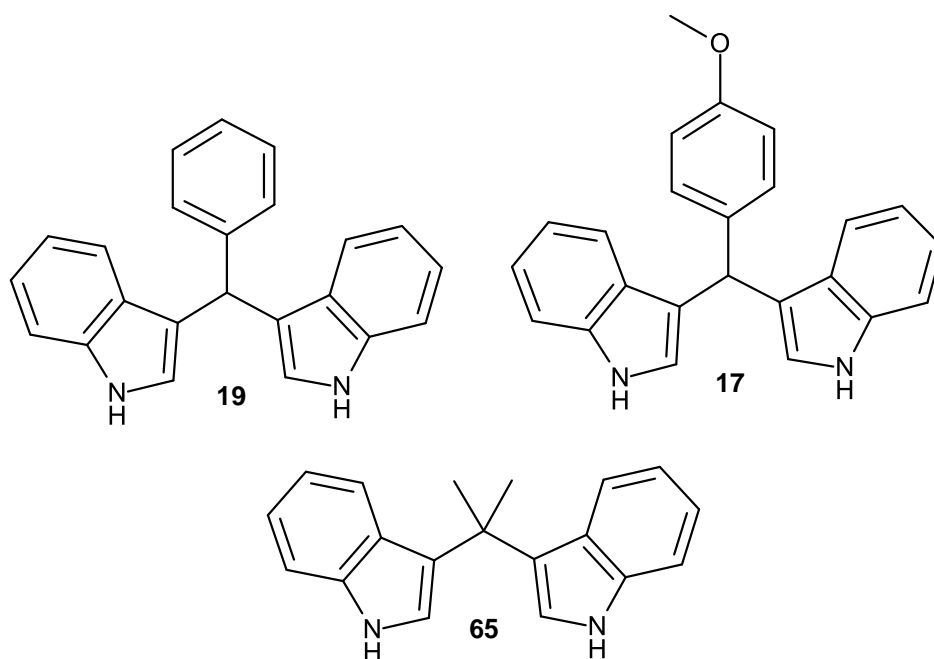


Figure 2 – The structures of compounds **19**, **17** and **65**, the compounds that exhibited the best anti-glioblastoma activity.

To conclude, this project identifies c-DIM analogues, that display respectable anti-cancer activity towards glioblastoma cells. The active compounds synthesised in this project, provide a good basis for the future synthesis of a wider library of compounds, and further investigation into the use of DIM derivatives for the treatment of glioblastoma.

Table of contents

STUDENT DECLARATION FORM.....	1
ABSTRACT.....	2
TABLE OF CONTENTS.....	4
ACKNOWLEDGEMENTS.....	8
LIST OF ILLUSTRATIVE MATERIALS.....	9
List of figures.....	9
List of schemes.....	12
List of tables.....	14
List of graphs.....	15
List of equations.....	16
LIST OF ABBREVIATIONS.....	17
CHAPTER ONE – INTRODUCTION.....	20
1.1 Cancer.....	21
1.2 Brain tumours.....	23
1.2.1 Brain tumours.....	23
1.2.2 Causes of brain tumours.....	25
1.2.3 Signs and symptoms.....	26
1.2.4 Diagnosis.....	26
1.3 Glioblastoma.....	28
1.3.1 Classification of glioblastoma.....	28
1.3.2 Current treatments.....	29
1.3.3 Conclusion.....	34
1.4 The anti-cancer effect of 3,3'-diindolylmethane (DIM) and its derivatives.....	35
1.4.1 Introduction.....	35
1.4.2 3,3'-Diindolylmethane.....	37
1.4.2.1 The structure of 3,3'-diindolylmethane.....	37
1.4.2.2 The anti-cancer effect of 3,3'-diindolylmethane.....	38
1.4.3 c-substituted 3,3'-diindolylmethane derivatives.....	40

1.4.4 Physiochemical properties of c-substituted 3,3'-diindolymethanes.....	44
1.5 Conclusion.....	47
1.6 Project aims.....	47
1.6.1 Specific aims.....	47
CHAPTER TWO – SYNTHETIC METHODS FOR C-SUBSTITUTED 3,3'-DIINDOLYLMETHANES.....	48
2.1 Introduction.....	49
2.2 c-substituted 3,3'-diindolymethanes from indole and aldehydes or ketones.....	50
2.3 c-substituted 3,3'-diindolymethanes from indoles with alcohols, amines or related compounds.....	57
2.3.1 c-substituted 3,3'-diindolymethanes from indoles and alcohols.....	57
2.3.2 c-substituted 3,3'-diindolymethanes from indoles and amines, imines or related derivatives.....	59
2.4 Conclusion.....	63
CHAPTER THREE – RESULTS AND DISCUSSION.....	64
3.1 Synthetic results and discussion.....	65
3.1.1 Compound synthesis.....	65
3.1.2 Attempted syntheses and optimisation of syntheses.....	68
3.1.2.1 Optimisation of synthesis for 3-[1-(1H-Indol-3-yl)-1-methyl-ethyl]-1H-indole.....	68
3.1.2.2 Optimisation of synthesis for 2-Methyl-3-[(2-methyl-1H-indol-3-yl)-phenyl-methyl]-1H-indole and 2-Phenyl-3-[phenyl-(2-phenyl-1H-indol-3-yl)methyl]-1H-indole	69

3.1.2.3	Attempted synthesis of 3-[1H-Indol-3-yl(diphenyl)methyl]-1H-indole	70
3.1.3	Challenges encountered in compound synthesis.....	71
3.2	Cell viability results and discussion.....	73
3.2.1	Materials.....	73
3.2.2	Cell culture methods.....	73
3.2.2.1	Defrosting cells.....	73
3.2.2.2	Cell maintenance.....	73
3.2.2.3	MTS cell viability assay.....	74
3.2.2.4	Statistical analysis.....	77
3.2.3	Series one cell viability results and discussion.....	77
3.2.3.1	Cell viability assay	77
3.2.3.2	Series one cell viability results.....	79
3.2.3.3	Series one cell viability discussion.....	80
3.2.4	Series two cell viability results and discussion.....	82
3.2.4.1	Series two cell viability results.....	82
3.2.4.2	Series two cell viability discussion.....	84
3.2.5	Discussion of results from within the Snape research group.....	84
3.2.6	Discussion of results in comparison to temozolomide.....	86
3.2.7	Challenges encountered during cytotoxicity testing	87
3.2.7.1	Solubility of compounds.....	87
3.2.7.2	Contamination of cells.....	90

CHAPTER FOUR – CONCLUSION.....	92
4.1 Conclusion.....	93
4.2 Future work	94
CHAPTER FIVE – EXPERIMENTAL.....	95
5.1 Materials.....	96
5.2 3-[1H-Indol-3-yl(phenyl)methyl]-1H-indole.....	97
5.3 3-[1H-Indol-3-yl-(4-methoxyphenyl)methyl]-1H-indole.....	98
5.4 3-[1H-Indol-3-yl-(4-nitrophenyl)methyl]-1H-indole.....	99
5.5 3-[1-(1H-Indol-3-yl)-1-methyl-ethyl]-1H-indole.....	100
5.6 3-[1H-Indol-3-yl-(4-fluorophenyl)methyl]-1H-indole.....	101
5.7 2-Methyl-3-[(2-methyl-1H-indol-3-yl)-phenyl-methyl]-1H-indole.....	102
5.8 2-Phenyl-3-[phenyl-(2-phenyl-1H-indol-3-yl)methyl]-1H-indole.....	103
5.9 1-Methyl-3-[(1-methylindol-3-yl)-phenyl-methyl]indole.....	104
REFERENCES.....	105
APPENDIX.....	120

Acknowledgements

I would firstly like to thank my project supervisor Dr Tim Snape, whom without, this project would not have been possible. I appreciate all of his advice and assistance throughout this degree. I also wish to express my gratitude to Julie and Amanda, for all their help in tissue culture. Likewise, my thanks go out to Tamar, Pat, Pete and Samira for always being of assistance in the analytical lab. I also have to thank my boyfriend Jack, for his ongoing support during this masters project. Lastly, but by no means the least, I want to thank my parents Andrew and Lynda and my grandparents, Beryl and Maurice for their constant encouragement and for everything they have done for me throughout my time at university.

List of illustrative materials

List of figures

Figure 1 - The structure of the lead compound, 3,3'-diindolylmethane (8).....	2
Figure 2 - The structures of compounds 19 , 17 and 65 , the compounds that exhibited the best anti-glioblastoma activity.....	3
Figure 3 – Pie charts showing new cases of cancer in 2018 (left), and the number of cancer deaths in 2018 (right).....	21
Figure 4 – Lifetime risk of cancer for specific cancer types vs number of total stem cell divisions.....	22
Figure 5 – CT and MRI scan combined with a PET/CT scan of a 62 year old male with glioblastoma to produce a radiotherapy plan.....	27
Figure 6- CT and MRI scan combined with a PET/CT scan of a 50 year old male with nodular atypical meningioma to create a radiotherapy plan.....	27
Figure 7 – Photo taken during glioblastoma resection using 5-ALA. Under white light (left) it seems tumour has been entirely removed. The yellow line indicates tumour border according to MRI. Under blue light (right) residual tumour is seen.....	31
Figure 8 - CT scan of a grade IV glioblastoma patient showing planning volumes for RT treatment.....	32
Figure 9 - Chemical structures of anti-cancer agent mitomycin C (9) and the amino acid tryptophan (10).....	37
Figure 10 - Chemical structures of indole containing chemotherapy drugs vincristine (11) and vinblastine (12).....	38
Figure 11 – The chemical structure of 3,3'-diindolylmethane (8).....	38
Figure 12 – Chemical structures of 2,2'-methyl-substituted DIM derivatives (13-16) tested for anti-proliferative effects against breast cancer cells.....	40

Figure 13 – c-DIM compounds; DIM-c- <i>p</i> PhOCH ₃ (17) and DIM-c- <i>p</i> PhOH (18), which were tested on lung and prostate cancer cell lines. The Same research group investigated the effects of 17 and c-DIM-Ph (19) as Nur77 agonists.....	41
Figure 14 - Chemical structures of DIM-c- <i>p</i> PhF (20) and its 2,2'-methyl substituted (21) and <i>N,N'</i> -methylated (23) derivatives.....	43
Figure 15 – Alkyl substituted c-DIM (23) tested against the FaO hepatoma cell line by Tocco et al.....	43
Figure 16 - Applying Lipinski rule of five to DIM-c-Ph, (19).....	44
Figure 17 – Naturally occurring c-DIM derivatives.....	49
Figure 18 – ¹³ C NMR of compound 64 . The CH peak of compound 64 is assumed to be hidden underneath the DMSO solvent peak.....	71
Figure 19 - DEPT-90 NMR of compound 64 , the CH peak was visible on a DEPT-90 NMR spectra, as only CH peaks are seen.....	72
Figure 20 - Serial dilution scheme followed to prepare the 250 μM, 100 μM, 10 μM and 1 μM concentrations of I3C, DIM and the compounds synthesised.....	75
Figure 21 - Plate map for cell viability experiment. Control wells = cells and media. Media wells = media, no cells.....	76
Figure 22 - 2-Arylindoles previously tested against the U87MG glioma cell line within the Snape research group.....	83
Figure 23 – Compounds tested against glioblastoma U-87 MG cell lines within the Snape research group. 2-Arylindoles 69-71 , DIM derivatives 72-74 and their IC ₅₀ values.....	85
Figure 24 – Left: Low density U-87 MG cells as seen under the microscope (magnification x100). Right: Compound 17 oiling-out in media (magnification x100).....	88

Figure 25 - Top row: the usual serial dilution followed to create the 250 μ M concentration. Bottom row: the serial dilution followed to create the 250 μ M concentration for compound **17** as this avoided the compound precipitating out in media.....89

List of schemes

Scheme 1 - Reaction scheme showing the formation of PpIX from 5-ALA during the heme synthesis. M, methyl side chain. V, vinyl side chain.....	30
Scheme 2 – Mechanism showing the metabolism of TMZ (1) in aqueous media.....	33
Scheme 3 – The metabolism of glucobrassicin into I3C (7) and DIM (8).....	36
Scheme 4 – Scheme showing glucuronidation of a phenolic group via nucleophilic attack to carbon of UDP-glucuronic acid. Histidine assists hydrogen abstraction from phenolic group.....	45
Scheme 5 – Mechanism for c-DIM (29) formation, from indole (26) reacting with a carbonyl compound.....	50
Scheme 6 - Reaction scheme showing the intermediate (31) isolated from an acid catalysed reaction between 3-formindole (30) and indole (26).....	51
Scheme 7 - Reaction between isobutylaldehyde and <i>N</i> -methylindole (32).....	51
Scheme 8 – Synthesis of c-DIMs in water using an in situ generated iron(III) dodecyl sulfate LASC.....	53
Scheme 9 – Synthesis of c-DIMs from indole (26) and an α,β -unsaturated ketone (35).....	54
Scheme 10 – Ultrasound assisted synthesis of <i>N</i> -methylindole (32) and benzaldehyde (37) to yield <i>N,N'</i> -dimethyl c-DIM (38).....	55
Scheme 11 – Photoirradiation c-DIM synthesis.....	55
Scheme 12 - Preparation of 2,2'-dimethyl c-DIMs (42) from 2-methylindole (39) and various aldehydes (41), using glycerol as a reaction medium.....	56
Scheme 13 – Synthesis of 5-carboxylic acid c-DIMs (45) via indole-5-carboxylic acids (43) with benzyl alcohols (44) in water.....	57
Scheme 14 – Preparation of DIM-c-Ph (19) using 1H-indole-3-yl-(phenyl)methanol (46) and indole (26).....	58
Scheme 15 – Reaction scheme showing the chemoselective reaction of primary (47) and secondary alcohols (48) with indole (26).....	58

Scheme 16 – A plausible mechanism for the synthesis of c-DIM 19 via <i>N</i> -benzylamines (50) and indole (26).....	59
Scheme 17 – Indole (26) reacting with benzylamine (54) to produce c-DIM (19).....	60
Scheme 18 – Friedel crafts alkylation of imine (55) with <i>N</i> -methylindole (32).....	60
Scheme 19 – Synthesis of 2-substituted c-DIMs (58) from 2-methylindole (39) and α -amido sulfones (57).....	61
Scheme 20 – Reaction between the benzyl nitron of propanal (59) and indole (26) to produce c-DIM (23) and by-product (60).....	62
Scheme 21 – Utilization of nitron (61) with indole (26) to develop c-DIM (62), derived from marine sponge <i>Orina Sp</i>	62
Scheme 22 - Reaction scheme for c-DIM compounds (19 , 17 , 64 , 65 and 20) and 2,2'-substituted c-DIM compounds synthesised (66 and 67), and yields.....	65
Scheme 23 - Reaction mechanism for the synthesis of compound 19 via the reaction of indole (26) and benzaldehyde (39).....	66
Scheme 24 - Synthesis of compound 38 via <i>N,N'</i> -methylation of compound 19	67
Scheme 25 - Attempted synthesis of 3-[1-(1H-indol-3-yl)-1-methyl-ethyl]-1H-indole, 65	68
Scheme 26 – Attempted synthesis of 66 and 67 in the same reaction. Due to solubility issues of the products, Purification via flash column chromatography was not possible.....	69
Scheme 27- Attempted synthesis of 3-[1H-indol-3-yl(diphenyl)methyl]-1H-indole (68).....	70
Scheme 28 – Reduction of MTS to the formazan product.....	74
Scheme 29 – Chemical structure of phenol red and its colour change reaction.....	90

List of tables

Table 1 - Grading of select brain tumours according to the WHO 2016.....	24
Table 2 – Key characteristics of IDH-wildtype glioblastoma and IDH-mutant glioblastoma.....	29
Table 3 – IC ₅₀ values for I3C, DIM and compounds 19 , 17 , 64 and 65 against the U-87 MG cell line for 48 hours.....	79
Table 4 – IC ₅₀ values for compounds 20 , 66 , 67 and 68 against the U-87 MG cell line for 48 hours.....	82

List of graphs

Graph 1 - Cell viability graph of U-87 MG cells after treatment with DIM after 48 hours.....	78
Graph 2 - Bar chart showing IC ₅₀ values of I3C, DIM and compounds tested (excluding compound 20), in comparison to temozolomide.....	87
Graph 3 - U-87 MG % cell viability graph of U-87 MG cells after treatment with compound 17 after 48 hours.....	89

List of equations

Equation 1 – Cell viability (%) equation.....77

List of abbreviations

AhR – Aryl hydrocarbon receptor
AIC – 5-Aminoimidazole-4-carboxamide
AlCl₃ – Aluminium trichloride
BF₃.Et₂O – Boron trifluoride etherate
Bi(NO₃)₃.5H₂O – Bismuth (III) nitrate pentahydrate
BBB – Blood brain barrier
c-DIM – c-substituted 3,3'-diindolylmethane
CF₃CO₂H – Trifluoroacetic acid
CHOP – C/EBP-homologous protein
CH₃CN – Acetonitrile
ClSiMe₃ - Trimethylchlorosilane
CNS – Central nervous system
CO₂ – Carbon dioxide
CT – Computerised tomography
CTV – Clinical target volume
CYP-450 – Cytochromes P450
Da – Dalton
DBSA - Dodecylbenzenesulfonic acid
DCM - Dichloromethane
DEPT-90 - Distortionless enhancement by polarization transfer-90
DEPT-135 – Distortionless enhancement by polarization transfer-135
DIM – 3,3'-diindolylmethane
DMSO – Dimethyl sulfoxide
DNA – Deoxyribonucleic acid
DSA - Dodecylsulfonic acid
EGFR – Epidermal growth factor
EMEM – Eagles minimum essential medium
EOR – Extent of removal
ER – Endoplasmic reticulum
ESI – Electrospray ionization
FBS – Foetal bovine serum
FCC – Flash column chromatography
FDG – Fluorodeoxyglucose
(Fe(DS)₃) - Iron(III) dodecyl sulfate

Fe(OTf)₃- Iron(III) trifluoromethanesulfonate
FGS – Fluorescence guided surgery
GB – Glioblastoma
GLOBOCAN – Global cancer observatory
GTV – Gross tumour volume
HBF₄.SiO₂ – Fluoroboric acid adsorbed on silica-gel
HCl – Hydrochloric acid
HClO₄ – Perchloric acid
HGG – High grade glioma
HPLC – High performance liquid chromatography
HPV – Human papillomavirus
IC₅₀ – Half maximal inhibitory concentration
IDH – Isocitrate dehydrogenase
IMS – Industrial methylated spirit
IR – Infrared
I3C – Indole-3-carbinol
InCl₃ – Indium (III) chloride
LASC – Lewis acid-surfactant combined catalyst
LC-MS – Liquid-chromatography-mass spectrometry
Log P – Partition coefficient
LOH – Loss of heterozygosity
MGMT – O⁶-methylguanine-DNA transferase
MMR – DNA mismatch repair
MTIC - methyl-(triazene-1-yl)imidazole-4-carboxamide
MRI – magnetic resonance imaging
m.p – melting point
MTS - (3-(4,5-dimethylthiazol-2-yl)-5-(3-carboxymethoxyphenyl)-2-(4-sulfophenyl)-2H-tetrazolium
MW – Molecular weight
NADPH – Nicotinamide adenine dinucleotide phosphate
NaH – Sodium hydride
NaHCO₃ – Sodium bicarbonate
NEAA – Non-essential amino acids
NLC – Nano structured lipid carrier
NOS – Not otherwise specified

Nur77- Nerve growth factor-induced Balpha
OS – Overall survival
PARP - poly (ADP-ribose) polymerase
PBS – Phospahte buffer solution
Pen-Strep – Penicillin Streptomycin
Pd(OAc)₂ – Palladium (II) acetate
PET – Positron emission tomography
PPAR γ – Peroxisome proliferator -activated receptor
PpIX – Protoporphyrin IX
PTV – Planning total volume
S_N2 – Nucleophilic bimolecular substitution reaction
TFA – Trifluoroacetic acid
THF – Tetrahydrofuran
TLC – Thin layer chromatography
TfOSiMe₃ – Trimethylsilyl Triflate
TMZ – Temozolomide
U.S – Ultra sonic
U.V – Ultra violet
WBRT – Whole brain radiotherapy
WHO – World Health Organisation
5-ALA – 5-aminolevulinic acid
[Et₃NH]⁺[HSO₄]⁻ – triethylammonium hydrogen sulfate
[bnmim]⁺[HSO₄]⁻ – 1-benzyl-3-methyl imidazolium hydrogen sulfate
[Msim]⁺[Cl]⁻ - 3-methyl-1-sulfonic acid imidazolium chloride
[(*n*-propyl)₂NH₂]⁺[HSO₄]⁻ - di-*n*-propylammoniumhydrogensulfate

CHAPTER ONE - INTRODUCTION

Chapter 1 – Introduction

1.1 Cancer

Cancer is a worldwide burden on the population, affecting people of any age, gender or ethnicity. According to GLOBOCAN 2018, there were approximately 18.1 million new cases of cancer and 9.6 million deaths last year. It is estimated that 1 in 2 people will develop cancer at some point of their lives, and although cancer survival rates are higher than ever, this is still a stark statistic to comprehend.^[11]

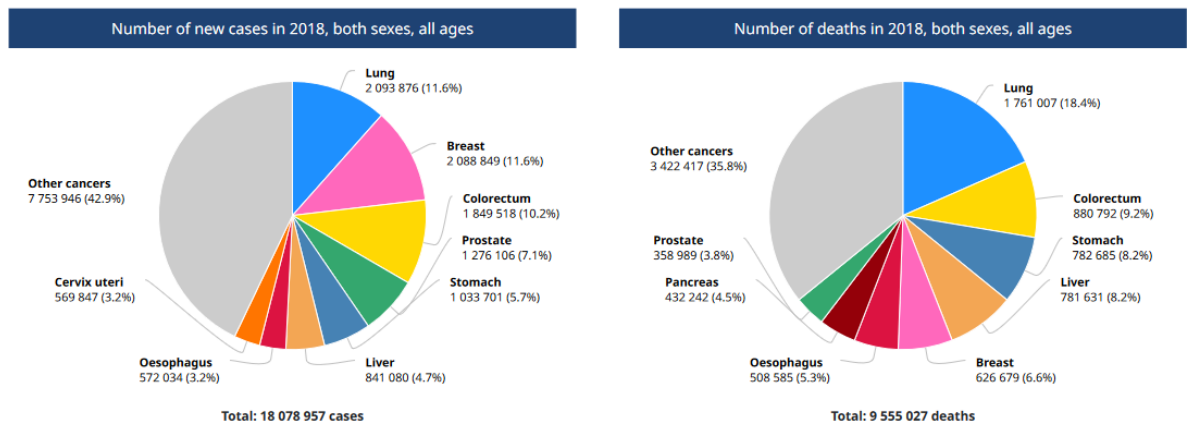


Figure 3 – Pie charts showing new cases of cancer in 2018 (left), and the number of cancer deaths in 2018 (right).^[11]

Over a century ago, German cytologist Theodor Boveri proposed that chromosomal defects could cause a cell to proliferate abnormally, essentially suggesting that cancer is a “disease of the genome”.^[12] This took 70 years to prove, by showing the presence of mutated cancer-causing genes. Some years later, the main types of cancer causing and cancer suppressing genes (oncogenes and tumour suppressor genes) had been identified, alongside the genomic alterations that give rise to these cancer-causing genes (e.g. nucleotide substitutions, DNA rearrangements and chromosomal copy number alterations).^[13] These findings hinted at the complexity of the genetic mutations that cause cancer, as these genes vary across tumour types and the fact that multiple genes contribute to oncogenesis.

Over the past few decades, extensive research has been carried out to identify risks associated with cancer, factors that may cause or encourage the genetic mutations that cancer arises from. For several cancers, there are established environmental factors in cancer causation, for example, smoking and lung

cancer, human papillomavirus (HPV) and cervical cancer, UV radiation exposure and skin cancer and *Helicobacter pylori* (*H.pylori*) and gastric cancer.^[14] Hereditary factors also play a role, confirmed by twin studies and the identification of genetic predispositions for particular cancers, for example mutations of the BRCA1 or BRCA 2 genes can increase the risk of breast and ovarian cancer. However, only around 5-10% of cancers are caused by inherited genes.^[15]

The increase in incidences of cancer can generally be attributed to the increase in life expectancy and the ever-expanding population. The ageing process is considered the most significant factor in the development of cancer, as cancer is a result of random mutations during DNA replication which occurs more as a person ages. Figure 4 shows how the risk of cancer increases with the number of cell divisions relative to the tissue type the cancer arises from. Surprisingly, only one third of cancer risk is currently known to be caused by environmental or hereditary factors and sadly, the remaining two thirds are down to “bad luck”.^{[15][16][17]}

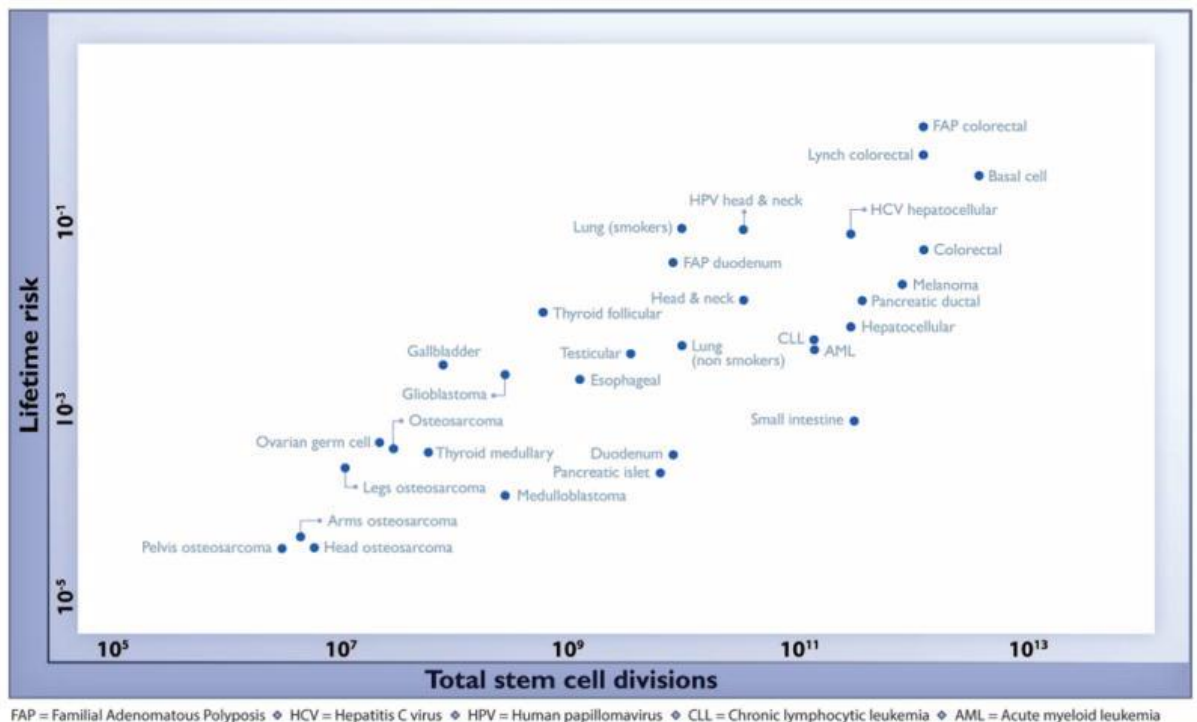


Figure 4 – Lifetime risk of cancer for specific cancer types vs number of total stem cell divisions.^[17]

1.2 – Brain tumours

1.2.1 – Brain tumours

Brain tumours, better described as intracranial neoplasms, are tumours that arise from cells within the brain. They can be either malignant (cancerous) or benign (non-cancerous) tumours, they can then be divided into primary tumours or secondary tumours. Primary brain tumours arise from tissues within the brain, they are significantly more prevalent in children under 15 years of age and the elderly.^[18] The most frequent primary brain tumours are: gliomas (50.4%), meningiomas (20.8%), pituitary adenomas (15%) and nerve sheath tumours (8%).^[19] Secondary brain tumours are metastatic, whereby cancer from elsewhere in the body has spread to the brain. This most commonly occurs from bladder cancer, breast cancer, melanoma, kidney cancer and leukaemia.^[20] The World Health Organisation (WHO) provides a grading of brain tumours (Table 1) that is recognised globally, this allows for worldwide research and epidemiological studies. Brain tumours are graded depending on their malignancy, suspected cell type of origin and rate of cell proliferation. For example, tumours that originate from ependymocytes are termed ependymomas, whereas tumours derived from astrocytes are known as astrocytomas. The malignancy is graded from I-IV, whereby grade I and II tumours have low mitotic activity, are unlikely to spread and are associated with good prognosis. However, grade III and IV tumours are very malignant, have a high rate of proliferation, infiltrate other areas of the brain and are associated with poor prognosis.^{[1][21]}

Diffuse astrocytic and oligodendroglial tumours	
Diffuse astrocytoma, IDH-mutant	II
Anaplastic astrocytoma, IDH-mutant	III
Glioblastoma, IDH-wildtype	IV
Glioblastoma, IDH-mutant	IV
Diffuse midline glioma, H3 K27M-mutant	IV
Oligodendroglioma, IDH-mutant and 1p/19q-codeleted	II
Anaplastic oligodendroglioma, IDH-mutant and 1p/19q-codeleted	III
Other astrocytic tumours	
Pilocytic astrocytoma	I
Subependymal giant cell astrocytoma	I
Pleomorphic xanthoastrocytoma	II
Anaplastic pleomorphic xanthoastrocytoma	III
Ependymal tumours	
Subependymoma	I
Myxopapillary ependymoma	I
Ependymoma	II
Ependymoma, <i>RELA</i> fusion-positive	II or III
Anaplastic ependymoma	III
Tumours of the pineal region	
Pineocytoma	I
Pineal parenchymal tumour of intermediate differentiation	II or III
Pineoblastoma	IV
Papillary tumour of the pineal region	II or III
Embryonal tumours	
Medulloblastoma (all subtypes)	IV
Embryonal tumour with multilayered rosettes, C19MC-altered	IV
Medulloepithelioma	IV
CNS embryonal tumour, NOS	IV
Atypical teratoid/rhabdoid tumour	IV
CNS embryonal tumour with rhabdoid features	IV
Tumours of the cranial and paraspinal nerves	
Schwannoma	I
Neurofibroma	I
Perineurioma	I
Malignant peripheral nerve sheath tumour (MPNST)	II, III or IV
Meningiomas	
Meningioma	I
Atypical meningioma	II
Anaplastic (malignant) meningioma	III

Table 1 – Grading of select brain tumours according to the WHO 2016.^[1]

GLOBOCAN 2018 states, 296,581 people worldwide were diagnosed with a brain or central nervous system (CNS) tumour, and in the same year there were 241,037 deaths as a result of brain and CNS tumours.^[22] Although the diagnostic figures seem low in comparison to other cancers such as breast and lung cancer, the survival rates are much poorer. Only 14% of people diagnosed with a brain tumour will survive for more than 10 years and only 40% of patients with a malignant brain tumour will live over one year.^[23] Brain tumours propose a significant challenge in terms of diagnosis, treatment and survival. Thus, a much more effective regime is required.

1.2.2 – Causes of brain tumours

The etiology of brain tumours has been widely researched, yet cause factors have not been established. Epidemiological studies have been burdened as a result of the rarity and complexity of these tumours, alongside the fact that brain tumours are thought to differ relative to the cell type the tumour originated from.^[24] A number of hereditary disorders such as tuberous sclerosis, von Hippel-Lindau disease and type 1 and 2 neurofibromatosis, have been associated with a genetic predisposition to the development of brain tumours.^[25] Neurofibromatosis type 1, also known as von Recklinghausen disease is the most frequent and is associated with gliomas of hamartomas and the optic nerves. On the other hand, neurofibromatosis type 2 is linked to meningiomas, ependymomas and schwannomas.^[26]

Certain occupations have been connected to a higher risk of developing brain tumours, for example, farmers as pesticide exposure is a suspected risk factor. A case-control study investigating the potential carcinogenetic effects of pesticide for agricultural purposes found a notable association between pesticide use and the development of gliomas later on in life. However, it is worth noting, that recall bias was an issue within this study, suggesting further research is required.^[27] A study by Provost *et al* investigated a link between brain tumours and pesticide exposure in southwestern France, which states that only a significantly high level of exposure could be associated with the development of brain tumours, gliomas especially.^[28] Occupations involving exposure to certain chemicals such as rubber, vinyl chloride, mercury and formaldehyde have also raised speculation in their role in the development of brain tumours.^[29]

There are other suspected risk factors linked to the causation of brain tumours, e.g. radiofrequency waves (use of mobile phones), previous head trauma, smoking and viral infections.^[29] However attempts to prove the relationships between these risk factors and brain tumours, sadly remains inconsistent.^[29]

1.2.3 – Signs and symptoms

Symptoms of brain tumours can vary dependent on its location within the brain, the type of tumour and tumour size. Symptoms are usually the result of the tumour pressing on the brain – intercranial pressure, blocking the movement of fluid flowing through the brain causing a build-up of fluid or by pressing on nerves in the brain.^[30] The most common symptoms include headaches, problems with memory and concentration, nausea and vomiting, poor vision, numbness of the limbs, seizures and loss of balance.^[31] As these symptoms can be caused by numerous other health conditions and a patient may only have a few of these symptoms, it can make early diagnosis of brain tumours difficult.

Psychological distress is extremely prevalent amongst brain tumour patients, depression in patients with highly malignant tumours was reported as high as 93%.^[32] Other issues such as extreme sleep disturbances, anxiety and fatigue are also common complaints amongst patients with high grade tumours.^[32]

1.2.4 - Diagnosis

The first stage of diagnosis is usually a neurological exam, consisting of checking reflexes, hearing, co-ordination, balance, and memory. Subsequently, imaging tests are carried out, the preferred modalities are magnetic resonance imaging (MRI) and computerised tomography (CT). These tests have an excellent ability to locate brain tumours, identify the size of the tumour, and evaluate complications such as oedema, hydrocephalus and brain haemorrhages.^[33] Additionally, doctors use these images to predict the tumour type. Positron Emission Tomography (PET) scans can also be used, with the assistance of radioactive tracer fluorodeoxyglucose (FDG) to represent the metabolic uptake of glucose.^{[34][35]} These scan images are usually combined to create treatment plans. Figure 5 illustrates a CT, MRI, PET/CT scan of a 62 year old male glioblastoma patient, the scan images were combined to calculate a radiotherapy plan. Similarly, Figure 6 also shows a CT, MRI, PET/CT scan and their combination in order to create a radiotherapy plan, however, for a 50 year old male with nodular atypical meningioma.^[36]

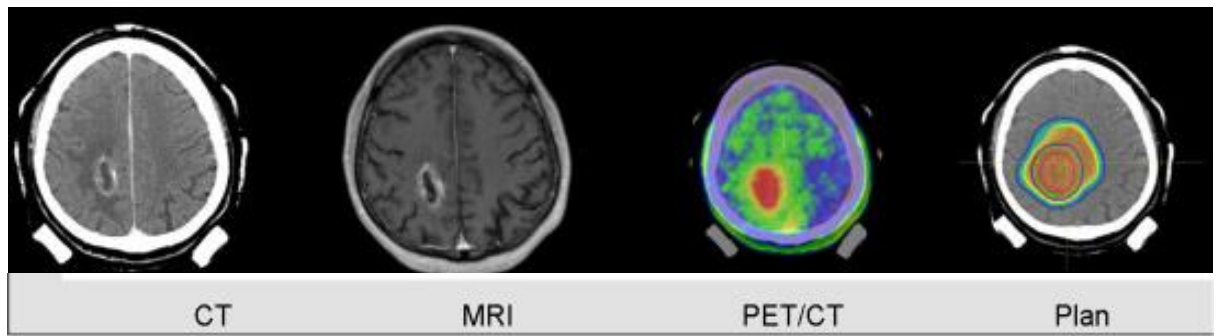


Figure 5 – CT and MRI scan combined with a PET/CT scan of a 62 year old male with glioblastoma to produce a radiotherapy plan.^[36]

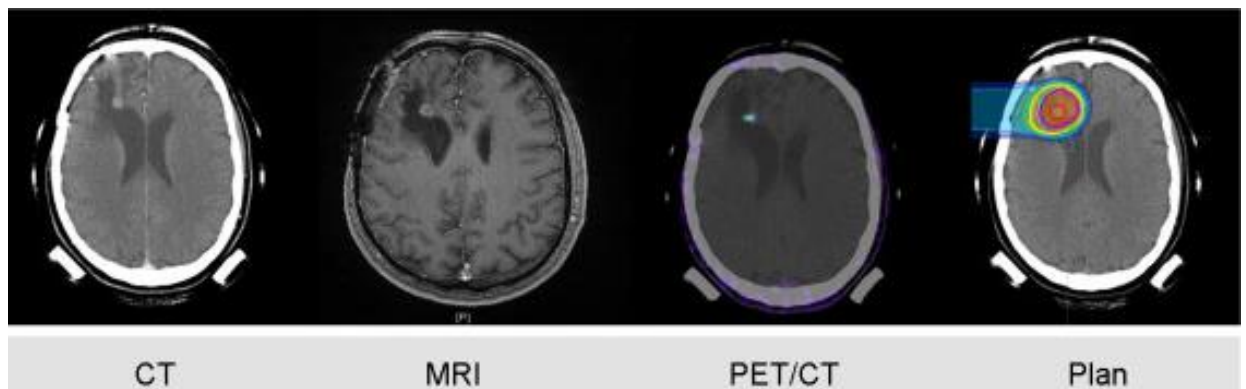


Figure 6 - CT and MRI scan combined with a PET/CT scan of a 50 year old male with nodular atypical meningioma to create a radiotherapy plan.^[36]

Despite the fact imaging techniques are extremely useful, MRI, FDG-PET and CT scans are unable to provide accurate insights into specific tumour type, therefore histological tests via biopsies are also required to make an accurate diagnosis.

1.3 – Glioblastoma

1.3.1 – Classification of glioblastoma

Glioblastoma (GB) is a grade IV astrocytoma, it can also be called a malignant astrocytic glioma.^[37] It is the most aggressive and lethal primary malignant brain tumour in adults, it is slightly more common in males and its incidence increases with age. GB has extremely poor prognosis, median survival for patients is around 6–9 months from time of diagnosis and even in the most positive circumstances long term survival is rare, with 25% of patients surviving two years.^{[1][2]}

Glioblastomas are conventionally split into primary and secondary tumours; the former, known as IDH-wildtype is a GB arising *de novo*, and the latter IDH-mutant are GB tumours derived from lower grade anaplastic astrocytomas or diffuse astrocytomas. GB tumours that are indistinguishable between primary and secondary are referred to as glioblastoma not otherwise specified (NOS).^{[1][38]} Primary and secondary GB tumours involve significant genetic differences, suggesting they evolve via different genetic pathways. Genetic characteristics typical of primary glioblastomas are, predominantly, loss of heterozygosity (LOH) on chromosome 10p (approximately 70% of cases), EGFR amplification, and mutation of protein PTEN. In contrast, secondary glioblastomas show TP53 mutations, the most common and earliest alteration to detect as it is already present in approximately 60% of low grade astrocytomas. Additionally, LOH is observed of chromosomes 13p, 17p, 19p and increased telomerase activity.^{[39][40][41]}

Primary GB is much more common, accounting for 90% of all cases and tend to grow quickly in elderly patients. Whereas, secondary tumours are less frequent, occur in younger patients, prefer developing within the frontal lobes of the brain and are associated with a more positive prognosis.^[1] Table 2 summaries the key characteristics associated with primary and secondary glioblastoma tumours, according to the WHO 2016.

	IDH-wildtype glioblastoma	IDH-mutant glioblastoma
Synonym	Primary glioblastoma, IDH-wildtype	Secondary glioblastoma, IDH-mutant
Precursor lesion	Not identifiable; develops de novo	Diffuse astrocytoma Anaplastic astrocytoma
Proportion of glioblastomas	~90%	~10%
Median age at diagnosis	~62 years	~44 years
Male-to-female ratio	1.42:1	1.05:1
Mean length of clinical history	4 months	15 months
Median overall survival		
Surgery + radiotherapy	9.9 months	24 months
Surgery + radiotherapy + chemotherapy	15 months	31 months
Location	Supratentorial	Preferentially frontal
Necrosis	Extensive	Limited

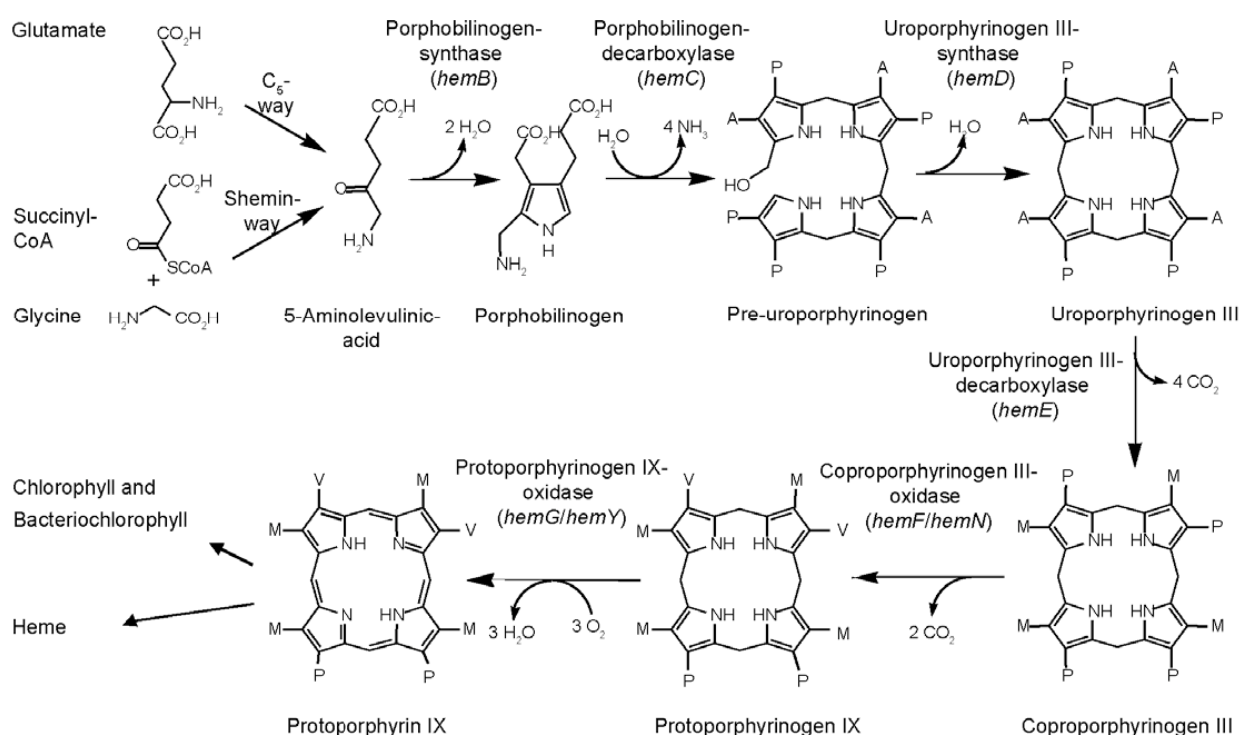
Table 2 – Key characteristics of IDH-wildtype glioblastoma and IDH-mutant glioblastoma.^[1]

1.3.2 – Current treatments

After diagnosis, surgical resection is the initial form of treatment, as studies demonstrate a positive correlation between extent of removal (EOR) and survival.^[42] Neurosurgeons aim to achieve a balance between maximum removal of tumour mass with minimal neurological impairment. Therefore, prior to surgery the EOR is determined in order to avoid damage to eloquent areas of the brain. If resection is expected to cause neurological impairment, then a stereotactic biopsy is performed. Although surgery is essential and extends survival significantly more in comparison with patients that only undergo biopsy (approximately 7 months vs 3.5 months, respectively), recurrence is 100%.^[43] Glioblastoma tumours have poor marginalisation, due to their extremely infiltrative nature. They tend to migrate along the white matter tracts of the brain and troublingly, they have been found to migrate up to 5 cm from their ‘visible’ margins.^[44]

Fluorescence guided surgery (FGS) is a surgical technique that may be used to improve the EOR, involving the use of fluorescent dyes with high tumour specificity, FGS can improve the visualisation of the tumours beyond their visible borders. The use of 5-aminolevulinic acid (5-ALA) is currently the only agent approved for high grade glioma (HGG) surgery in Japan, Canada and Europe.^[45]

5-ALA is a precursor of haemoglobin and is converted into fluorescent porphyrins (PpIX) during the heme synthesis in mammalian cells (Scheme 1).^[46]



Scheme 1 – Reaction scheme showing the formation of PpIX from 5-ALA during the heme synthesis. M, methyl side chain. V, vinyl side chain.^[46]

PpIX molecules have a preference for malignant glioma cells due to the variation in haemoglobin synthesis in tumour cells and normal cells, therefore the fluorophores accumulate within the tumour.^[47] PpIX emits light within the red region of the spectrum, producing pink fluorescence under blue-violet light conditions, allowing for differentiation between cancerous and normal tissues, which might otherwise be indistinguishable.^[48] In a 2006 a randomised controlled multi-institution phase III trial, investigating the effects of fluorescence-guided surgery with 5-ALA versus white light surgery was carried out. Resection of 65% was achieved for 5-ALA patients, in comparison to 36% for white light patients. Moreover, 6-month progression-free survival was found to be 41% for 5-ALA patients and 21.1% for white light patients.^{[49][50]}

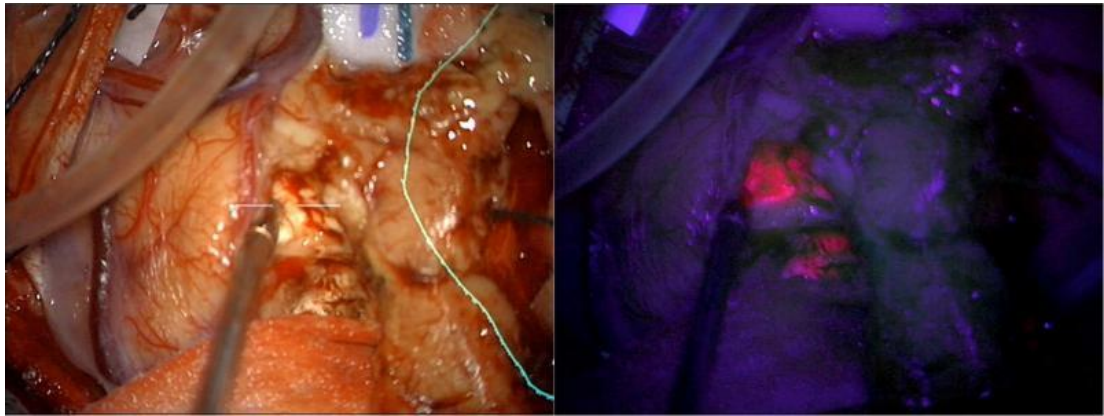


Figure 7 – Photo taken during glioblastoma resection using 5-ALA. Under white light (left) it seems tumour has been entirely removed. The yellow line indicates tumour border according to MRI. Under blue light (right), residual tumour is seen.^[50]

Despite demonstrating promising advancements in the resection of high grade gliomas (HGG's), 5-ALA does have disadvantages. PpIX can give false positive results via leaking into nearby fluid in the brain, giving the appearance more tumour is present.^[51] Also, side effects such as photosensitivity, nausea, hypotension and raised liver enzyme levels were reported up to 48 hours after the drug was administered.^[51]

Although surgery is the most efficient intervention in extending the overall survival (OS) and relieving patients of painful symptoms, such as headaches and seizures, residual tumour cells always remain after surgery and recurrence is inevitable. Therefore, follow up treatments are essential.^[51]

Radiotherapy (RT) has played a key role in GB treatment since the 1980's, when it was discovered that post-surgery therapeutics aid overall survival.^{[52][53]} RT is based on ionising radiation dealing damage to the DNA of tumour cells, disrupting the mechanisms associated with cell division and thus preventing tumour growth. Radiotherapy treatment is usually started 4 to 6 weeks after surgery, over a 6 to 7 week period, the standard dose is a total of 60 gray units (Gy) in daily doses of 2Gy, 5 days a week.^[54]

In the past, GB patients were given whole brain radiotherapy (WBRT), however, it was associated with cognitive issues and high doses were required.^{[55][56]} Currently, sophisticated planning is carried out using CT scans before RT is administered. There are three essential volumes to consider; the first is the known

gross tumour volume (GTV), which is usually the visible tumour mass. The second is the clinical target volume (CTV), which encases the GTV and accounts for tumour spread that is not visible. Finally, the planning target volume (PTV) which takes into account both internal and external uncertainties.^{[57][58]}

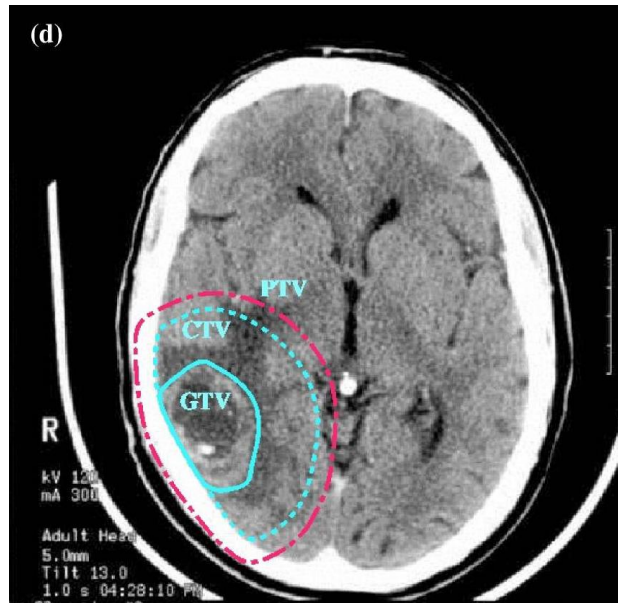
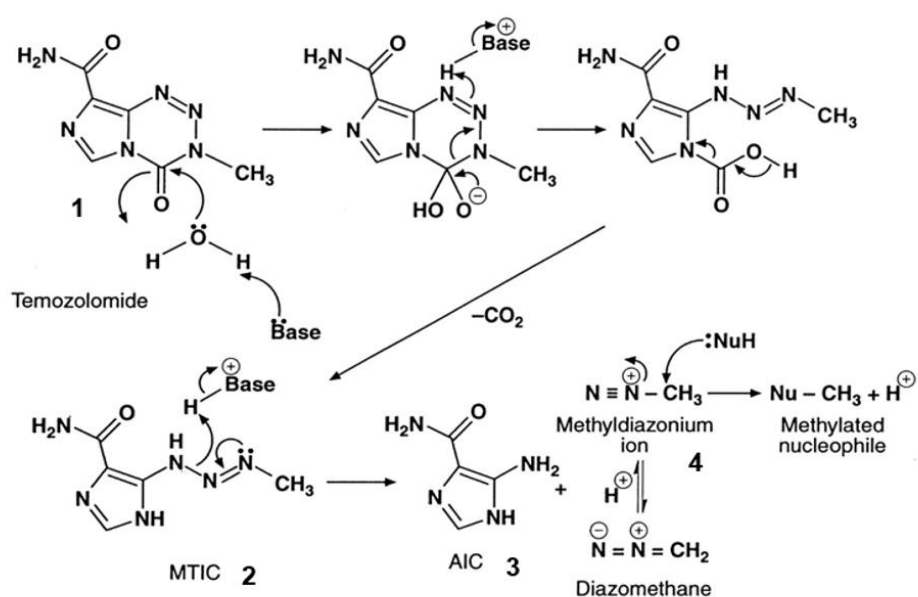


Figure 8 - CT scan of a grade IV glioblastoma patient showing planning volumes for RT treatment.^[58]

In addition to maximum surgical resection and RT, the use of pharmaceutical agents are also used to further destroy and inhibit the growth of glioblastoma cells. After surgery, chemotherapy treatment is started, either at the same time or shortly after RT.^[59] Oncologists devise carefully tailored chemotherapy plans for glioblastoma patients, due to the extremely heterogeneous nature of glioblastoma tumours.^[60] Carmustine is a commonly used medication for the treatment of high-grade gliomas, Bevacizumab can be used as a secondary treatment for recurrent glioblastoma, Lomustine is a drug sometimes used alongside Bevacizumab to improve the effectiveness of Bevacizumab.^[61] Chemotherapy medications can be administered orally, intravenously and in special circumstances injected into the intrathecal space of the spine.^[61] Carmustine can also be implanted into the tumour cavity in a biodegradable wafer, known as gliadel wafers.^{[61][62]} However, the use of these wafers is controversial, the implantation of wafers offer a slight improvement of less than six weeks. Moreover, side effects reported include myelosuppression, intracranial infections and worsening of neurological deficits.^[62]

Currently, the initial chemotherapeutic agent of choice for the treatment of newly diagnosed glioblastoma patients is temozolomide.^[63] Initially, radiotherapy was trialled as a monotherapy after surgery in the treatment of glioblastoma. However, in 2005 a phase III randomised controlled trial concluded that radiation therapy combined with temozolomide increased the OS of glioblastoma patients by 2.5 months (12.1 versus 14.6 months OS). Since then, this has become the gold standard of care for healthy adults with recently diagnosed GB.^[63] Typically, the recommended dose of TMZ for newly diagnosed GB patients receiving concomitant radiation plus chemotherapy, is 75mg per day for 5 days over a 6-week period. Side effects such as nausea, tiredness and sleep problems were reported but otherwise TMZ is well tolerated.^[64]

TMZ (**1**) is an oral alkylating drug belonging to the imidazotetrazine family, it is a small molecule with a molecular weight of 194 g/mol, thus is easily absorbed into the bloodstream, its bioavailability is approximately 100%. Its lipophilic properties also allow it to penetrate the blood brain barrier (BBB).^[65] TMZ acts as a prodrug, stable in the acidic environment of the stomach, however, labile once absorbed into the bloodstream (pH 7). TMZ undergoes spontaneous hydrolysis to yield 3-methyl-(triazene-1-yl)imidazole-4-carboxamide (MTIC, **2**). MTIC then reacts with water to liberate 5-aminoimidazole-4-carboxamide (AIC, **3**) and the active species - the methyl diazonium cation (**4**, see Scheme 2).^{[66][67]}



Scheme 2 – Mechanism showing the metabolism of TMZ (**1**) in aqueous media.^[67]

The methyldiazonium (4) ion formed via the metabolism of TMZ (1), methylates guanine and adenine residues within DNA, most frequently occurring at the N7-position of guanine, then the N3-position of adenine, followed by the O6-position of guanine (O6-MeG). While the (O6-MeG) lesion is the least common methylation, it is responsible for the cytotoxic effects of TMZ towards GB cells.^[67] In normal cells the enzyme methylguanine methyltransferase (MGMT) removes the methyl group and restores guanine. However, in MGMT deficient cells, during DNA replication, O6-MeG pairs with thymine instead of cytosine, in turn activating DNA mismatch repair (MMR), which identifies the mismatch and destroys the daughter strand of DNA. As the O6-MeG still exists in the template strand, this causes repetitive DNA strand breaks and ultimately cell apoptosis via G₂/M cell cycle arrest.^{[68][69]}

Glioblastoma tumours that initially respond well to chemotherapy, can eventually develop a resistance to the drug – this is known as acquired resistance. Explained by Darwinian evolution, acquired resistance to TMZ is the outcome of drug-induced changes to genes in neoplastic cells. By inducing and selecting genes that have a survival advantage.^[70] Patients experiencing an ineffectiveness of TMZ can be attributed to having increased levels of MGMT and insufficient MMR. Zhang *et al* reported that increased up-regulation of MGMT in U373 glioblastoma cells that were treated with TMZ, showed a 4-fold resistance to TMZ.^[71] In addition, cancer stem cells and the presence of efflux pumps that actively pump drugs out of the tumour cells, such as P-glycoprotein, have been associated with resistance to treatment.^[72]

1.3.3 – Conclusion

To conclude, glioblastoma is a deadly brain tumour and despite the advancements in imaging, radiotherapy, surgery and chemical agents, prognosis is dismal. A more effective regime, in the diagnosis and treatment of glioblastoma is essential, preferably earlier diagnosis and the development of more effective pharmaceutical agents with high tumour specificity, the ability to pass the BBB and minimal adverse side effects.

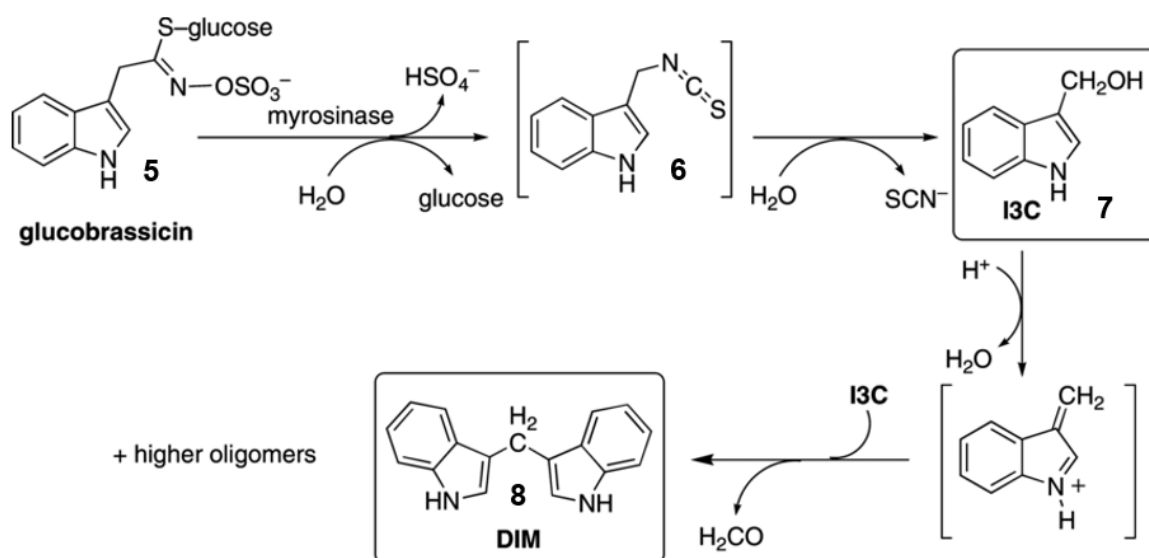
1.4 - The anti-cancer effect of 3,3'-diindolylmethane (DIM) and its derivatives

1.4.1 – Introduction

Dietary intake has always contributed to defining a person's health, and an increased consumption of fruit and vegetables is recommended in order to avoid the development of chronic diseases, including cancer. According to The World Cancer Research Fund, approximately 3 to 4 million cases of cancer worldwide could be avoided via making healthy lifestyle choices, it is proposed that micronutrients such as antioxidants and phytochemicals may possibly have anti-cancer properties.^[73] This has led to research aiming to establish this link and to identify the components responsible for the chemopreventive properties.^[74] A meta-analysis of 14 case-controlled studies concluded that the risk of developing breast cancer was decreased by 25% by an increased vegetable intake.^[75] Epidemiological studies have also been carried out to investigate the effects of higher vegetable consumption amongst populations and occurrences of cancer. A study involving Dutch men and women found that those with the highest vegetable intake were at lower risk of developing colon cancer than those with lesser intakes.^[76] In a review analysing results from 206 epidemiological studies and 22 animal studies, there was evidence that a higher fruit and vegetable consumption provides a protective effect for several cancers, including pancreas, endometrium, lung, pharynx and colon.^[77] The type of fruit and vegetables that most frequently demonstrated the protective effect were cruciferous vegetables. Cruciferous vegetables are vegetables of the *Brassicaceae* family, including broccoli, cabbage, cauliflower, watercress and collard greens. Considerable research has found possible associations between cruciferous vegetable intake and reduced risks of cancer.^{[78][79][80]} This includes a meta-analysis carried out in the US, that found women who consumed more than 5 servings of cruciferous vegetables per week had a reduced risk of lung cancer.^[81] This association between reduced risk of cancer and increased cruciferous vegetable intake, has led to the study of cruciferous vegetables' bioactive constituents being studied for use in the prevention and treatment of cancer.^[82]

Cruciferous vegetables are a rich source of glucosinolates – substituted β -thioglucoside *N*-hydrosulfates - glucosinolates are derived from amino acids, which upon hydrolysis form isothiocyanates, with the exception of those derived from tryptophan which yield indoles. The composition varies significantly with the

type of plant. For example, watercress is rich in gluconasturtiin, whereas broccoli has a high glucoraphanin content. The levels of glucosinolates can also vary dependent on environmental factors such as soil pH, iron presence and temperature.^{[83][84]} Glucosinolates are hydrolysed via the enzyme myrosinase to produce a variety of isothiocyanates and indoles. A glucosinate of interest, namely glucobrassicin (**5**), upon hydrolysis produces indole-3-methyl isothiocyanate (**6**) via a C-N (Lossen) rearrangement, this rapidly yields the corresponding alcohol - indole-3-carbinol (I3C, **7**) and a thiocyanate ion (see Scheme 3).^[85] In the acidic environment of the gut, indole-3-carbinol is extremely unstable and undergoes reactions to produce a spectrum of products, at least 15 different oligomeric products. However, primarily formed is the dimeric product of I3C – 3,3'-diindolylmethane (DIM, **8**, Scheme 3) - thought to be the most biologically active and most stable metabolite of I3C, and it is DIM that is believed to have the anti-cancer effect.^{[8][86]} Attempts to investigate the chemopreventive and anti-carcinogenic properties of I3C have proved difficult due to its instability in aqueous media. For example, a phase I trial administered oral doses of I3C (400-1200 mg) to women, subsequently, serial plasma samples were analysed via HPLC. No I3C was detected in plasma and the only derivative product of I3C detectable in plasma was DIM.^[87]



Scheme 3 – The metabolism of glucobrassicin into I3C (**7**) and DIM (**8**).^[85]

1.4.2 – 3,3'-Diindolylmethane

1.4.2.1 – The structure of 3,3'-diindolylmethane

Indole is a planar bicyclic molecule consisting of a benzene ring fused to a nitrogen-containing pyrrole ring. Thought to be one of the most privileged heterocycles known, this particular structure is found in many natural and synthetic products. For example, the anti-tumour agent mitomycin C (Figure 9, **9**) which undergoes bio-reductive activation, causing the formation of cross-links with DNA to prevent replication of cancer cells. Also, the naturally occurring amino acid tryptophan (Figure 9, **10**).^{[8][88]}

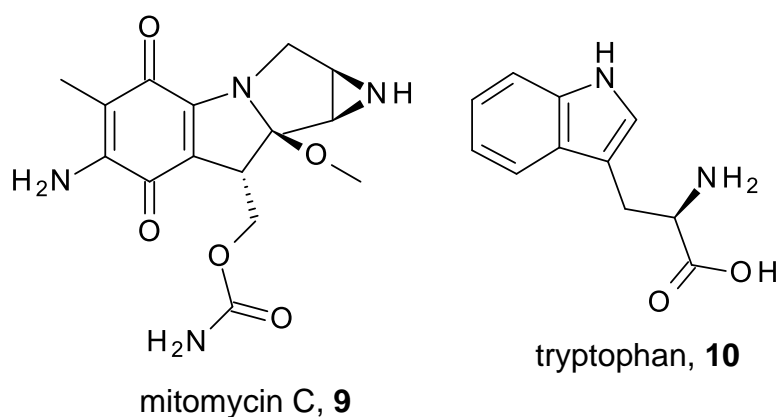


Figure 9 - Chemical structures of anti-cancer agent mitomycin C and the amino acid tryptophan.

Due to the biological activity of the indole nucleus, its derivatives have therefore been widely implemented in drug design. For example, vincristine (**11**) and vinblastine (**12**, see Figure 10) are indole containing chemotherapeutic agents that have been used when treating Hodgkin's lymphoma, leukaemia and breast cancer.^[89]

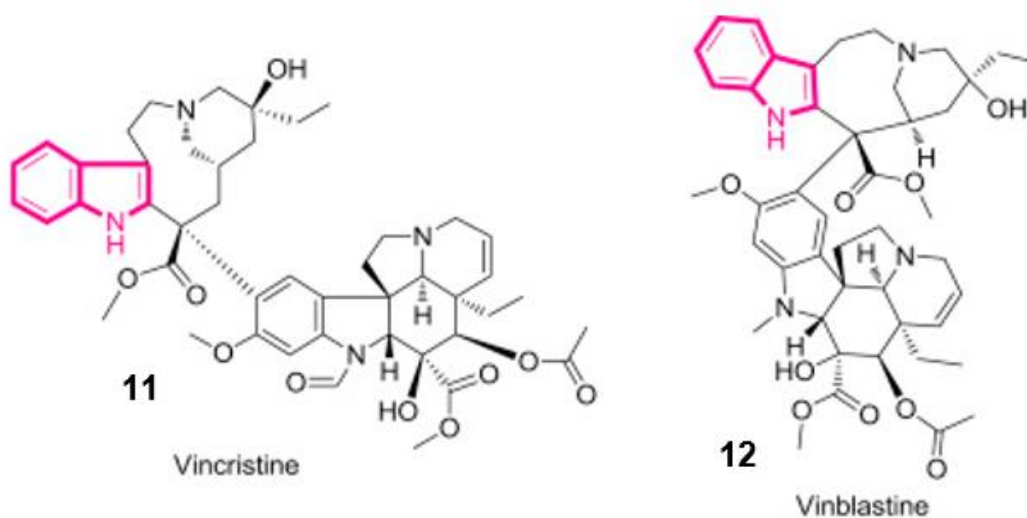


Figure 10 - Chemical structures of indole containing chemotherapy drugs vincristine and vinblastine.^[89]

The 3,3'-diindolylmethane (**8**) skeleton is a symmetrical structure comprised of two indole rings bound by a methylene bridge at position-3 of the indole rings (Figure 11).

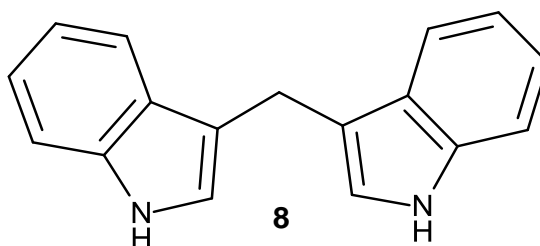


Figure 11 – The chemical structure of 3,3'-diindolylmethane (**8**).

1.4.2.2 – The anti-cancer effect of 3,3'-diindolylmethane

Studies have established the anti-cancer effects of DIM against a number of cancer cell lines. A study by Nicastro *et al*, investigated the effects of DIM at different concentrations (0-25 μ M), on breast cancer growth.^[90] It was established that DIM inhibited tumour growth, showing a positive correlation between DIM concentration and tumour growth inhibition. From 30 minutes to 24 hours of administration DIM inhibited cell proliferation by 54% and cell migration by 66%.^[90] Importantly, DIM did not have an effect on non-tumorigenic cell lines, demonstrating its ability to distinguish between healthy and cancerous cells; enhancing its applicability to a clinical setting. A similar investigation was carried

out by Vivar *et al*, in which they tested the effects of DIM against human prostate cancer cells.^[7] It was concluded that DIM inhibited the growth of prostate cancer cells, and specifically, it was identified that DIM prevented the progression of cancer cells into the S phase via inducing a G₁ phase-specific cell cycle arrest.^[7] Additionally, research by Li *et al* shows that DIM inhibits gastric cancer cells via G₁ phase cell cycle arrest by decreasing levels of cyclin dependant kinases. DIM also increased cellular pro-apoptotic protein and p53 levels.^[91]

There is also evidence DIM exhibits anti-carcinogenic effects against other types of cancer such as; oesophageal, colorectal, liver and pancreatic.^{[92][93][94][95]} The mechanisms by which DIM inhibits the growth of cancer cells varies amongst cancer types but are well studied. The most commonly noted ones include; induction of endoplasmic reticulum (ER) stress, G₀ and G₁ cell cycle arrest, apoptosis and activation of the aryl hydrocarbon receptor (AhR).^{[96][97]} In the USA, DIM is currently used in the adjuvant therapy of recurrent respiratory papillomatosis, a rare disease caused by HPV, whereby tumours form in the upper respiratory tract.^{[98][99]}

In addition to the basic DIM structure, *in vitro* screening studies have established that 2,2'-substituted DIM compounds also demonstrate an anti-proliferative effect towards breast cancer by inhibiting the epidermal growth factor (EGFR) pathway.^[100] Ghosh *et al*, identified that 2,2'-diphenyl DIM (**13**, Figure 12), induced a 50% decrease in cell proliferation (IC₅₀ value of 50 µM) at concentrations below 20 µM in breast cancer cell lines. The cytotoxicity of 2,2'-phenyl DIM (**13**) towards non-cancerous cells was also investigated, in which it was concluded that **13** was non-cytotoxic to healthy cells up to concentrations of 50 µM.^[100]

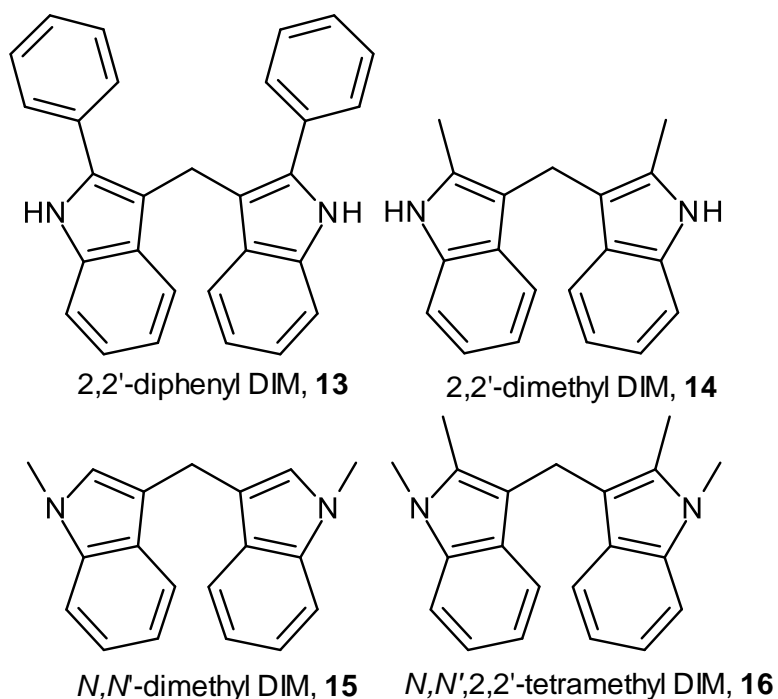


Figure 12 – Chemical structures of *N,N'*- and 2,2'-methyl-substituted DIM derivatives (**13-16**) tested for anti-proliferative effects against breast cancer cells.^{[100][101]}

Similar to the research carried out by Ghosh *et al*, Safe *et al* investigated the effects of methyl-substituted DIM analogues against breast cancer cells. They found that 2,2'- (**14**), *N,N'*-dimethyl DIM (**15**) and *N,N',2,2'*-tetramethyl DIM (**16**) (Figure 12) all inhibited estrogen-induced T47D breast cancer cell growth by acting as selective FDG modulators.^[101]

1.4.3 – c-substituted 3,3'-diindolylmethane derivatives

The previously discussed findings provide evidence of the anti-cancer effects of DIM. Using DIM as a template, additional research into the anti-tumorigenic properties of c-functionalised DIM derivatives (c-DIMs) show promising prospects for DIM derivatives as anti-cancer agents. c-DIMs are characterised by substitution at the carbon of the methylene bridge, this includes the addition of more than one group to the conjoining carbon (examples in Figure 13). Functionalisation can also occur around the indole ring.

Research has identified two c-DIM compounds; DIM-c-*p*PhOCH₃ (**17**) and DIM-c-*p*PhOH (**18**, Figure 13), that have exhibited cytotoxic effects towards lung cancer cells, potentially by acting as TR3 inactivators, thus preventing cell progression to the S-Phase of the cell cycle. Compounds **17** and **18** were found

to be active against A549 cells, with 24-hour IC₅₀ values of 14.29 ± 2.30 μM and 16.18 ± 1.59 μM respectively. The study also established, the DIM analogues were active against H460, LnCap and PC3 cell lines.^[10] The H460 cell line is derived from non-small cell lung cancer cells, whereas LnCap and PC3 cell lines are derived from prostate cancer cells.

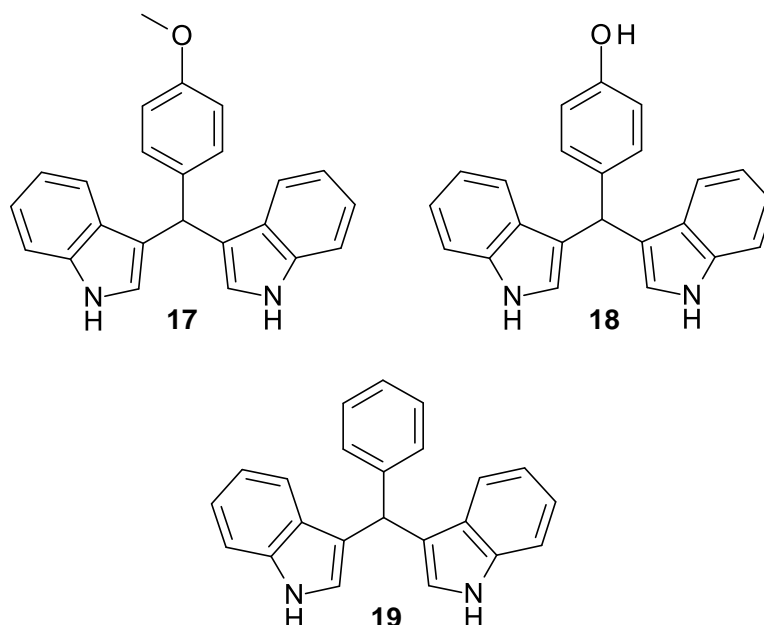


Figure 13 – *c*-DIM compounds; DIM-*c*-*p*PhOCH₃ (**17**) and DIM-*c*-*p*PhOH (**18**), which were tested on lung and prostate cancer cell lines.^[10] The same research group investigated the effects of **17** and *c*-DIM-Ph (**19**) as Nur77 agonists.^[103]

Moreover, investigations by the same research group, demonstrated that DIM-*c*-*p*PhOCH₃ (**17**) and DIM-*c*-Ph (**19**) act as agonists for nerve growth factor-induced Balpha (Nur77) – an orphan nuclear receptor expressed in a number of cancer types including, colon, pancreatic, breast, prostate cancer, and interestingly, cerebral cells.^[102] The compounds were also tested for PPAR_γ (peroxisome proliferator-activated receptor γ) activation, but the results were negative. Activation of Nu77 causes initiation of cell death via TRAIL (tumour necrosis factor-related apoptosis-inducing ligand), and cleavage of PARP (poly (ADP-ribose) polymerase). The methoxy group on DIM-*c*-*p*PhOCH₃ (**17**) was changed to the *meta* and *ortho* positions of the phenyl ring to carry out structure-dependant activation of Nu77 tests, whereby only the *para*-substituted *c*-DIM was found to be active. Furthermore, 2,2'-methyl and *N,N'*-methyl indole substitutions of DIM-*c*-*p*PhOCH₃ (**17**) and DIM-*c*-Ph (**19**) were tested and did not show Nu77

activation. It is also worth noting that DIM-c-*p*PhOH (**18**) was also tested in this study but did not demonstrate activation of either Nu77 or PPAR γ .^{[103][104]}

Moreover, Kassouf *et al* synthesised c-DIMs DIM-C-Ph (**19**), DIM-C-*p*PhCF₃ and DIM-c-*p*Ph-t-butyl, which were tested against bladder cancer cells, using PPAR γ as a target.^[106] PPAR γ is a ligand activated nuclear receptor belonging to the nuclear hormone receptor family and is thought to be a good target for anti-cancer therapy. Due to PPAR γ activation resulting in; apoptosis, prevention of G₀/G₁ to S-phase progress, and reduced proliferation. Also, PPAR γ is over-expressed in many different tumour samples and cell lines including lung, colon, breast and glioblastoma cell lines.^[105] The study established that all three c-DIMs had anti-cancer effects *in vitro* and in orthotopic bladder tumours in mice, DIM-C-PhCF₃ demonstrated the best activity, significantly inhibiting the growth of the orthotopic tumours by 32%.^[106]

Further research investigated the activity of halogenated phenyl substituted c-DIMs; DIM-c-*p*PhBr and DIM-c-*p*PhF (**20**, see Figure 14), against colon cancer cell lines. SW480 and RKO cell lines were treated with both c-DIMs for 12 hours and both inhibited cell growth *in vitro* by activation of ER stress, caused by induction of CHOP (C/EBP homologous protein) and cleavage of PARP. The *ortho*- and *meta*-substituted analogues also exhibited activity but were much less potent than the *para*-substituted c-DIMs, the order of activity established was *para* > *meta* > *ortho*. Moreover, the 2-methyl-substituted analogues (**21**) and *N,N'*-methylated-substituted analogues (**22**) were also tested for activity. The former displayed good anti-proliferative activity, showing a 40-60% reduction in cell viability. Whereas, the latter were completely inactive – suggesting the free NH groups are necessary for activity, more specifically for the induction of CHOP.^[107]

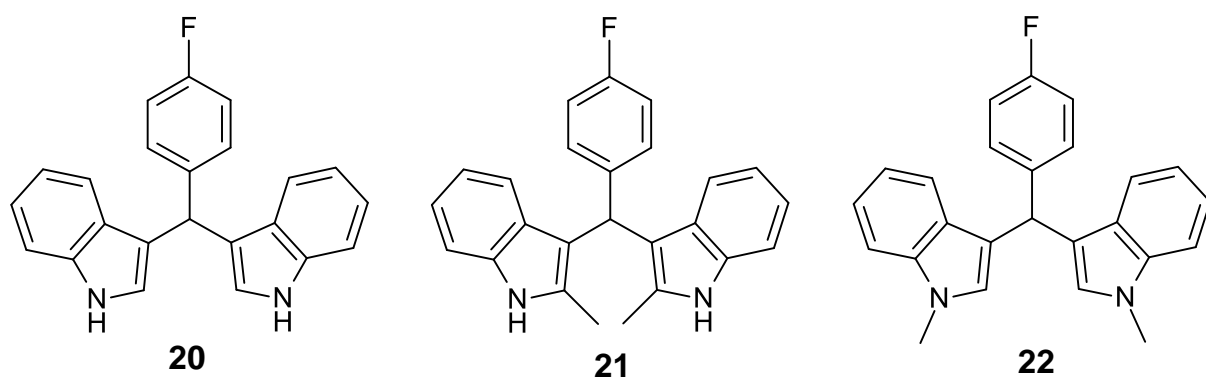


Figure 14 - Chemical structures of DIM-c-pPhF (**20**) and its 2,2'-methyl substituted (**21**) and N,N'-methylated (**22**) derivatives.^[107]

Similar research, again involving DIM-c-pPhF (**20**, Figure 14) and DIM-c-pPhBr, concluded that both of the halogenated phenyl c-DIMs decreased cell proliferation and induced apoptosis in oral squamous cell carcinoma tumours.^[108]

Furthermore, as various studies have determined that aromatic-substituted c-DIMs display anti-proliferative effects towards cancer cell lines, Tocco *et al* decided to carry out preliminary research into the activity of alkyl substituted c-DIMs against hepatocarcinoma, the fifth most common type of primary liver cancer. Using the rat hepatoma cell line, FaO, the c-DIM (**23**), shown in Figure 15, demonstrated a 55% reduction in cell viability at 100 μ M, which was four-fold more potent than I3C.^[109]

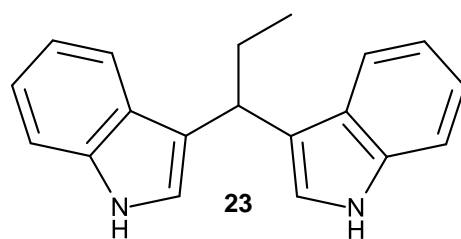
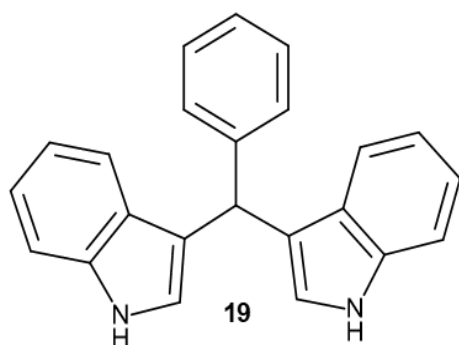


Figure 15 – Alkyl substituted c-DIM (**23**) tested against the FaO hepatoma cell line by Tocco *et al*.^[109]

1.4.4 - Physiochemical properties of c-substituted 3,3'-diindolymethane derivatives

Nearly 40% of new pharmaceutical agents are associated with poor oral bioavailability.^[110] A way of predicting whether orally administered drugs will have poor absorption and bioavailability, is by applying the Lipinski rule of five (Figure 16), a method well known by medicinal chemists.^[111]



- . Molecular weight less than 500 Da ✓
- . Log P value less than 5 ✗
- . Less than 5-bond donors (the sum of NH and OH groups) ✓
- . Less than 10 H-bond acceptors (the sum of N and O) ✓

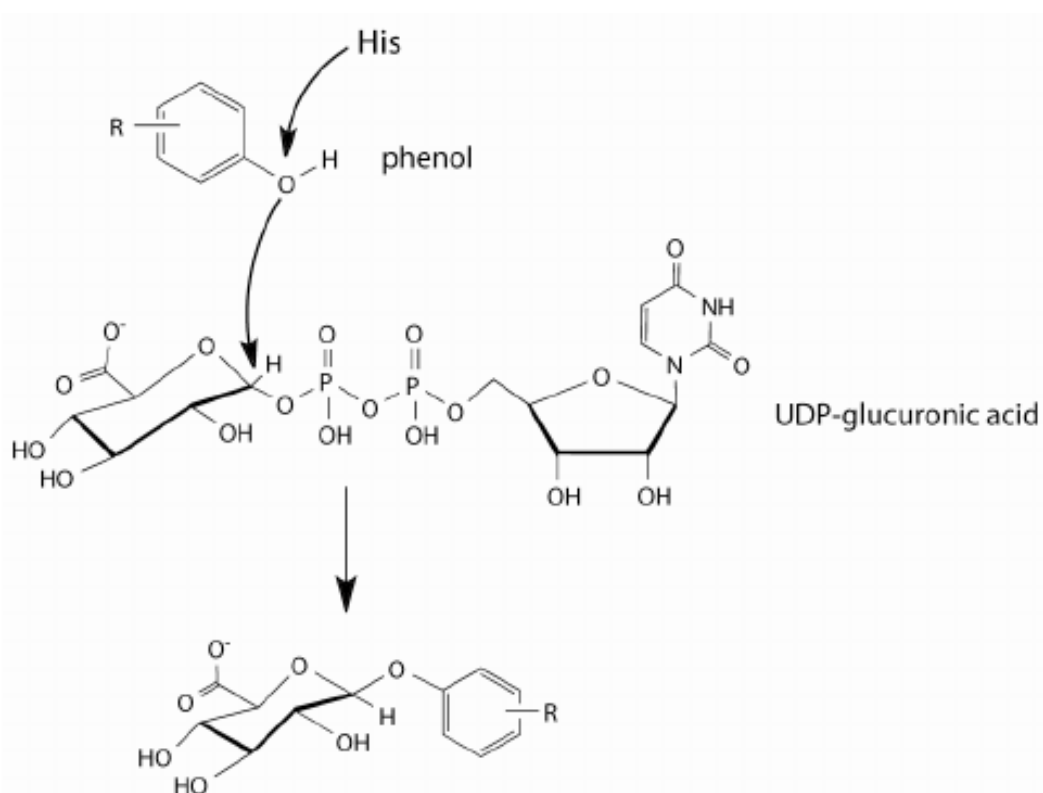
Figure 16 - Applying Lipinski rule of five to DIM-c-Ph (**19**), ✓ indicates rule applies to compound **19**, whereas, ✗ indicates rule does not apply to compound **19**.^[111]

By applying this rule to the basic aromatic substituted c-DIM, **19** (Figure 16), we would expect c-DIMs to have poor bioavailability, as the Log P value of DIM-c-Ph is thought to be around 5.40.^[112] However, it is worth noting, the Lipinski rule of five is only applicable to compounds that are not substrates for active transports. Additionally, the violation of one rule, does not essentially result in poor absorption and bioavailability. The probability of poor bioavailability increases with number of rules broken and to the magnitude which they are exceeded.^[111]

The physiochemical properties of substituted c-DIMs are not seemingly widely documented, however, it is known that DIM has poor oral bioavailability, as a result of its high lipophilicity/low solubility. A study administering DIM to rats via intraperitoneal injection, found DIM induced CYP-450 (cytochrome P450) to a much higher extent than in rats that had DIM administered orally. This is suggestive of poor drug absorption through the gastrointestinal tract.^[113]

Interestingly, Safe *et al* carried out investigative work into the neuroprotective efficacy of para-phenyl substituted DIM's (**17**, **18** and DIM-c-pPhCl) in a mouse model of Parkinson's disease.^[114] Although this study does not discuss the effects of c-DIMs against cancer, the study explores the pharmacokinetic behaviour of c-DIMs when administered orally and intravenously and states their concentration within brain tissues. This is of interest as one of the biggest challenges in the development of chemotherapeutic agents for the treatment of glioblastoma, is entry into the brain. Oral bioavailability was measured based on the compound's total exposure.

After oral administration, DIM-c-pPhOCH₃ and DIM-c-pPhCl exhibited the highest oral bioavailability (38% and 42% respectively). However, DIM-c-pPhOH only demonstrated 6% bioavailability, potentially, due to the presence of a phenol group, it undergoes glucuronide conjugation as shown in Scheme 4.^[114]



Scheme 4 – Scheme showing glucuronidation of a phenolic group via nucleophilic attack to carbon of UDP-glucuronic acid. Histidine assists hydrogen abstraction from phenolic group.^[115]

Although the highest concentrations of the c-DIMs were found in the intestines, followed by the liver, reasonable distribution to the brain was observed. Oral administration resulted in higher compound accumulation within brain tissue than

intravenous administration, substantially increasing the concentration of DIM-c-*p*PhOCH₃ from 272 ng/mL to 1173 ng/mL. DIM-c-*p*PhOH showed the lowest concentration in brain tissue (31.2 ng/mL) with DIM-c-*p*PhOCH₃ being the highest (1173 ng/mL).^[114]

This investigation demonstrates that although the solubility of c-DIM compounds is thought to be poor as a result of its high log P value (approximately 5.40), some does manage to enter the brain in *in vivo* studies using rats.^{[112][114]} However, it is worth mentioning that results observed from using rats cannot be generalised to humans, thus, ideally, further research should be conducted into the physiochemical properties of c-DIMs *in vivo*, to identify how they would behave within the body. It is also important that the development of drug delivery methods for the treatment of glioblastoma are carried out, to identify effective ways to deliver therapeutic agents to tumour sites within the brain. For example, Safe *et al*, carried out pharmacokinetic studies into the permeability and oral bioavailability of two c-DIM compounds (DIM-c-*p*PhCN and DIM-c-*p*PhOCH₃, **17**). In previous research these c-DIMs had demonstrated significant anti-cancer effects towards several breast cancer cell lines (IC₅₀ values in the range of 10-20 µM across the varying cell lines).^[116] The oral bioavailability of these compounds was less than 20%, and permeability studies suggested the permeability of these compounds is also poor.^[116] To tackle this issue, the research team developed c-DIM nano structured lipid carrier (NLC's) based formulations. Using the NLC formulation approach, the bioavailability of the c-DIMs increased by ten-fold, enabling the dosage to be reduced by almost a third. Pharmacokinetic studies were also carried out in dogs, whereby the oral bioavailability of DIM-c-*p*PhCN increased from 27% (free drug) to 80% (NCL formulation). The reason behind this increase in drug oral bioavailability when using NLC formulations, is because there is an increased solubility in nanoparticle form. Also, nanoparticles have increased absorption via lymphatic and other alternative gastrointestinal uptake mechanisms.^[116] This study shows that despite the poor oral bioavailability of the c-DIMs investigated, methods exist to improve the bioavailability and permeability, indicative that this class of compounds can still be employed in a clinical setting.

1.5 - Conclusion

The research discussed in this section provides clear evidence of the anti-cancer effects of DIM and c-DIMs against several cancer types and tumours including pancreatic, bladder, colon and breast, via various cellular mechanisms. On the contrary, the effect of DIM and c-DIMs when tested against brain tumours and specifically to this project, glioblastoma, is currently unknown. Thus, it seems, therefore necessary to carry out an investigation into the potential anti-cancer effects of DIM, and its methylene-substituted derivatives towards glioblastoma cells.

1.6 – Project aims

The aim of this study is to carry out preliminary research into the potential anti-cancer activity of DIM and its symmetrical c-substituted derivatives (c-DIMs) towards glioblastoma.

1.6.1 – Specific aims

- Using DIM as the lead compound, synthesise a preliminary series of c-DIM analogues (series one)
- Measure the anti-cancer activity of I3C, DIM, and the compounds in series one, against the glioblastoma cell line U-87 MG, using the MTS cell viability assay.
- Analyse the data obtained from the cell viability assays, calculate IC_{50} values for the compounds tested in series one. Determine structure activity relationships from the preliminary analogues. Then, synthesise a second series of c-DIM analogues, derived from the preliminary series one.
- Measure the anti-glioblastoma activity of the second c-DIM series, again using the MTS assay to obtain IC_{50} values for each compound tested in series two
- Discuss the overall structure activity relationships between compounds synthesised in this project, and between compounds tested for anti-cancer activity against glioblastoma within the Snape research group.

CHAPTER TWO – SYNTHETIC METHODS FOR C-SUBSTITUTED 3,3'-DIINDOLYLMETHANES

2.1 – Introduction

The c-diindolylmethane (c-DIM) scaffold is a privileged structure, present in many natural and synthetic compounds.^[117] Streptindole (**25**, Figure 17) is derived from *Streptococcus faecium* IB 37 and is found in human waste products. Whilst, compounds such as vibrindole A, trisindoline (**24**), deoxytopsentin and arsindoline (**23**) are c-DIM structures found in marine bacteria (Figure 17).^[117] Over recent years the synthesis of c-DIMs has gained considerable attention owing to their variety of bioactive properties; anticancer, antifungal, anti-inflammatory, antibacterial and analgesic properties.^{[118][119]}

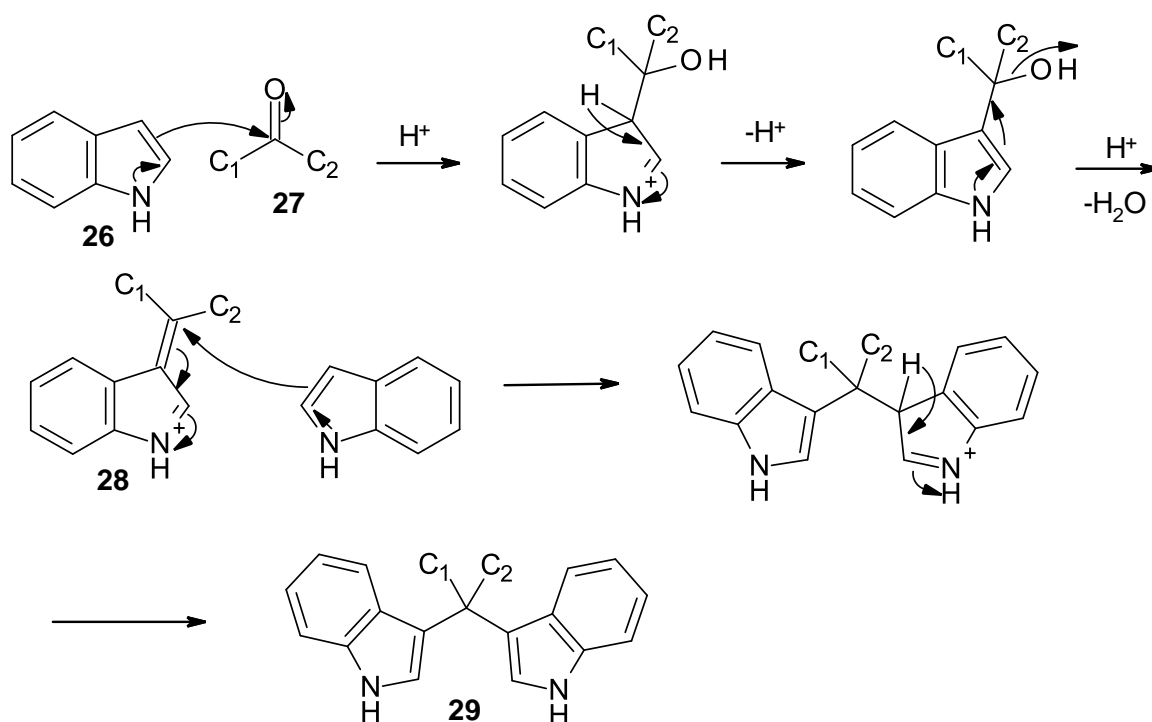


Figure 17 – Naturally occurring c-DIM derivatives.^[119]

This project will entail attempts to synthesise a number of symmetrical c-substituted diindolylmethane analogues, after which their cytotoxic activity towards glioblastoma cells will then be tested and IC₅₀ values obtained. This section will discuss the various synthetic methods that are available to synthesise c-DIMs.

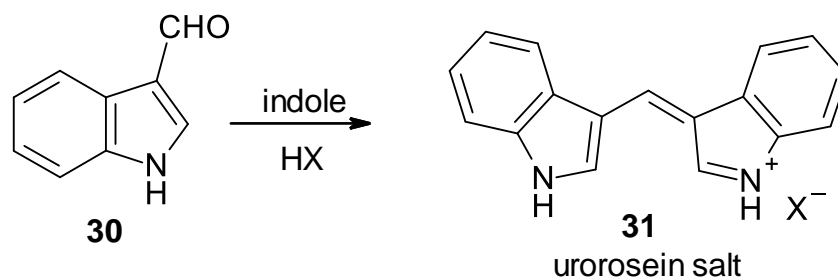
2.2 – c-substituted 3,3'-diindolylmethanes from indole and aldehydes or ketones

The most common and direct method to prepare c-substituted 3,3'-diindolylmethane derivatives was initially pioneered by Fischer in 1886, using an acid catalysed Friedel-Crafts reaction. An electrophilic substitution reaction of indole (**26**) with aliphatic or aromatic aldehydes and ketones (**27**) yields an intermediate azafulvenium salt (**28**), which undergoes a further addition reaction with a second molecule of indole to form the final c-DIM (**29**).^[120] The mechanism is shown in Scheme 5 below.



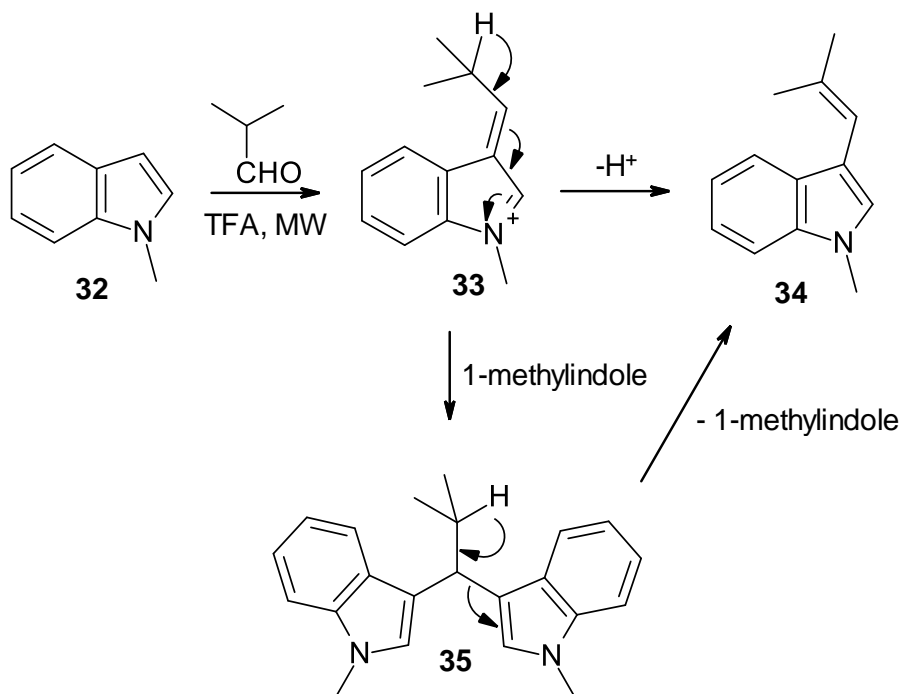
Scheme 5 – Mechanism for c-DIM (**29**) formation, from indole (**26**) reacting with a carbonyl compound.

The following reactions follow the same mechanism, confirming the intermediate azafulvenium salt formed in the production of c-DIMs. For example, the intermediate formed during a reaction between 3-formylindole (**30**) and indole (**26**) in the presence of HClO₄ or HCl, was isolated and identified as the formation of urorosein salt (**31**, Scheme 6).^[121]



Scheme 6 - Reaction scheme showing the intermediate (**31**) isolated from an acid catalysed reaction between 3-formylindole (**30**) and indole (**26**).^[121]

Similarly, when isobutylaldehyde reacts with *N*-methylindole (**32**) with TFA in toluene for 10, 20, 60 and 120 minutes, under microwave conditions, 3-vinylindole (**34**) and bisindolylalkane (**35**) were produced via the azafulvenium intermediate (**33**), in ratios of 80:20, 90:10, 96:4, and 100:0 respectively (Scheme 7).^[122]



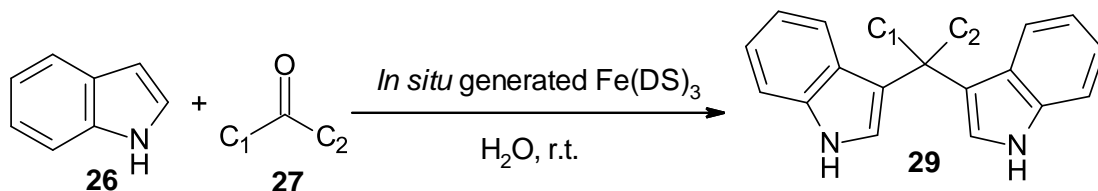
Scheme 7 - Reaction between isobutylaldehyde and *N*-methylindole (**32**).^[122]

The condensation of indoles with carbonyl compounds is typically catalysed by protic acids or Lewis acids. Protic acids usually employed include; H₂SO₄, TFA, HCl and oxalic acid, and popular Lewis acids used are AlCl₃, InCl₃ and BF₃.Et₂O.^{[123][124]} Research by Wang *et al* investigated the efficiency of a variety of Lewis acids in the reaction between benzaldehyde and indole, whereby zirconium tetrachloride prevailed in terms of reaction rate and yield (30 minutes, 96%).^[125] However, many Lewis acid catalysts are required in excess of stoichiometric amounts due to these acids being susceptible to decomposition or deactivation in the presence of nitrogen containing compounds. This can be avoided by using lithium perchlorate, although this can involve extensive reaction times and can be expensive. Additionally, Lewis catalysts can involve long reaction times and are usually not environmentally benign.^[126] As a result, many alternative catalysts have been developed.

Ionic liquids have gained interest as catalysts, due to their easy recyclability and negligible vapour pressure. Vadhat *et al* developed a protocol for the synthesis of c-DIMs at room temperature, using ethyl ammonium nitrate as a catalyst in water with yields of up to 95%.^[127] Other ionic liquids employed include [Et₃NH][HSO₄], [bnmim][HSO₄] and [Msim]Cl.^{[128][129][130]}

More recently, the employment of Lewis acid – surfactant-combined catalysts (LASC's) has become attractive for the synthesis of c-DIMs from indole and aldehydes or ketones in water, because being able to obtain high yields using water as a solvent means the use of hazardous organic solvents can be avoided. LASC's act as an acid catalyst and increase the solubility of indole in water by acting as surface-active agents, forming a stable colloidal dispersion system. Examples include dodecylsulfonic acid (DSA) and dodecylbenzenesulfonic acid (DBSA).^[131]

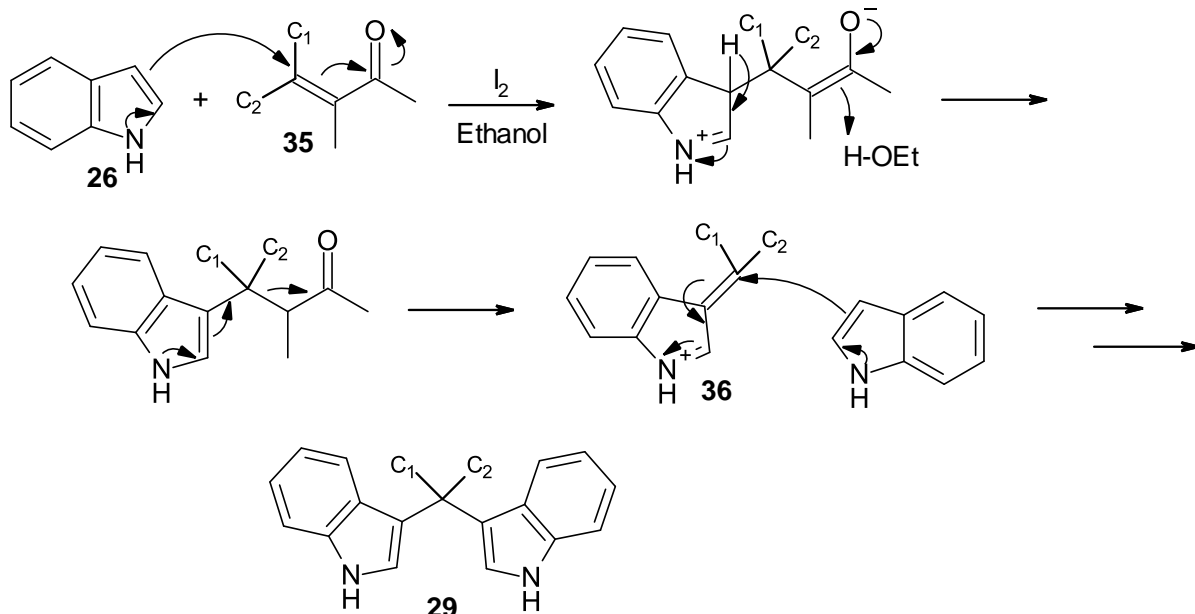
Veisi *et al* reports the use of *in situ* generated iron(III) dodecyl sulfate ($\text{Fe}(\text{DS})_3$), as an efficient LASC for the synthesis of c-DIMs (**29**) from indole (**26**) and aldehydes or ketones (**27**) in water (Scheme 8), yields of 85-95% were obtained.^[132]



Scheme 8 – Synthesis of c-DIMs in water using an *in situ* generated iron(III) dodecyl sulfate LASC.^[132]

Numerous zeolites have been reported to efficiently promote the synthesis of c-DIMs from indoles and aldehydes.^[133] Karthik *et al* investigated the efficiency of zeolites HY, H β and H-ZSM-5 for the synthesis of vibrindole A. All zeolites demonstrated excellent catalytic activity in the order HY>H β >H-ZSM-5, which is in accord with the acid site density of the zeolite. The catalysts could be used up to five times without loss of activity with yields of up to 88%.^[134] Although eco-friendly, zeolite catalysts can often require high activation temperatures.

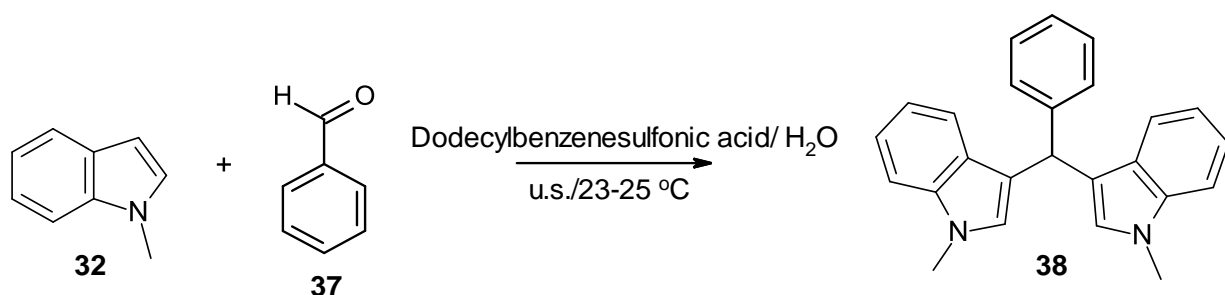
Research by Malik *et al* identified that iodine catalysed synthesis of c-DIMs from indole (**26**) and unsaturated α,β -ketones (**35**) in ethanol, produced yields of 52-63% over 4 hours. The c-DIMs (**29**) were produced via the formation of an azafulvenium salt (**36**); the reaction mechanism can be seen in Scheme 9.^[135]



Scheme 9 – Synthesis of c-DIMs from indole (**26**) and an α,β -unsaturated ketone (**35**).^[135]

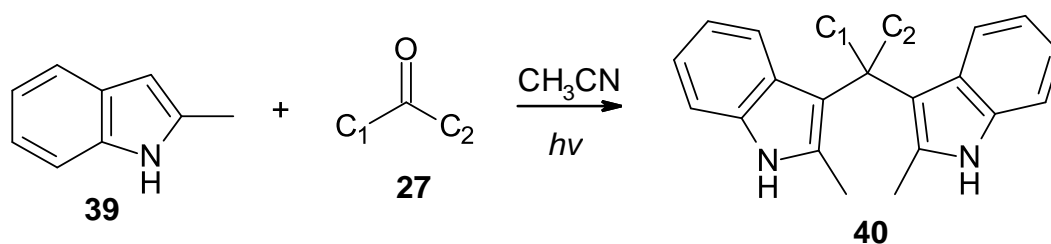
Zahran *et al* present an efficient synthesis of 2-substituted c-DIM analogues using glacial acetic acid as a catalyst under microwave irradiation.^[136] The results show excellent reaction times between 1-10 minutes and moderately good yields (56-96%), shorter reaction times and higher yields were observed for the reaction of indole with aromatic aldehydes. However, the use of aliphatic aldehydes resulted in longer reaction times and lower yields. The study also states that heating by microwave irradiation produced much higher yields than conventional heating.^[136] Further research by Das demonstrates the synthesis of c-DIM derivatives by reaction of indole with aldehydes and ketones, using $[(n\text{-propyl})_2\text{NH}_2][\text{HSO}_4]$ ionic liquid catalyst and microwave irradiation. c-DIMs were produced in extremely high yields (85-99%) in under 6 minutes.^[137]

Furthermore, numerous syntheses involving ultrasound irradiation in the production of c-DIMs have been reported. Joshi *et al*/state the synthesis of c-DIM analogues from indole and aromatic aldehydes in water, using 1-hexenesulfonic acid sodium salt to catalyse the reaction. The reaction mixture underwent ultra sonic waves for 45 minutes and produced good yields of 82-94%.^[138] Similarly, Li *et al*/reports the ultrasound assisted synthesis of *N, N'*-dimethyl c-DIM derivatives (**38**) by reaction of *N*-methylindole (**32**) with benzaldehyde (**37**) in water, dodecylbenzenesulfonic acid was employed as a catalyst, and the reaction mixture was put under ultrasound irradiation at 23-25 °C (Scheme 10).^[139]



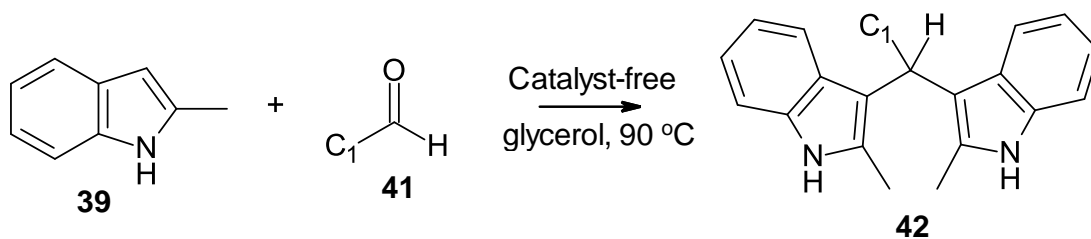
Scheme 10 – Ultrasound assisted synthesis of *N*-methylindole (**32**) and benzaldehyde (**37**) to yield *N, N'*-dimethyl c-DIM (**38**).^[139]

In addition to microwave and ultrasound irradiation, the photochemical synthesis of DIM derivatives has been reported. D’Azuria synthesised 2-substituted c-DIM analogues (**40**) by reaction of indole or 2-methylindole (**39**) with aldehydes or ketones (**27**) in acetonitrile (see Scheme 11). Yields of 47-52% were observed.^[140]



Scheme 11 – Photoirradiation c-DIM synthesis.^[140]

It is also worth noting, the formation of c-DIMs in the absence of catalyst in glycerol at 90 °C also has been observed. He *et al*/investigated the use of glycerol in the electrophilic activation of aldehydes. Yields as high as 98% were obtained for aromatic substituted c-DIMs, featuring methyl substitution at position-2 of the indole rings (Scheme 12).^[141]



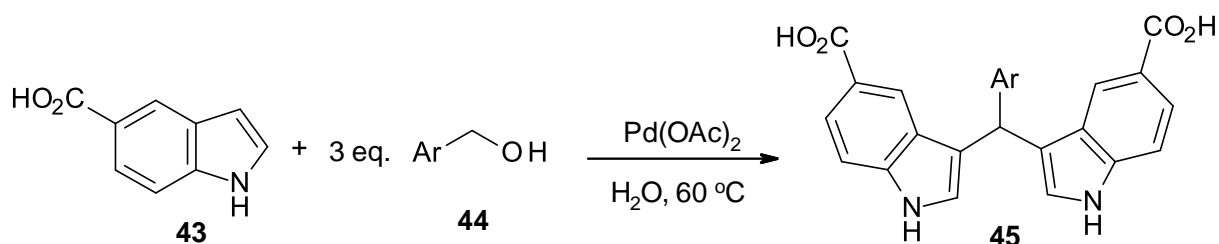
Scheme 12 – Preparation of 2,2'-dimethyl c-DIMs (**42**) from 2-methylindole (**39**) and various aldehydes (**41**), using glycerol as a reaction medium.^[141]

2.3 – c-DIMs from indoles with alcohols, amines and related compounds

Although these methods are less frequently employed, the synthesis of c-DIMs has been achieved without the use of aldehydes or ketones. This section will discuss alternative pathways towards the production of symmetrical c-DIM derivatives.

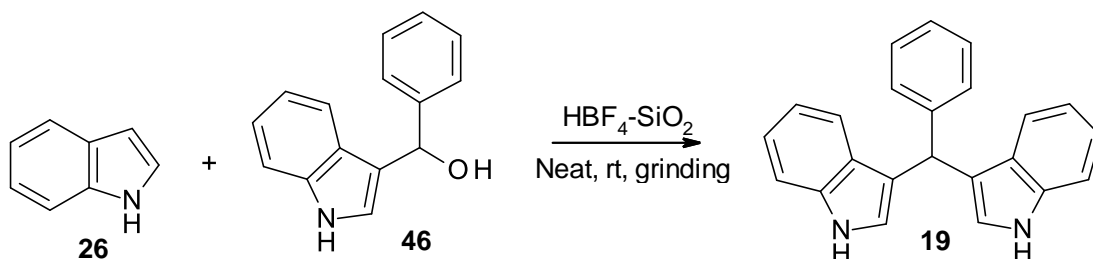
2.3.1 – c-DIMs from indoles and alcohols

Hikawa *et al* has developed a unique method of c-DIM synthesis by the reaction of indole-5-carboxylic acid (**43**) with benzyl alcohols (**44**) in the presence of a palladium catalyst ($\text{Pd}(\text{OAc})_2$) in water (Scheme 13).^[142] The study states that the reaction proceeds as water protonates the hydroxyl group of the benzyl alcohol which leads to the formation of a (η^3 -benzyl)palladium intermediate, which then undergoes transformation reactions to produce 5-carboxylic acid c-DIMs (**45**) in good yields (63-93%).^[142]



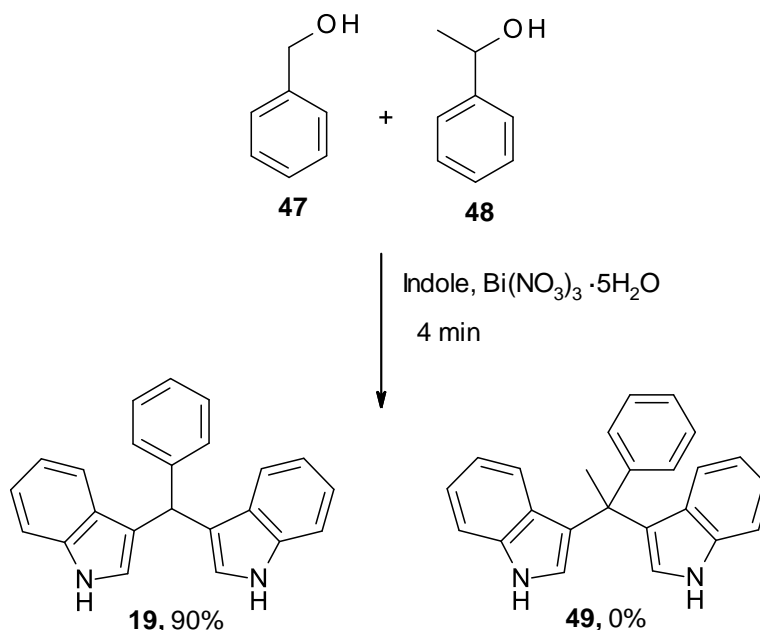
Scheme 13 – Synthesis of 5-carboxylic acid c-DIMs (**45**) via indole-5-carboxylic acids (**43**) with benzyl alcohols (**44**) in water.^[142]

Research by Bandgar *et al* synthesised a library of c-DIM analogues by the reaction of indole (**26**) with 1H-indole-3-yl-(phenyl)methanol (**29**) and its derivatives, under solvent free conditions at room temperature and catalysed by $\text{HBF}_4\text{-SiO}_2$ (Scheme 14). Although the reaction was successful, producing good yields (75-90%) and short reaction times (10 minutes), the same research group report c-DIM synthesis involving the condensation of indoles with aldehydes which produced higher yields (85-94%) and the same reaction time.^[143]



Scheme 14 – Preparation of DIM-c-Ph (**19**) using 1H-indole-3-yl-(phenyl)methanol (**46**) and indole (**26**).^[143]

The one-pot conversion of primary alcohols (**47**) to their corresponding c-DIM (**19**), has been carried out by Khosropour *et al*, under solvent-free conditions and promoted by $\text{Bi}(\text{NO}_3)_3 \cdot 5\text{H}_2\text{O}$ (Scheme 15). The reactions proceeded in under 6 minutes and demonstrated excellent yields of up to 95%. Additionally, when secondary alcohols (**48**) were added to the reaction mixture, none of these alcohols produced their corresponding c-DIMs (**49**), suggesting the reaction is chemoselective towards primary alcohols.^[144]



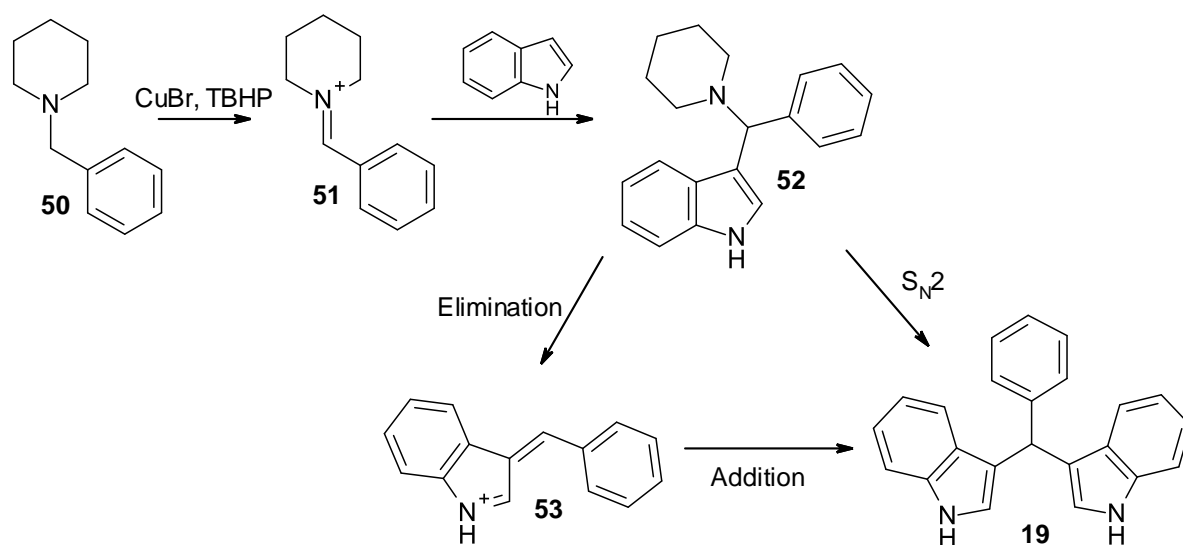
Scheme 15 – Reaction scheme showing the chemoselective reaction of primary (**47**) and secondary alcohols (**48**) with indole (**26**).^[144]

Similarly, Nikoofar also reports the one-pot synthesis of c-DIMs from primary alcohols. The reaction was carried out in an undivided electrochemical cell, using acetonitrile as a solvent and LiClO_4 as a catalyst. The alcohol is oxidised at the anode, yielding the corresponding aldehyde, for example, benzyl alcohol is

oxidised to benzaldehyde. Upon addition of indole to the reaction mixture, the indole anion is formed via cathodic electron absorbance, leading to nucleophilic attack of indole to the aldehyde to yield the desired c-DIM.^[145]

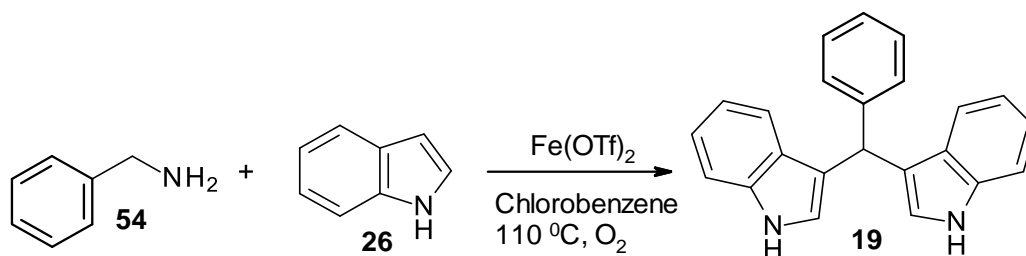
2.3.2 – c-DIMs from indoles and amines, imines or related derivatives

A variety of c-substituted diindolylmethane derivatives were prepared by Yang, by the CuBr catalysed cleavage of C-N bonds in the oxidative cross-dehydrogenative-coupling of various *N*-benzylamines (**50**) with indoles, in the presence of *tert*-butyl hydroperoxide. *N*-Benzyl pyrrolidine produced the highest yields (61-80%), its derivatives; *N*-(3-methylbenzyl) pyrrolidine and *N*-(4-chlorobenzyl) pyrrolidine produced moderately good yields – possibly due to steric hinderance. However, when *N*-ethyl pyrrolidine was employed, no DIM product was observed. The exact mechanism for this reaction is unknown, although a plausible pathway can be seen in Scheme 16. The initial step is thought to be an iminium ion (**51**) being formed through the development of a copper complex. Secondly, a Friedel-Crafts type reaction yields the intermediate (**52**), then two possibilities for the transformation of **52** to **19** exist; either a substitution (S_N2) reaction or an elimination reaction followed by a Michael addition. Intermediates **52** and **53** were both present in the reaction mixture after the reaction, suggesting the latter is more probable.^[146]



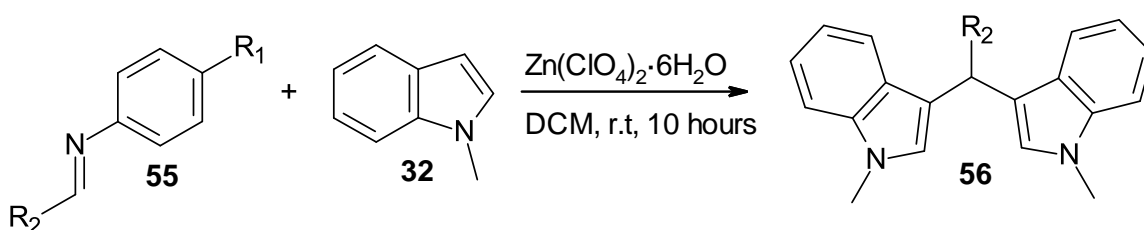
Scheme 16 – A plausible pathway for the synthesis of c-DIM **19** via *N*-benzylamines (**50**) and indole (**26**).^[146]

Similar work was carried out by Gopalaiah, his team synthesised 27 different c-DIM analogues via the oxidative coupling of benzylamines with indole.^[147] The reaction was promoted by iron(II) triflate in chlorobenzene, in an atmosphere of molecular oxygen at 110 °C. Scheme 17 shows the reaction between benzylamine (**54**) and indole (**26**) to produce compound **19**. Yields of up to 93% were obtained, the electronic substituents of the aromatic benzylamines did not significantly reduce the yield, except for a trifluoromethyl group at the meta position of the benzylamine. Secondary benzylamines worked efficiently as substrates with yields of 74%, whereas aliphatic amines, for example octylamine and hexylamine, produced significantly lesser yields; 55 and 48% respectively.^[147]



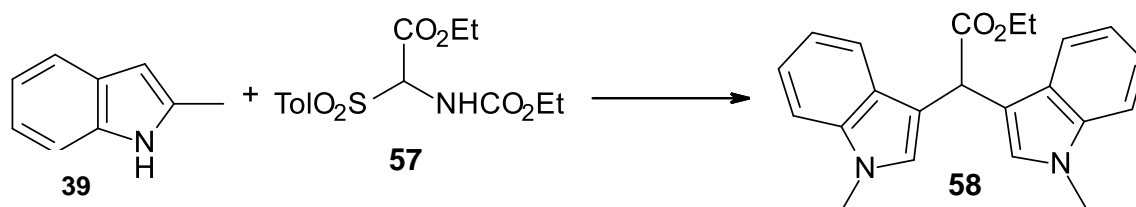
Scheme 17– Indole (**26**) reacting with benzylamine (**54**) to produce c-DIM (**19**).^[147]

Imines are much less reactive towards nucleophiles in comparison to ketones and aldehydes, however there are reports of imines reacting with *N*-indoles to produce c-DIMs in decent yields. For example, Xie *et al* have developed an efficient procedure for the synthesis of c-DIMs (Scheme 18) by reacting various imine derivatives (**55**) with *N*-methylindole (**32**), using a dithiocarbohydrazone Schiff base (Zn(ClO₄)₂·6H₂O). Initially, R² of the imine were aromatic substituents and gave high yields of 86-99%, regardless of whether R₁ was an electron-donating or electron-withdrawing group. However, the use of hydroxyl imines produced considerably lower yields (63-73%).^[148]



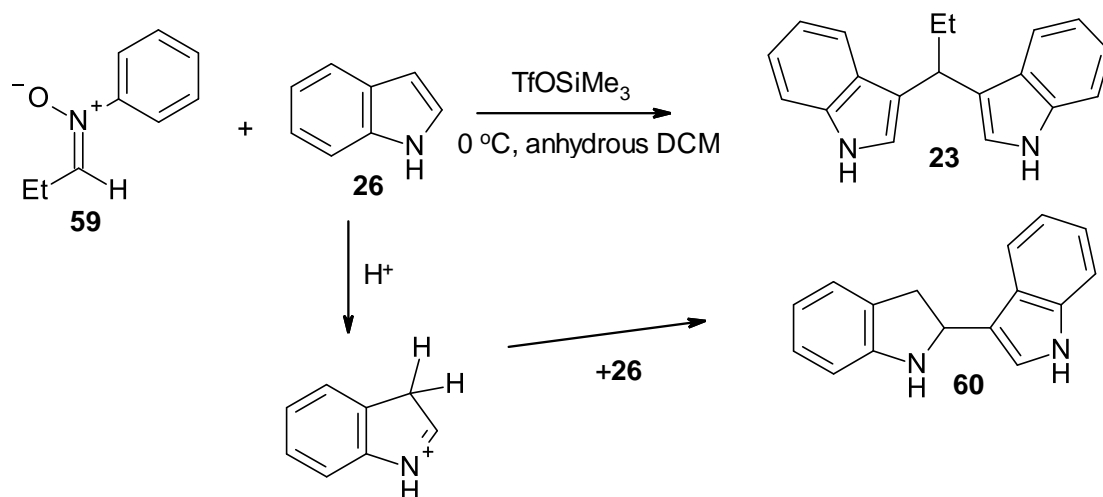
Scheme 18 – Friedel crafts alkylation of imine (**55**) with *N*-methylindole (**32**).^[148]

Typically, nucleophilic substitution of amines, alcohols and chemically similar compounds with indole, results in the alkylation of indoles. However, when Ballini *et al* attempted the alkylation of 2-methylindole (**39**) using α -amido sulfones (**57**), in the absence of solvent and catalysed by K-10 montmorillonite clay, c-DIMs (**58**) were unexpectedly produced in 58% yield (Scheme 19).^[149]



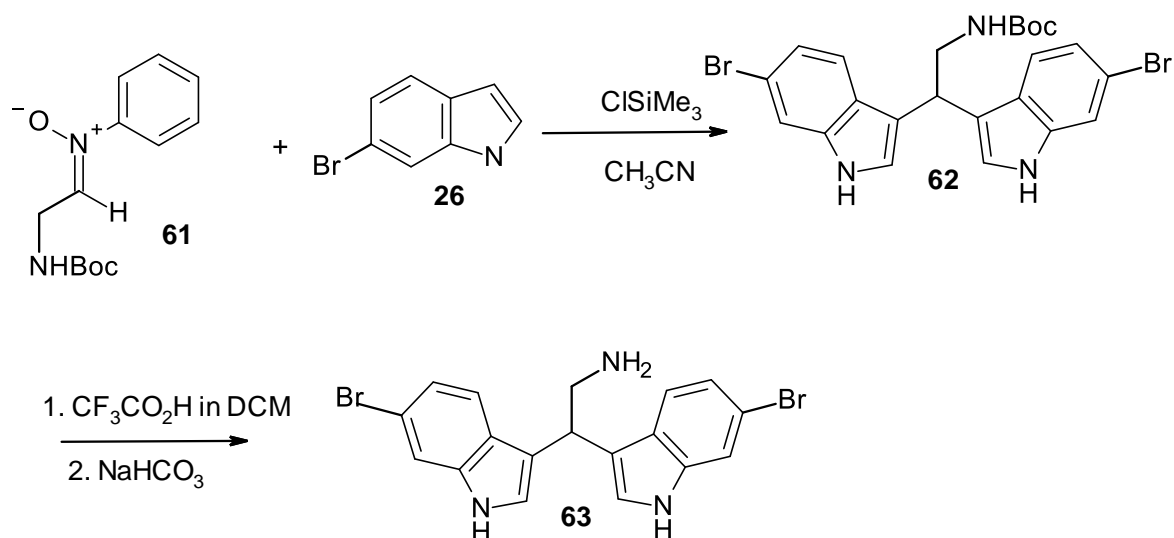
Scheme 19 – Synthesis of 2-substituted c-DIMs (**58**) from 2-methylindole (**39**) and α -amido sulfones (**57**).^[149]

In addition to amines and imines, nitrones can also react with indoles to form c-DIMs. Vallee *et al* synthesised symmetrical c-DIM derivatives by reacting the benzylnitronone of propanal (**59**) with indole (**26**) at room temperature in the presence of TfOSiMe_3 , in anhydrous DCM for 2 hours (Scheme 20).^[150] Once the reaction had reached completion, 3-[1-(1H-indol-3-yl)propyl]-1H-indole (**23**) was the major product formed with a yield of 70%, However, some indole dimer was also formed (**60**, 5%). This by-product is the result of the triflic acid formed from the catalyst protonating indole which then attacks another indole molecule. Although it was a minor product, the similarity in R_f value made it inseparable from the major product by flash column chromatography (FCC). To counter this problem, TfOSiMe_3 was substituted for the use of ClSiMe_3 whereby the desired c-DIM (**23**) was produced in 85% yield and the indole by-product was not detected.^[150]



Scheme 20 – Reaction between the benzyl nitronal of propanal (59) and indole (26) to produce c-DIM (23) and by-product (60).^[150]

Applying the same strategy, the same research group synthesised a naturally occurring c-DIM analogue (63), which is derived from the marine sponge *Orina Sp.* with a yield of 85%. The reaction scheme they used can be seen below. (Scheme 21).^[151]



Scheme 21 – Utilization of nitronal (61) with indole (26) to develop c-DIM (62), derived from marine sponge *Orina Sp.*^[151]

2.4 – Conclusion

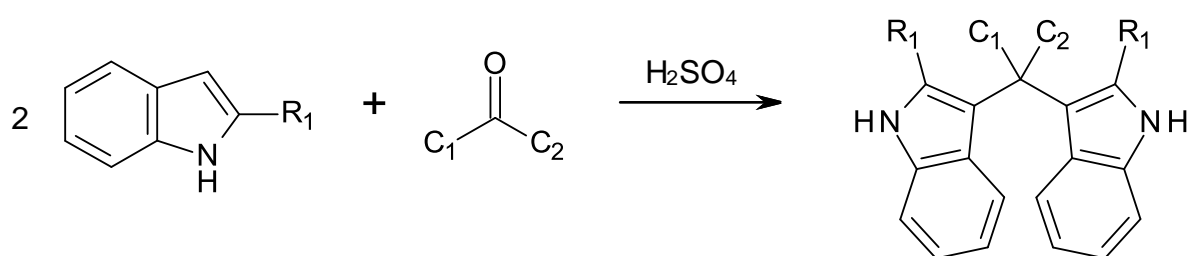
Such an extensive range of synthetic methods are available for the preparation of c-DIMs and their derivatives. However, this project will use the condensation of indoles with aldehydes or ketones to synthesise a library of c-DIM analogues, as it is an extremely direct and well understood method, which can be carried out in the absence of non-green organic solvents. It also involves the use of many readily available and inexpensive reagents and catalysts. The reaction between indoles with aldehydes and ketones can be employed to develop a wide variety of c-DIMs to be tested against glioblastoma cell lines.

CHAPTER THREE – RESULTS AND DISCUSSION

3.1 – Synthetic results and discussion

3.1.1 - Compound synthesis

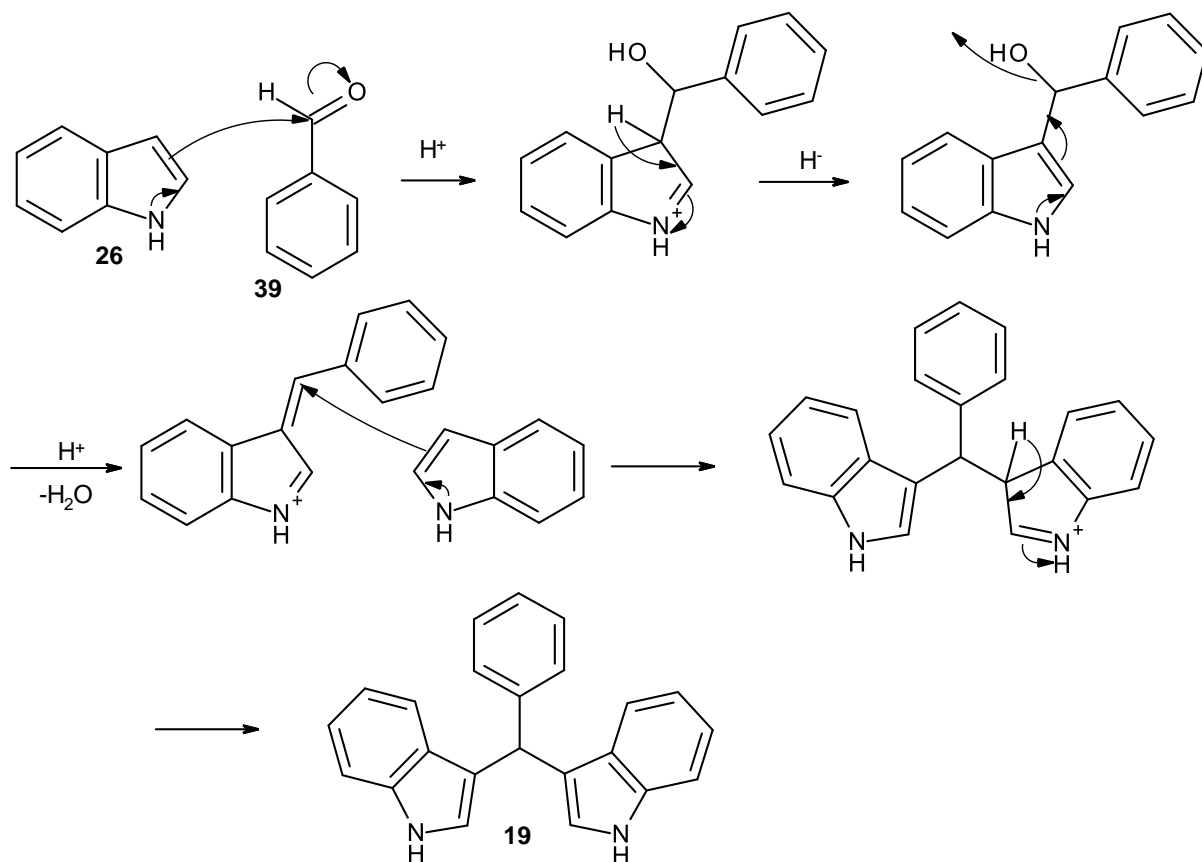
As previously mentioned in chapter two, there are many synthetic routes available to produce symmetrical c-DIM compounds. However, this project employed the electrophilic substitution of indoles with various aldehydes and ketones – a very direct and well understood method.^[120] The compounds shown in Scheme 22, were catalysed by concentrated sulfuric acid; the first 5 compounds (**19**, **17**, **64**, **65** and **20**) shown in Scheme 22 were carried out using water as a reaction medium, as the reactions proceeded well in water and produced good yields. Using water in replacement of an organic solvent offers advantages such as; safe handling, reduced expense and environmental compatibility. However, for the synthesis of compounds **66** and **67** the use of water was not possible. Water was not a suitable reaction medium for the synthesis of **66** and **67** due to the insolubility of the reagents 2-methylindole and 2-phenylindole in water. Therefore, reaction conditions were optimised.



Compound	C ₁	C ₂	R ₁	Yield (%)
19	Ph	H	H	88
17	PhpMeO	H	H	58
64	PhpNO ₂	H	H	73
65	Me	Me	H	38
20	PhpF	H	H	71
66	Ph	H	Me	65
67	Ph	H	Ph	72

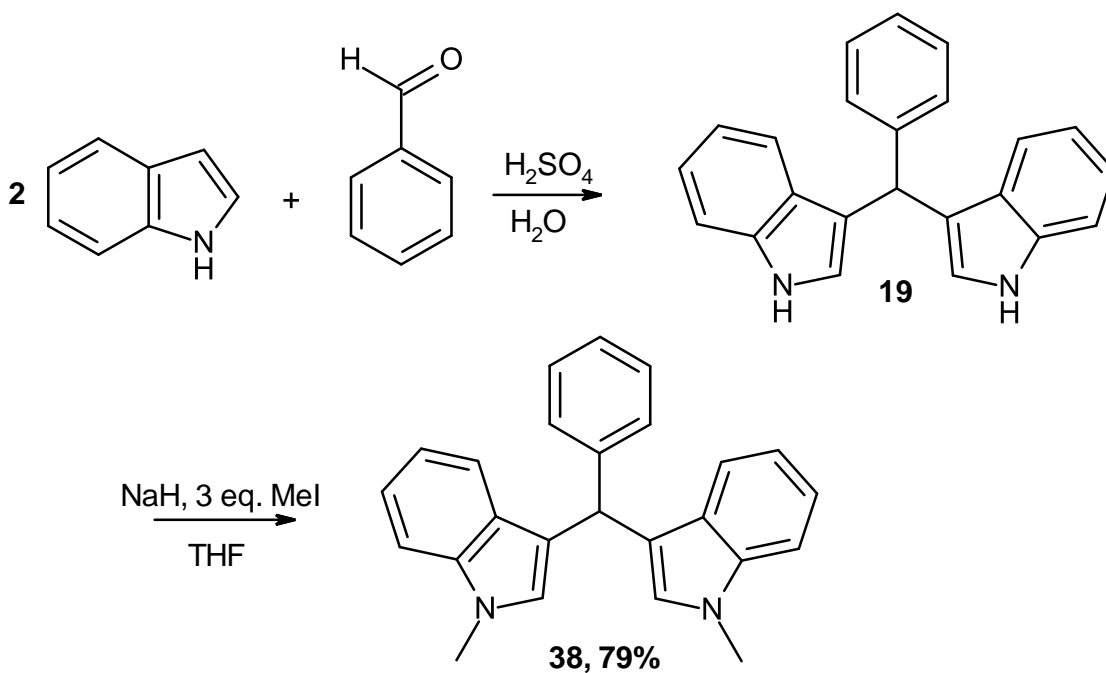
Scheme 22 - Reaction scheme for c-DIM compounds (**19**, **17**, **64**, **65** and **20**) and 2,2'-substituted c-DIM compounds synthesised (**66** and **67**), and yields.

Scheme 23 below, shows reaction mechanism employed for the formation of compound **19**, occurring by an acid catalysed Friedel-Crafts alkylation reaction between indole and benzaldehyde.



Scheme 23 – Reaction mechanism for the synthesis of compound **19** via the reaction of indole (**26**) and benzaldehyde (**39**).

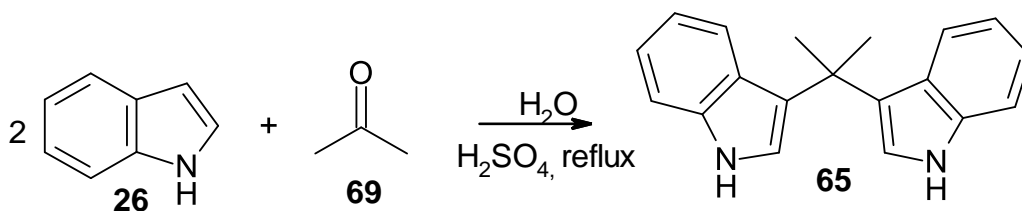
The reaction between indole (2 eq.) and benzaldehyde yielded compound **19** (Scheme 23). Compound **19** then underwent *N,N*-dimethylation in dried THF to produce compound **38**. Methyl iodide is a popular methylation reagent used in organic synthesis, as the iodide ion is an excellent leaving group, thus *N*-methylation reactions using methyl iodide often have high conversion rates. Also, the low boiling point of methyl iodide (42 °C), means that it can be removed from the reaction mixture with ease *in vacuo*. Likewise, NaH is also easily removed from the reaction, during the acidic 1 M aqueous HCl extraction, by being miscible with the aqueous phase. This reaction proceeded well and produced a decent yield of 79% (Scheme 24). The formation of this compound was identifiable by ¹H NMR by the loss of the N-H peak and the appearance of a CH₃ peak, integrating to 6 H at 3.70ppm.



Scheme 24 - Synthesis of compound **38** via *N,N'*-methylation of compound **19**.

3.1.2 - Attempted synthesis and optimisation of synthesis

3.1.2.1 - Optimisation of synthesis for 3-[1-(1H-Indol-3-yl)-1-methyl-ethyl]-1H-indole (Compound 65)



Scheme 25 - Attempted synthesis of 3-[1-(1H-indol-3-yl)-1-methyl-ethyl]-1H-indole (**65**).

To begin with, the reaction shown in Scheme 25 was carried out to synthesise **65**. However, after 3 days stirring no reaction was observed.

Next, the same reaction was carried out, however heat (50 °C) was applied to the reaction. Due to the low boiling point of acetone (**69**), an air cooled reflux condenser was used to prevent the evaporation of acetone whilst under heating. Still, no substantial product (**65**) was observed.

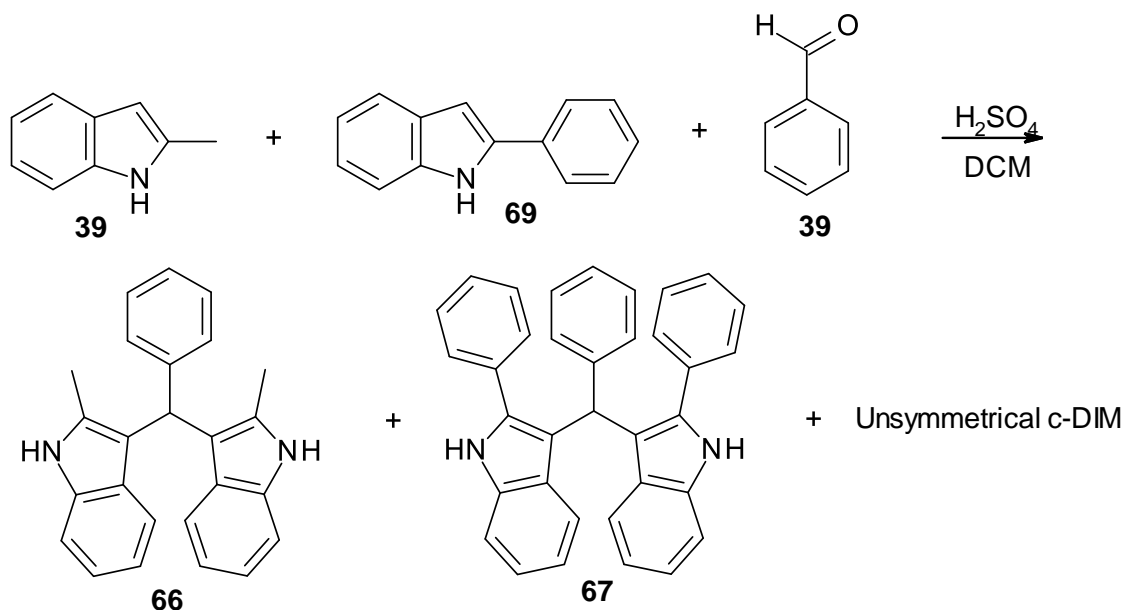
It was clear that heating the reaction mixture made a slight improvement on the reaction, however the lack of product formed prompted the use of an excess of acetone (2 mL), as it would not have a detrimental effect on the reaction. The heat of the reaction mixture was increased to 60 °C. After 4 days a reasonable amount of product was visible by TLC and the reaction was stopped.

Purification was an issue with this compound. Initially, it seemed only two products were present by TLC, however when separated by flash column chromatography (40:60 ethyl acetate: petroleum ether) the ¹H NMR showed a mixture of products. After experimenting with various TLC solvent systems, a TLC was ran in 8:92 ethyl acetate: toluene and was stained using *p*-anisaldehyde. When gently heating the TLC after staining, two different coloured products (pink and purple) were visible within what initially seemed to be one product. Flash column chromatography was then carried out again using 8:92 ethyl acetate: toluene to yield compound **65**.

The use of a ketone in this reaction, as opposed to an aldehyde made it more difficult to obtain the desired c-DIM and resulted in a lower yield. Firstly, due to steric effects. Ketones have two groups attached to the carbonyl carbon,

therefore, steric hinderance impedes nucleophilic attack of the carbonyl carbon. Secondly, as a result of electronic effects. As the carbonyl group in ketones is attached to two groups, the partial positive charge of the carbonyl carbon is less than that of an aldehyde.

3.1.2.2 - Optimisation of synthesis for 2-Methyl-3-[(2-methyl-1H-indol-3-yl)-phenyl-methyl]-1H-indole (66) and 2-Phenyl-3-[phenyl-(2-phenyl-1H-indol-3-yl)methyl]-1H-indole (67)



Scheme 26 – Attempted synthesis of **66** and **67** in the same reaction. Due to solubility issues of the products, purification via flash column chromatography was not possible.

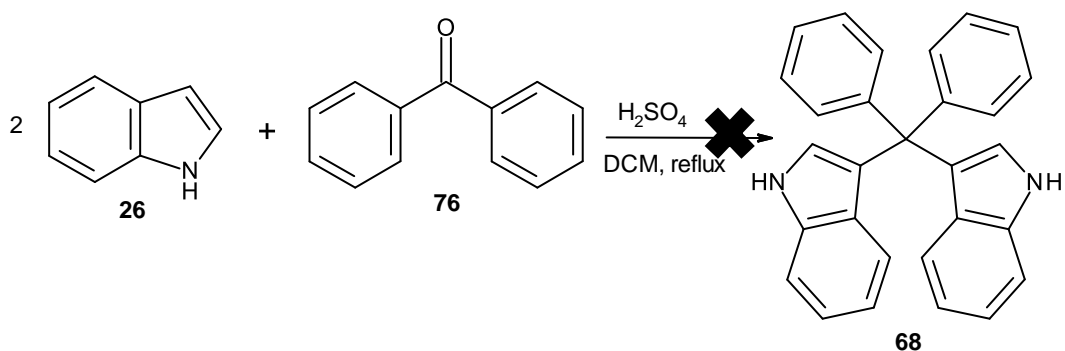
Originally, an attempt was made to synthesise both compounds **66** and **67** in the same reaction mixture, with the intention of purifying the products by flash column chromatography in order to obtain three different 2,2'-substituted c-DIMs. Due to the insolubility of 2-methylindole and 2-phenylindole in water no reaction was observed.

Then, the reaction solvent was changed to DCM as the 2-indole reagents were soluble in this, the reaction scheme can be seen in Scheme 26. During this reaction a solid precipitated out. The crude ^1H NMR showed the formation of a mixture of products. Due to the insolubility of the crude product in common solvents such as DCM, ethyl acetate, petroleum ether, diethyl ether, the product

was extremely difficult to purify by flash column chromatography. This issue of solubility also made it problematic to follow the reaction by TLC.

Therefore, for ease of purification, the reactions were carried out separately. Again, due to the insolubility of the products, they were not identifiable by TLC. However, the depletion of 2-methylindole and 2-phenylindole from the reaction mixtures were visible by TLC. The desired 2,2'-substituted c-DIMs precipitated out in the reaction mixture, the product was filtered and washed with 20:80 ethyl acetate: DCM to yield products **66** and **67**.

3.1.2.3 - Attempted synthesis of 3-[1H-Indol-3-yl(diphenyl)methyl]-1H-indole (**68**)



Scheme 27 - Attempted synthesis of 3-[1H-indol-3-yl(diphenyl)methyl]-1H-indole (**68**)

The reaction scheme above was attempted, however no reaction was observed. Similar to compound **65**, due to the steric hinderance of two benzene rings around the carbonyl group of benzophenone, this ketone was not easily susceptible to nucleophilic attack. Additionally, the partial positive charge of the carbon is reduced by the benzene groups attached to the carbonyl carbon, therefore the desired product was not formed during this reaction.

The same reaction was carried out in using amberlyst-15 as a catalyst, however, thought to be due to the same reasons of steric and electronic effects, no product was formed.

3.1.3 - Challenges encountered in compound synthesis

Compounds **64**, **66** and **67** presented solubility issues with regards to carrying out NMR analysis. DMSO was the only NMR solvent found that the compounds would dissolve in to a sufficient extent. For example, the high molecular weight of compound **67** (474 Da), meant a high concentration sample was required for ^{13}C and DEPT-135 NMR analysis.

When analysing the ^{13}C NMR and DEPT-135 spectra, it became apparent that the peak of the C-H bond of the bridge joining the indole rings, was masked by the broad DMSO solvent septet, however, the C-H peak was clearly visible in the ^1H NMR spectrum. Analysing the ^{13}C and DEPT-135 NMR of structurally similar compounds **19**, **17**, and **20**, which were soluble in deuterated chloroform, the CH bridge peaks are visible at 40.2, 39.3 and 38.9 ppm respectively. Figure **18** shows that in the ^{13}C NMR of compound **64**, the DMSO solvent peak covers the range you would expect the CH bridge peak to lie.

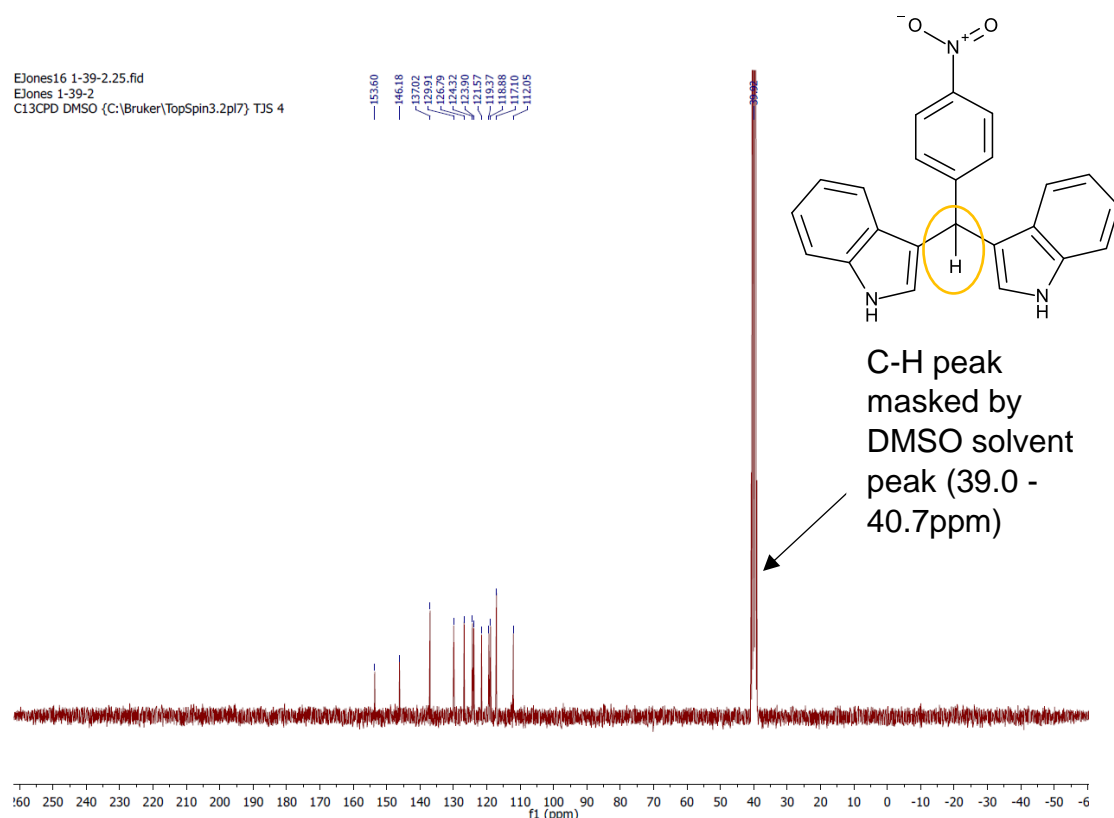


Figure 18 - ^{13}C NMR of compound **64**. The CH peak of compound **64** is assumed to be hidden underneath the DMSO solvent peak.

To counter this issue, DEPT-90 NMR was run for compounds **64**, **66** and **67**. As DEPT-90 spectra only show CH peaks, DMSO was not visible, meanwhile, the desired CH peaks were. See Figure 19, for DEPT-90 NMR spectrum of compound **64**.

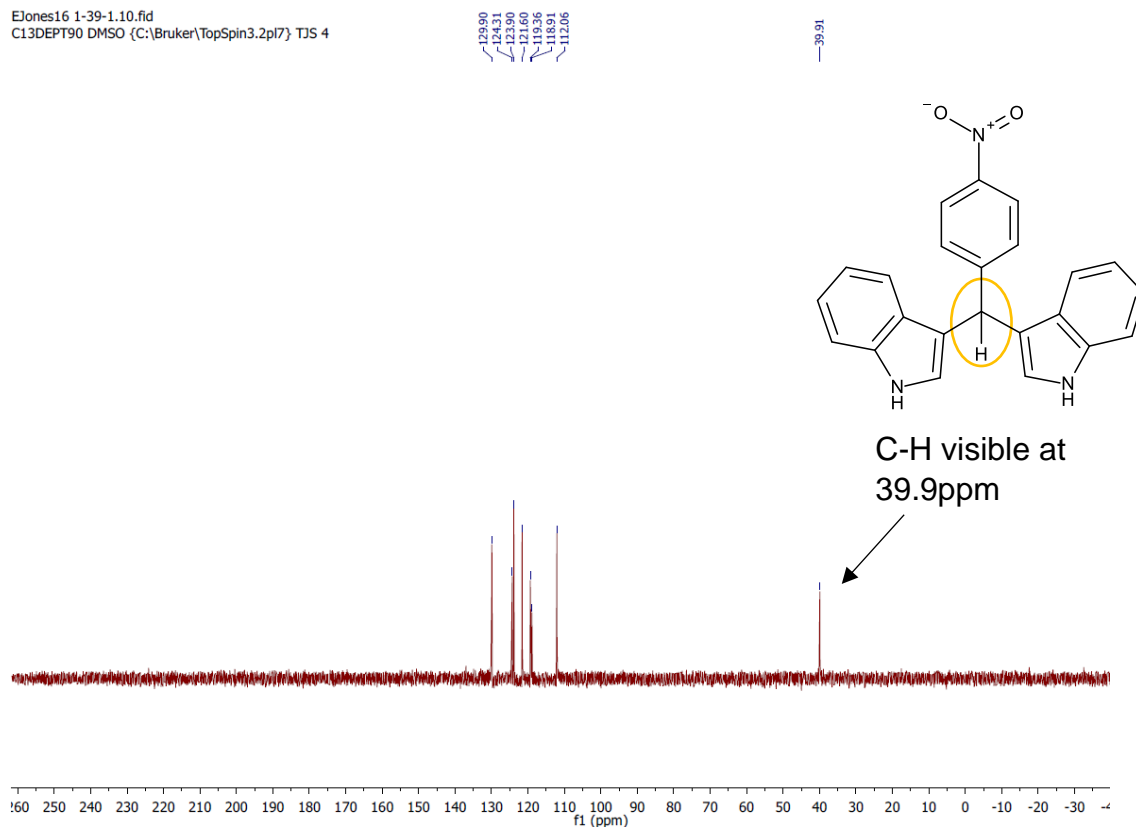


Figure 19 – DEPT-90 NMR of compound **64**, the CH peak was visible on a DEPT-90 NMR spectrum, as only CH peaks are seen.

3.2 - Cell viability results and discussion

3.2.1 - Materials

Ethanol, 96 well plates, 75 cm² angled neck tissue culture flasks, 15 mL and 50 mL centrifuge tubes, serological pipettes, PBS (phosphate buffered solution) tablets, foetal bovine serum were purchased from ThermoFisher Scientific. Sterile DMSO was purchased from Sigma-Aldrich. Eagles Minimum Essential Medium (EMEM), non-essential amino acids, trypsin and sodium pyruvate solution were purchased from Lonza. The U87-MG human glioblastoma cell line was originally from ECACC. MTS assay; CellTiter 96® Aqueous One Solution Cell Proliferation Assay was purchased from Promega Corporation.

A Matic AE2000 microscope was used for observing and counting cells. Absorbance was measured at 485 nm using a GENios pro plate reader with 4 seconds shaking.

3.2.2 - Cell culture methods

3.2.2.1 - Defrosting cells

Wearing gloves and a full face shield, a vial of cryopreserved U-87 MG cells were removed from -180 °C liquid nitrogen. Cells were stored in dry ice whilst being transported to the tissue culture laboratory. Cells were then held in a 37 °C water bath, carefully as to not submerge the vial under the water as this can encourage contamination. Once defrosted, the vial of cells were placed in the fume hood and carefully pipetted into a 75 cm³ flask. 10 mL of EMEM was then added and the contents of the flask was resuspended by gently pipetting up and down, to ensure the cells were dispersed in the media. Cells were then viewed under the microscope and incubated at 37 °C in a humidified atmosphere with 5% CO₂, until they had reached 75-85% confluence and passaging was required.

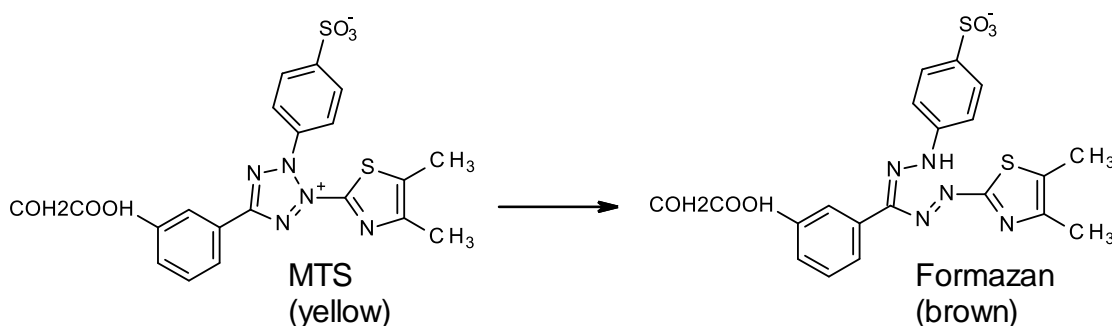
3.2.2.2 - Cell maintenance

U-87 MG cells were maintained in Eagles Minimum Essential Medium (EMEM-500 mL) supplemented with 10% foetal bovine serum (FBS-50 mL), L-glutamine (2 mM-5 mL), 1% non-essential amino acids (NEAA-5 mL) and sodium pyruvate (1 mM-5 mL) and incubated at 37 °C in a humidified atmosphere with 5% CO₂.

When an average of 75-85% confluence was reached, cells were washed with 5 mL PBS solution, which was then aspirated. 2 mL of 1x trypsin was added and cells were returned to the incubator to detach them from flask for 3-5 minutes. Cells were observed under the microscope to ensure they had detached and 2 mL of supplemented EMEM was added. Cells were transferred to a 15 mL centrifuge tube and centrifuged at 1000rpm for 5 minutes, subsequently the supernatant was removed. Cells were either resuspended in an appropriate media volume and passaged into suitable ratios. Or a single cell suspension was obtained, and cells were seeded into 96 well plates for experimental analysis.

3.2.2.3 - MTS cell viability assay

The protocol for the MTS assay, which is explained below, was provided by the manufacturer; Promega, and was followed extremely carefully.^[152] The MTS assay is a colorimetric technique based on the reduction of a tetrazolium dye by NAD(P)H-dependent dehydrogenase enzymes in mammalian cells. MTS is reduced to a formazan product (Scheme 28), causing a colour change (yellow to brown) which can be quantified by measuring absorbance at 485 nm, providing a measure of cell viability. The colour change to brown indicates a high quantity of living cells, whereas yellow means the majority of cells are dead (or non-viable).



Scheme 28 – Reduction of MTS to the formazan product.^[145]

Concentrations of 250 μ M, 100 μ M, 10 μ M and 1 μ M of I3C, DIM and the c-DIM compounds were prepared in aseptic conditions using sterile DMSO and media.

This was carried out by serial dilutions; the serial dilution scheme followed is shown in Figure 20. Firstly, a 200 mM stock solution one was made. From this, 50 μ L was taken and diluted with 450 μ L DMSO to create 20 mM stock solution

two. Then a 10,000 μM working solution was made by taking 250 μL of stock solution 2 and diluting it with 250 μL media. 12.5 μL of the working solution was taken and made up to 0.5 mL with media to create the 250 μM concentration. 5 μL of the working solution was taken and again made up to 0.5 mL with media to make the 100 μM concentration. From the 100 μM concentration 50 μL was taken and 450 μL media added to make the 10 μM concentration, this serial dilution was repeated twice to make the 1 μM and 0.1 μM concentrations.

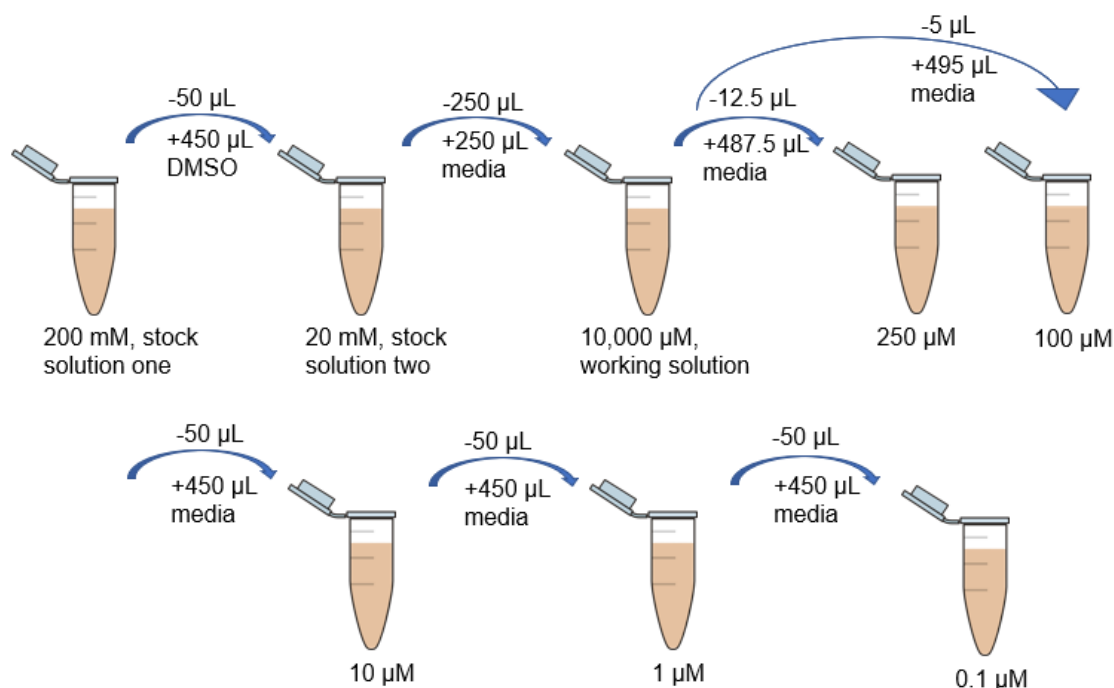


Figure 20 - Serial dilution scheme followed to prepare the 250 μM , 100 μM , 10 μM and 1 μM concentrations of I3C, DIM and the compounds synthesised.

Before cells could be seeded for experimental analysis, a cell count was performed. After the cells are centrifuged and a single cell suspension is created, 10 μL was removed and combined with 10 μL trypan blue. Trypan blue is a negatively charged chromophore with the inability to penetrate the cell membrane of live cells, therefore distinguishing between live and dead cells. The living cells in the solution of trypan blue were counted using a haemocytometer. The value of living cells obtained from the haemocytometer $\times 10^4$ equals the number of cells per mL of the cell suspension. This number is multiplied by 2, to correct for the dilution with trypan blue to give the total number of cells in the cell suspension.

To calculate what volume of the cell suspension was required to seed cells at 2000 per well, the total number of cells was divided by 2000 to give the value of

2000 cells per mL, dividing this value into 1000 then times by the number of wells provides the volume of cell suspension needed to seed 2000 cells per well. This volume was taken from the cell suspension and diluted to 10 mL with media. 100 μ L of the new stock solution was carefully pipetted into each well on the plate except for the media only wells, as these wells do not need cells (Figure 21).

Control	Control	Control	Control	Control	Control	Control	Control	Control	Control	Control	Control
DMSO 1,25%	DMSO 0,5%	1 μ M	10 μ M	100 μ M	250 μ M	DMSO 1,25%	DMSO 0,5%	1 μ M	10 μ M	100 μ M	250 μ M
DMSO 1,25%	DMSO 0,5%	1 μ M	10 μ M	100 μ M	250 μ M	DMSO 1,25%	DMSO 0,5%	1 μ M	10 μ M	100 μ M	250 μ M
DMSO 1,25%	DMSO 0,5%	1 μ M	10 μ M	100 μ M	250 μ M	DMSO 1,25%	DMSO 0,5%	1 μ M	10 μ M	100 μ M	250 μ M
DMSO 1,25%	DMSO 0,5%	1 μ M	10 μ M	100 μ M	250 μ M	DMSO 1,25%	DMSO 0,5%	1 μ M	10 μ M	100 μ M	250 μ M
DMSO 1,25%	DMSO 0,5%	1 μ M	10 μ M	100 μ M	250 μ M	DMSO 1,25%	DMSO 0,5%	1 μ M	10 μ M	100 μ M	250 μ M
Media	Media	Media	Media	Media	Media	Media	Media	Media	Media	Media	Media

Figure 21 – Plate map for cell viability experiment. Control wells = cells and media. Media wells = media, no cells.

Once cells were seeded at 2000 cells per well in 100 μ L EMEM, they were incubated for 24 hours. Next, the media was aspirated from each well except from the media wells. 100 μ L of each concentration (250 μ M, 100 μ M, 10 μ M and 1 μ M) of I3C, DIM and the compounds was added to the appropriate well on the plate (See Figure 21). 100 μ L of media was added to the control and media wells. Then, the DMSO control wells (0.5% and 1.25%) were also added in a 100 μ L volume. The plate was then incubated for 48 hours. Once treatment was completed, 10 μ L MTS reagent per well was added and the plate was incubated for 1 hour. Subsequently, the plate was transported to the plate reader wrapped in foil, as MTS reagent is light-sensitive. The absorbance was measured at 485 nm with 4 seconds of shaking using a 96 well plate reader.

3.2.2.4 - Statistical analysis

Statistical analysis was carried out using excel 2016. Results from each assay were normalised and expressed as a percentage of untreated cells for each concentration using equation 1. Absorbance values were expressed as the mean value of at least 3 assays in triplicate from different cell passages. Anomalous results were discounted if they were outlying from the mean value by 1 standard deviations.

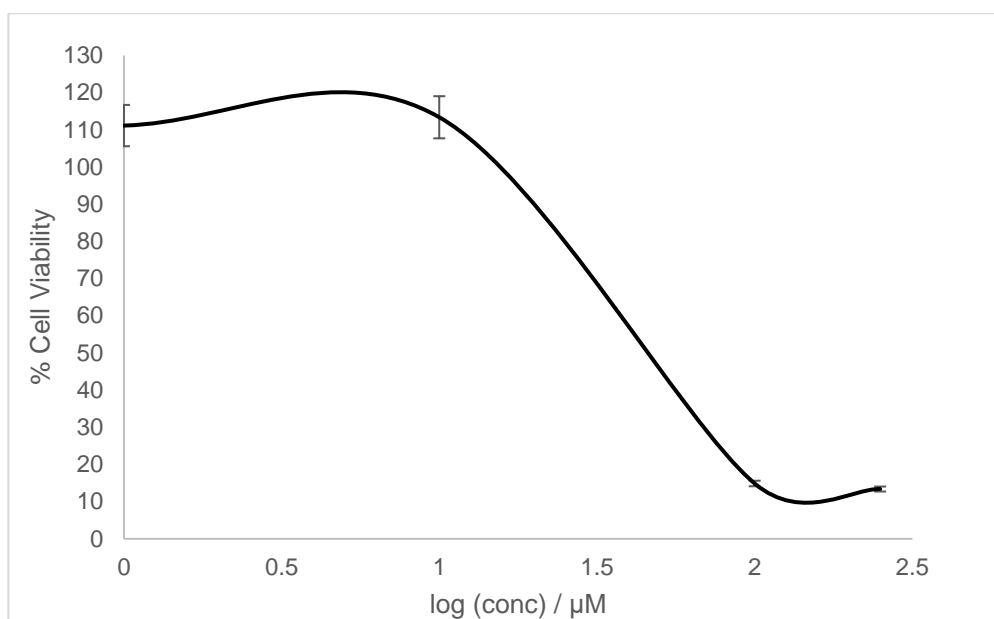
$$\frac{\text{Treated Absorbance} - \text{Media Absorbance}}{\text{DMSO Absorbance} - \text{Media Absorbance}} \times 100 = \text{cell viability (\%)}$$

Equation 1 – Cell viability (%) equation.

3.2.3 – Series one cell viability results and discussion

3.2.3.1 – Cell viability assay

The cell viability for I3C, DIM and the compounds synthesised was tested against U-87 MG human glioblastoma cells. This was measured using the MTS assay, this utilizes a colorimetric method for the quantification of viable mammalian cells. The MTS tetrazolium compound is reduced to a formazan dye by viable cells, which causes a colour change from yellow to brown. This colour change accounts for the amount of viable cells present in the cell culture, measuring the absorbance allows the cell viability to be quantified. Using the cell viability values obtained, cell viability graphs can be constructed, from which, IC₅₀ values can be calculated for each compound tested. For example, Graph 1 shows the cell viability graph for DIM. The IC₅₀ of a compound determines the concentration of the compound required for 50% inhibition of cancer cell lines. Once IC₅₀ values are obtained, it is possible for comparisons between the compounds to be made, as well as against the clinically relevant drug temozolomide.



Graph 1 - Cell viability graph of U-87 MG cells after treatment with DIM after 48 hours.

This section will entail the IC₅₀ values obtained for I3C, DIM and the compounds synthesised, alongside why the compounds from series one and two were synthesised and tested. Also, the structure activity relationship of the compounds with regards to their anti-proliferative effects towards U-87 MG cells will also be discussed. Cell viability results from series one and series two will be compared to compounds previously tested against glioblastoma cell lines within the Snape research group.

3.2.3.2– Series one cell viability results

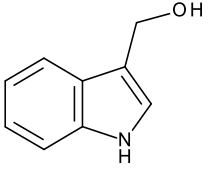
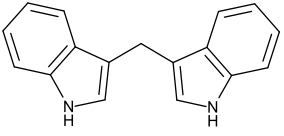
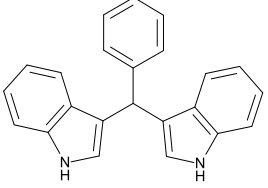
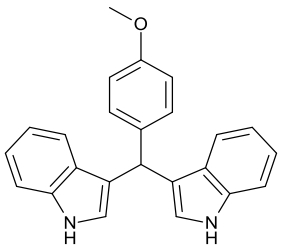
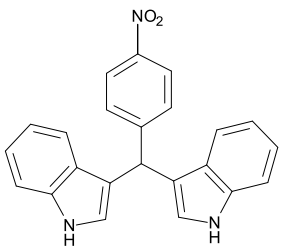
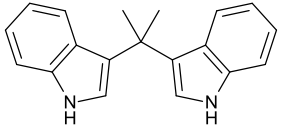
Compound	Chemical Structure	IC ₅₀ (μM)
I3C		158
DIM		46
19		32
17		52
64		38
65		33

Table 3 – IC₅₀ values for I3C, DIM and compounds **19**, **17**, **64** and **65** against the U-87 MG cell line for 48 hours.

As this project aimed to investigate whether DIM and its c-DIM derivatives display anti-cancer effects towards glioblastoma, series 1 consisted of preliminary compounds to test, including I3C and DIM (Table 3). This made it possible to establish whether DIM is active and compare its activity to I3C. Obtaining an IC₅₀ for DIM will also enable the evaluation of the effect substitution on the methylene

bridge has on activity. Compound **19**, with a phenyl group on the methylene bridge, acts as the neutral compound of the c-DIM series and will determine whether aromatic substituted c-DIMs demonstrate activity against the glioblastoma cell line. Then, compound **17** featuring a *para*-methoxy group on the phenyl ring, explores the effect of an electron donating group on the phenyl ring, as the lone pair on the oxygen delocalises into the ring. On the contrary, compound **64** bears a *para*-nitro group on the ring which heavily decreases the electron density of the aromatic ring as it draws electrons towards itself, away from the ring. Compound **65** investigates whether the introduction of two alkyl groups on the methylene bridge will affect the anti-cancer effects, and if so, in what capacity when compared to aromatic-substituted c-DIM compounds **19**, **17** and **64**.

3.2.3.3 - Series one cell viability discussion

As shown in Table 3, DIM displayed much better activity than I3C, (DIM 46 μM vs I3C 158 μM). This could possibly be due to I3C itself being active, or potentially and more likely, be the result of the conversion of I3C into its condensation product, DIM. Literature states that I3C rapidly converts into DIM at low pH and converts into DIM slowly at neutral pH.^{[153][154]} Therefore, as tissue culture medium is approximately pH 7-7.7, the activity of I3C stated in Table 3 may actually be due to the slow conversion of I3C to DIM *in vitro*. The IC₅₀ values obtained for I3C and DIM are accordance with literature involving other cancer cell lines. For example, Moiseeva *et al* report IC₅₀ values of 300 μM and 100 μM for I3C and DIM respectively when tested against breast cancer cell lines.^[155] Additionally, when I3C and DIM were tested against prostate cancer cell lines the IC₅₀ values were 50 μM (DIM) and 150 μM (I3C).^[156]

With regards to the c-substituted DIM derivatives, each of the compounds synthesised in series one, all demonstrated good activity against the glioblastoma cell line, with barely a difference between aromatic and alkyl substituents (32 μM compound **19** vs 33 μM compound **65**).

Compound **19**, the neutral c-DIM, displays very good activity against glioblastoma, this is consistent with the literature formerly discussed that c-DIMs demonstrate anti-proliferative activity against many types of cancer cells. The

IC₅₀ of compound **19** is a great improvement on that of I3C and is a small degree better than DIM, suggesting the incorporation of substituent on the methylene bridge of DIM slightly improves the anti-cancer effect. When comparing compound **19** to compounds **17** and **66**, the contrasting electronic effects of the methoxy and nitro groups on the phenyl ring do not seem to majorly effect the anti-cancer activity, however, it is worth noting the electron donating methoxy group very slightly reduces the activity (32 μ M [-H] and 38 μ M [-NO₂] vs 52 μ M [-OMe]).

Analogue **65**, with a gem-dimethyl group, also has respectable activity against the glioblastoma cell line. There essentially no difference observed between alkyl-containing compound **65** and phenyl-containing compound **19** (33 μ M and 32 μ M, respectively).

Overall, series one determines that both aromatic-substituted and alkyl-substituted c-DIMs demonstrate good anti-cancer properties towards the glioblastoma cell line, with compound **19** being superior. Thus, the compounds in series two were designed with the intention of improving the anti-cancer activity that was observed in series one.

3.2.4 – Series two cell viability results and discussion

3.2.4.1 – Series two cell viability results

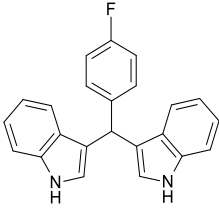
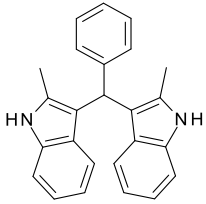
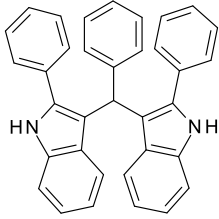
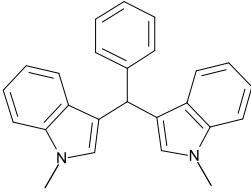
Compound	Chemical Structure	IC ₅₀ (μM)
20		>250 (91% cell viability at 250 μM)
66		200
67		209
38		186

Table 4 – IC₅₀ values for compounds **20**, **66**, **67** and **38** against the U-87 MG cell line for 48 hours.

The synthesis of compound **20** was firstly based on, as previously mentioned, a deactivating *para*-nitro group on the phenyl ring (compound **64**) displayed slightly improved activity in comparison to compound **17**, with a *para*-methoxy group (38 μM [-NO₂] vs 52 μM [-MeO]). Furthermore, formerly discussed literature states that halogenated phenyl substituted c-DIMs have an anti-proliferative effect towards colon cancer cells and oral squamous cell carcinoma.^{[107][108]} Therefore, it was of interest to investigate the effects of a *para*-halogenated phenyl c-DIM against glioblastoma cells.

Previous research carried out within the Snape research group, has identified that 2-substituted indoles **69**, **70** and **71**, as seen in Figure 22, display moderately good anti-glioblastoma activity.^{[157][158][159]}

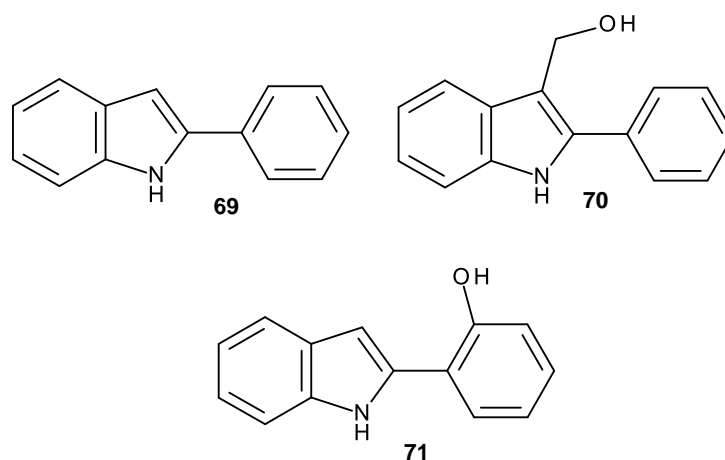


Figure 22 – 2-Arylimidazoles previously tested against the U87MG glioma cell line within the Snape research group.^{[157][158][159]}

Furthermore, previously discussed literature in section 1.4, states the anti-cancer activity of 2,2'-dimethyl and 2,2'-diphenyl DIM compounds towards breast cancer cell lines.^{[100][101]} Lei *et al* also reported a 40-60% reduction in cell viability of colon cancer cell lines after treatment with 2,2'-dimethyl DIM-*c-p*PhF.^[107] These findings suggest that adding methyl and phenyl substitution at position-2 of the indole rings, could potentially increase the anti-glioblastoma effects of *c*-DIMs.

Therefore, taking the structure of the compound that displayed the best activity from series one, which was compound **19**, and incorporating methyl and phenyl functionalisation at position-2 of the indole rings, provided the basis for the design of the 2,2'-substituted compounds **66** and **67**.

Studies regarding the anti-cancer activity of *N,N'*-methylated *c*-DIM compounds, state that *N,N'*-methylated DIM-*c-p*PhBr and DIM-*c-p*PhF compounds were totally inactive against colon cancer cells.^[107] However, *N,N'*-dimethyl DIM has been reported to reduce cell proliferation in breast cancer cell lines.^[101] Therefore, compound **38**, which was the *N,N'*-methylated derivative of compound **19**, was synthesised in order to analyse whether free NH groups were required for activity.

3.2.4.2 – Series two cell viability discussion

As shown in Table 4, surprisingly, compound **20** exhibited a drastic reduction in anti-cancer activity in comparison to the c-DIM compounds in series 1. An IC₅₀ value could not be established for this compound, therefore the cell viability at 250 µM is stated (91%). It would be expected that such a compound would demonstrate similar activity to compound **64** (IC₅₀ 38 µM), as they both contain an electron withdrawing substituent on the aromatic ring. However, only a slight positive effect was observed, with a 9% reduction in cell viability. Therefore, further research investigating the anti-glioblastoma effects of halogenated ring substituents should be carried out.

Comparing compounds **66** and **67** with compound **19**, shows that the addition of methyl and phenyl groups at position-2 of the indole rings dramatically reduced the activity of the compound. IC₅₀ values of 200 µM and 209 µM for compounds **66** and **67**, respectively, demonstrate that the absence of substitution at position-2 of the indole rings is required for anti-glioblastoma activity of symmetrical c-DIMs.

Compound **38** displays poor activity in comparison to compound **19** (32 µM vs 186 µM, respectively), despite the only difference structurally being methylation at the *N,N'*-positions. Similar results have been found in related research whereby methylated c-DIM compounds were inactive against colon cancer cells.^[107] These findings suggest that free NH groups are required for the anti-tumorigenic effect to glioblastoma cells.

3.2.5 - Discussion of results from within the Snape research group

Figure 23 shows 2-substituted indole compounds (**69-71**) and DIM derivatives (**72-75**) that have been tested against the U-87 MG glioblastoma cell line within the Snape research group. Compounds **69-71** each displayed good anti-glioblastoma effect towards U-87 MG cells.^{[157][158][159]} However, the 2,2'-disubstituted DIM compounds **72-74** demonstrated poor activity, these findings are concordant with the results obtained in series 2 for the 2,2'-dimethyl and -diphenyl substituted c-DIMs, compounds **66** and **67**.

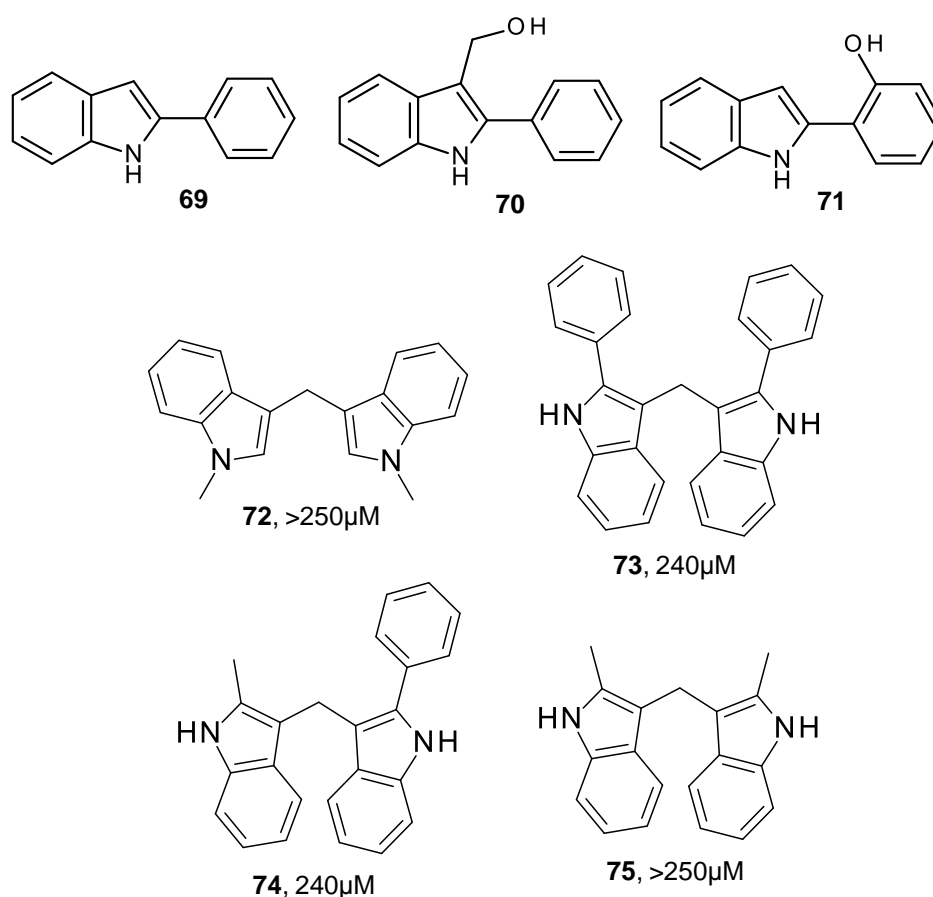


Figure 23 - Compounds tested against glioblastoma U-87 MG cell lines within the Snape research group. 2-Arylindoles **69-71**, DIM derivatives **72-74** and their IC_{50} values.^{[157][158][159]}

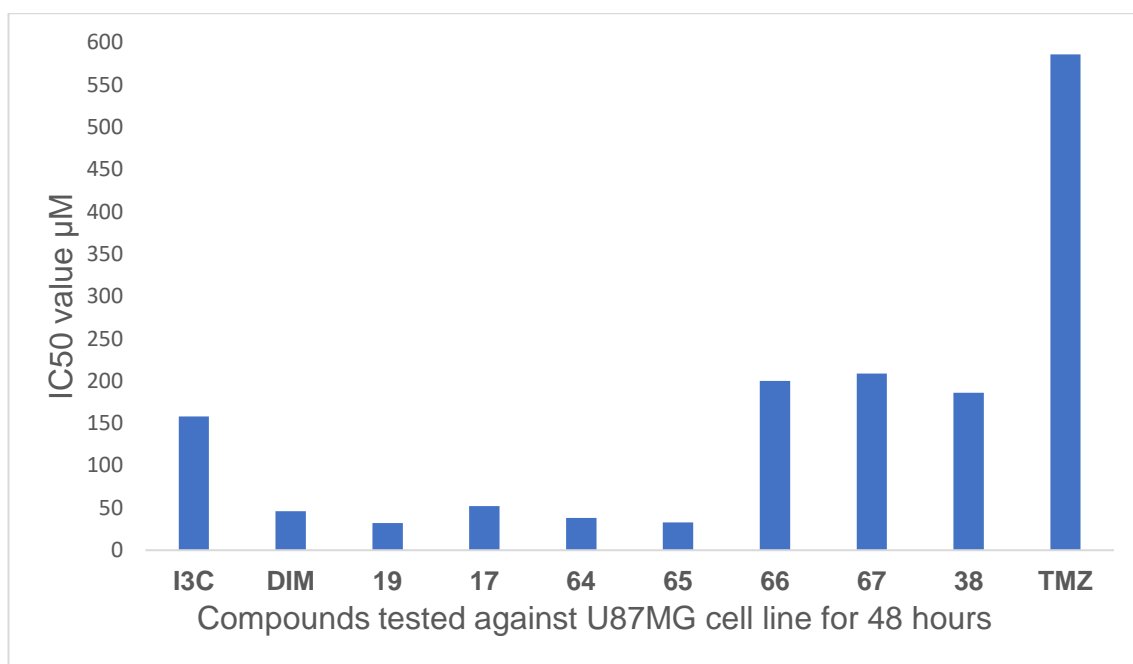
Therefore, the question arises, why do the c-DIM compounds featured in series one and 2-substituted indole compounds (**69-71**) display good anti-glioblastoma effects, whereas 2,2'-substituted DIM's and c-DIMs do not? For example, why is 2-phenylindole (**69**) active against glioblastoma cells, yet its dimeric product (**73**) and corresponding c-DIM (**67**) are both essentially inactive? A potential reason for this difference in activity could be that, the groups at position-2 force the molecule to conform to a different shape than the DIM/c-DIMs with no 2,2'-substitution. This possible difference in conformation, is indicative that the anti-cancer mechanism of DIM and c-DIMs is through binding to a three dimensional biological target, which requires a specific structural arrangement of the molecule.

Comparing compound **38**, the *N,N'*-methylated derivative of compound **19** (186.2 μ M) with compound **75**, *N,N'*-methylated DIM (>250 μ M, cell viability 92%), shows that methylation of the *N*-positions causes a significant reduction in activity.

These results are in accordance with each other, and previously mentioned literature.^[107] Again, this is suggestive that a free NH group is necessary for anti-glioblastoma activity, possibly due to the anti-cancer mechanism involving hydrogen bonding to a biological target via the amine groups of the indole motifs.^{[160][161]}

3.2.6 - Discussion of results in comparison to temozolomide

As previously discussed in section 1.3.2, temozolomide is currently the main chemotherapeutic agent used in the treatment of high grade gliomas. As shown in the Graph below, in comparison to temozolomide, all the c-DIM analogues tested in this project show more potent inhibition of U-87 MG cell proliferation than temozolomide when treated for 48 hours, except from compound **20** as only 91% cell viability was observed, thus, a reliable IC₅₀ value was not obtainable. Therefore, Graph 2 does not include compound **20**, Although each compound tested, including I3C and DIM, show improved anti-glioblastoma activity than temozolomide, compounds **19**, **17**, **64** and **65** especially demonstrate the most effective anti-proliferative effects against the malignant U-87 MG glioblastoma cell line, with compound **19** being superior overall. However, it is worth mentioning that temozolomide is an attractive chemotherapy drug due to its 100% oral bioavailability, whereby 100% of the drug enters the bloodstream when administered orally. Also, it has the ability to pass the blood brain barrier. The IC₅₀ value of temozolomide after 48 hours treatment against U-87 MG glioblastoma cells slightly varies across literature, therefore an average IC₅₀ value of 586 μ M was calculated and used for comparison purposes and for Graph 2.^{[162][163][164][165]}



Graph 2 – Graph showing IC_{50} values of I3C, DIM and compounds tested (excluding compound 20), in comparison to temozolomide.^{[162][163][164][165]}

3.2.7. – Challenges encountered during cytotoxicity testing

3.2.7.1 – Solubility of compounds

A common problem encountered within the cytotoxicity testing stage of this project, was the precipitation or oiling-out of the compounds synthesised at high concentrations, when coming into contact with media. Therefore, when making the 10,000 µM working solution (shown in dilution scheme, Figure, 20) each compound required thorough mixing and warming in a 37 °C water bath. Compound **17** especially, crystallised when coming into contact with media when making the 10,000 µM working solution, despite heating in the water bath and thorough mixing using a vortex. Thus, making it not possible to make the 250 µM, 100 µM, 10 µM and 1 µM concentrations required for the cell viability assays. The solution to this problem was to avoid making a 10,000 µM working solution, as this step involved the mixing of 250 µL of compound **17** and 250 µL media – and it was this step that was causing the precipitation of compound **17**. Figure 24 shows the serial dilution used for compound **17** in comparison to the other compounds, precipitation did not occur when using

the second serial dilution, as only half of the volume of 20 mM compound **17** was being diluted with media than it was in serial dilution one.

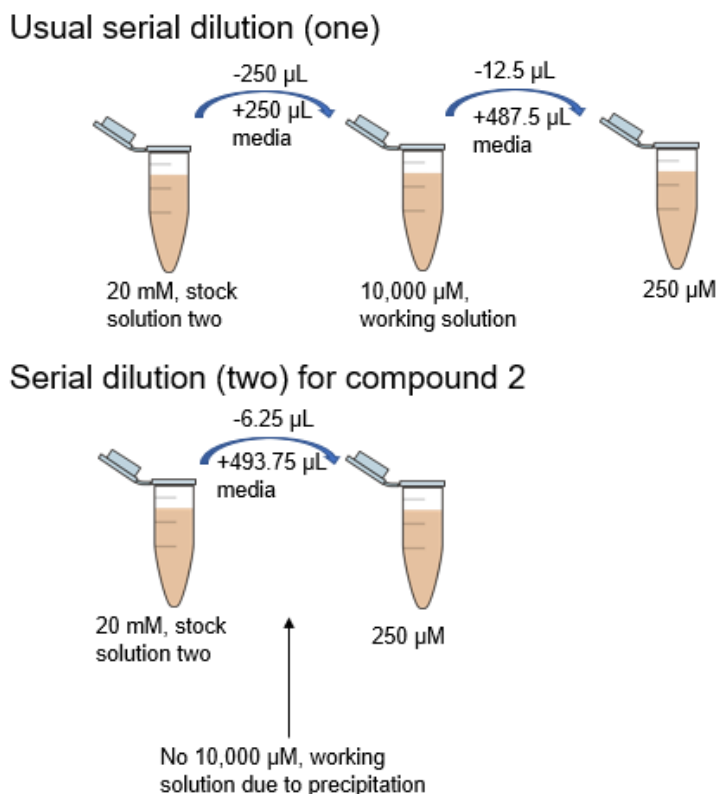


Figure 24 – Top row: the usual serial dilution followed to create the 250 μ M concentration. Bottom row: the serial dilution followed to create the 250 μ M concentration for compound **17** as this avoided the compound precipitating out in media.

After adding the compounds to the 96 well plates, the plates were studied under microscope often throughout the treatment stage. Crystallisation or oiling-out of compounds was easily identifiable amongst cells under the microscope, as crystals were larger, darker and visible as clusters under the microscope. Figure 25 shows U-87 MG cells on the left in comparison to compound **17** oiling out in media under the microscope.

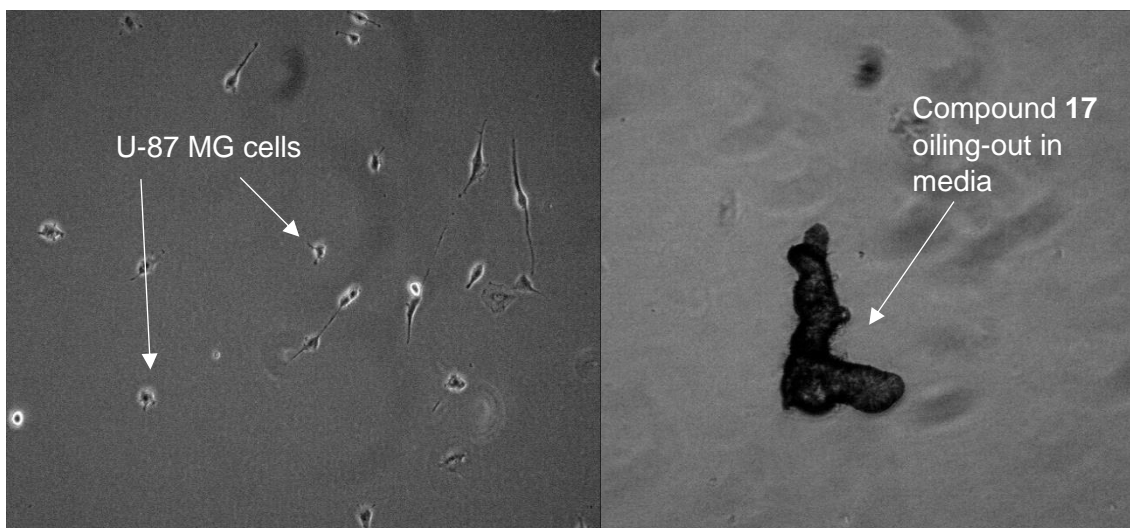
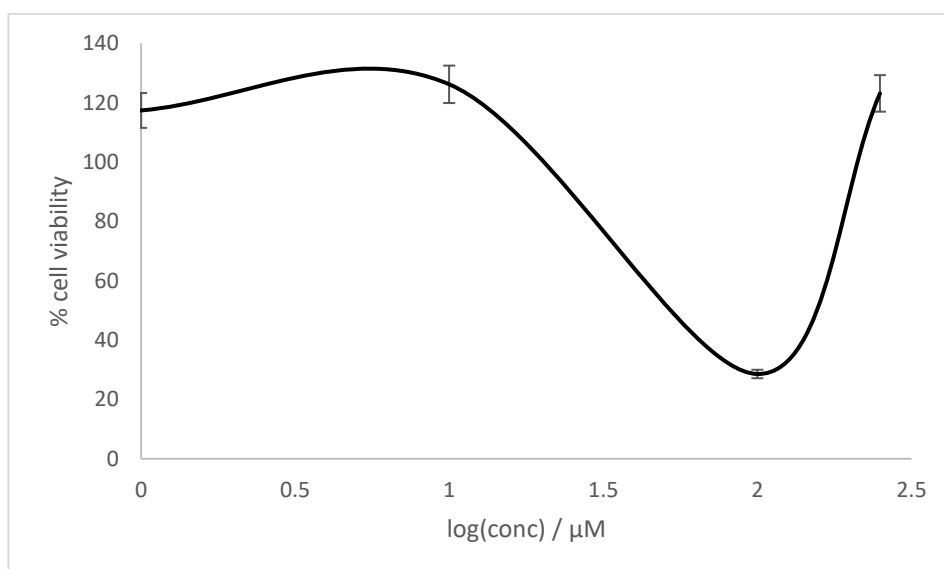


Figure 25 – Left: Low density U-87 MG cells as seen under the microscope (magnification x100). Right: Compound 17 oiling-out in media (magnification x100).

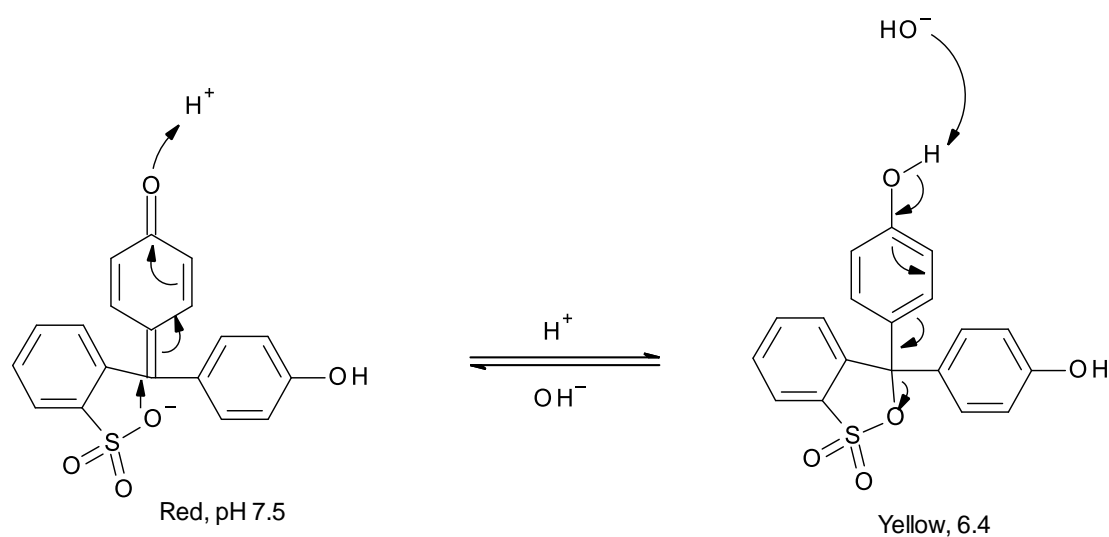
The precipitation of compound **17** at high concentrations, is also potentially visible in the cell viability graph shown below in Graph 3. The graph shows cell viability increasing at around 250 μM , this could possibly be a result of the compound crystallising over time at higher concentrations, and therefore having no effect on the cells.



Graph 3 - U-87 MG % cell viability graph of U-87 MG cells after treatment with compound **17** after 48 hours.

3.2.7.2 – Contamination of cells

Another recurring challenge in cytotoxicity testing was cell culture contamination, contaminants include bacteria, fungi, yeast, viruses and chemical contaminants. Bacterial and fungal contamination were the most common types of contamination encountered, however, they are also the easiest types to identify. Not only were bacterial and fungal contaminants easy to spot under the microscope, due to their difference in appearance to U-87 MG cells – bacteria/fungi are usually much darker and different structurally under the microscope. Culture medium contains a non-toxic pH indicator, called phenol red. As bacterial and fungal contamination results in the media becoming more acidic, a colour change from red (7.5 pH) to yellow (6.4 pH) is observed (Scheme 29). This obvious colour change made bacterial/fungal contaminated cultures easy to identify. Contaminated cultures were incinerated as soon as possible, new cryopreserved cells were then obtained from the liquid nitrogen freezer, defrosted and incubated in order to prepare for seeding.



Scheme 29 – Chemical structure of phenol red and its colour change reaction.

Cell culture contamination can arise from a number of different sources including;

- Contact with non-sterile media, solutions or equipment
- Airborne particles entering culture during passaging, seeding, treatment, transportation or incubating
- Over-crowding of cultures within the incubators
- Biological contaminants can grow or swim into culture vessels from outside of the vessels

As such a range of pathways can cause contamination, it was difficult to control, especially in a busy lab. The best way to reduce contamination problems was firstly, to practice good aseptic techniques; spray flasks and plates with 70% industrial methylated spirits (IMS) before placing cell cultures into fume hoods or incubators, to clean the fumehood before and after use, and clean the incubator on a regular basis using 70% Industrial methylated spirits (IMS) and Virkon. Virkon is a potent disinfectant that is effective in killing viruses, bacteria and fungi.

Antibiotics are frequently used in cell cultures as a way to prevent bacterial contamination. For example, Penicillin-Streptomycin (Pen-Strep) – a mixture of penicillin and streptomycin is often used within cell cultures to minimise bacterial contamination. However, they should only be used as a last resort or for a very short time period. This is because continuous use of antibiotics can encourage the progression of antibiotic resistant strains. Antibiotics in cell cultures can also mask low-level contamination, which can advance and spread into wide-scale contamination when the antibiotic is removed from the media. Therefore, the use of antibiotics was not an appropriate measure to control contamination during cell cytotoxicity testing.

CHAPTER FOUR – CONCLUSION

4.1 – Conclusion

Glioblastoma is the most aggressive and common malignant brain tumour in adults, with primary glioblastoma accounting for 90% of cases.^[1] Glioblastoma is associated with extremely poor prognosis, long term survival is uncommon, as only 25% of patients survive two years.^{[1][2]} Currently, the gold standard of care for the treatment glioblastoma is surgery, radiotherapy and the administration of the chemotherapeutic agent temozolomide. Although temozolomide extends the overall survival of patients, temozolomide resistance is a growing issue.^[70] Thus, the development of new, much more effective pharmaceutical agents are necessary for the treatment of glioblastoma.

Derived from cruciferous vegetables, the dimeric product of indole-3-carbinol (I3C) - 3,3'-diindolylmethane (DIM), has received considerable attention regarding its antitumorigenic activity towards various cancer cell lines.^{[7][90][91][92]} In addition to the basic structure of DIM, *in vitro* studies have also established anti-cancer effects of DIMs methylene bridge-substituted derivatives (c-DIMs), and its 2,2'-substituted derivatives.^{[10][100][101][103]} However, the effects of c-DIMs against glioblastoma cells are seemingly currently unknown.

This thesis successfully, for the first time, describes the anti-glioblastoma effects of c-substituted DIM derivatives. Using the MTS assay, cytotoxicity testing of I3C, DIM and the c-DIM compounds was carried out against the U-87 MG human glioblastoma cell line. From the *in vitro* studies, IC₅₀ values for each compound were established, and structure activity relationships were identified. DIM displayed much better activity than I3C, (46 µM vs 158 µM, respectively), possibly due to the slow conversion of I3C into DIM at neutral pH. Compounds **19**, **64** and **65** displayed the most effective activity (IC₅₀ values 31 µM, 38 µM and 33 µM, respectively), with compound **19** being superior overall. However, the *N,N'*- and 2,2'- substituted c-DIM analogues displayed a reduction in activity, suggestive that free indole groups are essential for anti-glioblastoma activity.

4.2 – Future work

Whilst this project demonstrates that c-DIMs display anti-glioblastoma effects, prospects remain to extend the scope of this research. Firstly, additional cytotoxicity testing of the best performing compounds **19**, **64** and **65**, should be carried out against alternative glioblastoma cell lines, as different genes are expressed within different cell lines. Therefore, comparisons can be made between cell viability results from other cell lines, popular alternative glioblastoma cell lines include U-118 MG and U-251 MG.

In addition to glioblastoma cell lines, the c-DIM compounds ought to be tested on primary glioblastoma cultures – these are tumours obtained directly from glioblastoma patients. This would reflect more accurately how the compounds would act against actual glioblastoma tumour tissue, as opposed to a cell line, as cell lines do not entail the true diversity of a living tumour.

Moreover, studies involving the testing of the compounds on healthy brain tissue should be carried out. This would establish the cytotoxicity of the compounds towards healthy brain cells. Ideally, anti-cancer agents should have the ability to distinguish between tumorigenic cells and normal, healthy cells.

With regards to the structure of the compounds tested, it would be interesting to test the effects of unsymmetrical 2-substituted c-DIMs. For example, incorporating a methyl group at position-2 of one indole ring of compound **19**. As the single-substituted c-DIM may not change in conformation to the extent we suspect the 2,2'-dimethyl c-DIM (**66**) did. Therefore, it would be of interest to compare the anti-glioblastoma activity of compound **19**, with its 2-methyl substituted and 2,2'-dimethyl substituted derivatives. It would also be of interest to extend the exploration of the effects of functionalisation around the indole ring, for example, analysing whether substitution at positions 5 or 6 would increase or reduce the anti-cancer in comparison to the activity described in this thesis.

Therefore, overall, this project has provided a good foundation for future investigation into the anti-cancer effects of c-DIM analogues towards glioblastoma.

CHAPTER FIVE – EXPERIMENTAL

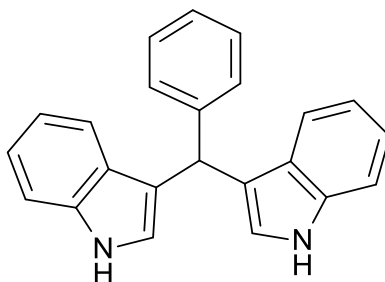
5.1 - Materials

Reactions were monitored using thin layer chromatography (TLC) using plastic-backed TLC plates coated in silica G/UV254, run in various solvent systems and visualised using a UVP CHROMATO-VUE cabinet under short wave (254 nm) and long wave (365 nm) UV light, with p-anisaldehyde or potassium permanganate stain. Commercially available solvents and reagents were purchased from Sigma Aldrich, TCI, Fluorochem or ThermoFisher Scientific and were used with no further purification unless stated otherwise in the syntheses. Flash column chromatography was carried out on DAVISIL silica 60 Å (40-63 µm) chromatography grade silica, under bellows pressure.

¹H and C¹³ NMR spectra were recorded using a Bruker Fourier 300 (300 MHz) or Bruker Advance III 400 (400 MHz). δ indicates chemical shift in ppm and J indicates coupling constants in Hertz (Hz). Multiplicity of NMR signals are abbreviated using: s = singlet, d = doublet, t = triplet, q = quartet, quin = quintet, sex = sextet, m = multiplet, dd = doublet of doublets, td = triplet of doublets. Assignments of NMR spectra was aided with the use of DEPT-135, and in some cases DEPT-90. LC-MS spectra were obtained using a Finnigan LCW Advantage Max, Finnigan PDA Plus detector. IR spectra were recorded using solid samples on a Thermo Nicolet IR-200 FT-IR. Melting points were obtained using Stuart digital melting point apparatus and are uncorrected.

Experimental

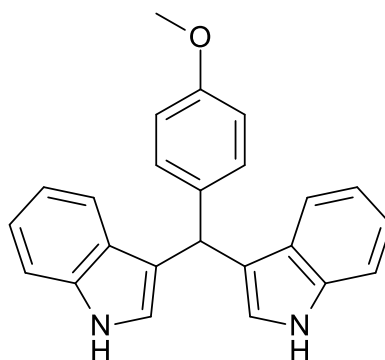
5.2 - 3-[1H-Indol-3-yl(phenyl)methyl]-1H-indole (EJ-1-33-2)



19

To a stirred solution of indole (0.50 g, 4.2 mmol, 2 eq.) and benzaldehyde (0.226 mL, 2.1 mmol, 1 eq.) in deionised water (15 mL), was added concentrated sulfuric acid (0.232 mL, 4.2 mmol) and stirred at room temperature. The reaction was monitored by TLC using ethyl acetate: petroleum ether (30:70). Once the reaction reached completion according to TLC, the reaction mixture was extracted with ethyl acetate (30 mL) and washed with brine (2 x 30 mL). The organic layer was dried with magnesium sulfate, filtered via vacuum filtration and the remaining solution was evaporated to dryness *in vacuo*, leaving a red oil that was left to dry overnight in the fumehood. The crude product had traces of starting reagents, so therefore was purified by flash column chromatography (30:70 ethyl acetate: petroleum ether) to yield compound **19** as a red solid (0.598 g, 88% yield). ¹H NMR (300 MHz, CDCl₃) δ_H= 7.88 (2H, s, NH), 7.33-7.41 (m, 6H, Ar H), 7.21-7.31 (m, 3H, Ar H), 7.18 (t, *J* = 7.5, 2H, Ar H), 6.99 (t, *J* = 7.5, 2H, Ar H), 6.64 (s, 2H, Ar H), 5.89 (1H, s, CH). ¹³C NMR (75MHz, CDCl₃): δ_C= 144.0 (Ar C), 136.7 (Ar C), 128.8 (Ar CH), 128.2 (Ar CH), 127.0 (Ar C), 126.1 (Ar CH), 123.7 (Ar CH), 121.9 (Ar CH), 120.0 (Ar CH), 119.7 (Ar C), 119.3 (Ar CH), 111.0 (Ar CH), 40.2 (CH). LC-MS (ESI) Calculated: 322.4, found: 321.56 (*m/z*). IR (neat, cm⁻¹) 3390 (N-H), 1335.50 (C-N). mp: 149-152 °C (ethyl acetate/ petroleum ether), literature mp: 142-144 °C.^[166]

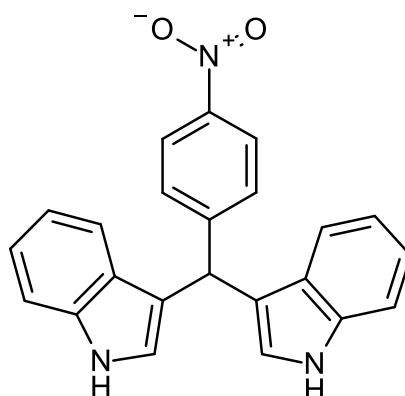
5.3 - 3-[1H-Indol-3-yl-(4-methoxyphenyl)methyl]-1H-indole (EJ 1-36-1)



17

Synthesised as compound **19** using 4-methoxybenzaldehyde (0.28 mL, 2.1 mmol) to yield compound **17** as a brown solid (0.425 g, 57% yield). Chromatography solvent 20:80 ethyl acetate: petroleum ether. ^1H NMR (300 MHz, CDCl_3): δ_{H} = 7.97 (s, 2H, NH), 7.39-7.45 (m, 4H, Ar H), 7.29-7.31 (m, 2H, Ar H), 7.22 (t, J = 7.5, 2H, Ar H), 7.06 (t, J = 7.0, 2H, Ar H), 6.87 (d, J = 8.0, 2H, Ar H), 6.70 (s, 2H, Ar H), 5.89 (s, 1H, CH), 3.84 (s, 3H, OCH_3). ^{13}C NMR (75 MHz, CDCl_3): δ_{C} = 157.9 (Ar C), 136.7 (Ar C), 136.2 (Ar C), 129.6 (Ar CH), 127.0 (Ar C), 125.5 (Ar CH), 123.5 (Ar CH), 121.9 (Ar CH), 120.0 (Ar CH), 120.0 (Ar C), 113.5 (Ar CH), 111.0 (Ar CH), 55.22 (C- OCH_3), 39.30 (CH). MS (ESI) calculated: 352.43, found: 351.31 m/z . IR (neat, cm^{-1}) 3392.96 (N-H), 1453.70 (C-H), 1344.71 (C-N), 1256.17 (C-O-C). mp: 184-186 °C (ethyl acetate/ petroleum ether), literature mp: 186-187 °C.^[166]

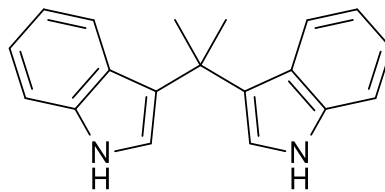
5.4 3-[1H-Indol-3-yl-(4-nitrophenyl)methyl]-1H-indole (EJ 1-39-2)



64

Synthesised as **19** using 4-nitrobenzaldehyde (0.3174 g, 2.1mmol) to yield compound **64** as a yellow solid (0.611 g, 73%). Chromatography solvent 30:70 ethyl acetate: petroleum ether. ^1H NMR (300 MHz, $\text{DMSO-}d_6$): $\delta_{\text{H}} = 10.96$ (s, 2H, NH), 8.15 (d, $J = 8.0$, 2H, Ar H), 7.61 (d, $J = 8.0$, 2H, Ar H), 7.36 (d, $J = 8.0$, 2H, Ar H), 7.29 (d, $J = 8.0$, 2H, Ar H), 7.05 (t, $J = 7.5$, 2H, Ar H), 6.86-6.90 (m, 4H, Ar H), 6.03 (s, 1H, CH). ^{13}C NMR (75 MHz, $\text{DMSO-}d_6$): $\delta_{\text{C}} = 153.60$ (Ar C), 146.18 (Ar C), 137.02 (Ar C), 129.91 (Ar CH), 126.79 (Ar C), 124.32 (Ar CH), 123.90 (Ar CH), 121.57 (Ar CH), 119.37 (Ar CH), 118.88 (Ar CH), 117.10 (Ar C), 112.05 (Ar CH), 39.9 (CH). MS (ESI) calculated: 367.4, found: 366.22 m/z . IR (neat cm^{-1}) 3448.48 (N-H), 1501.17 (N-O), 1340.51 (N-O), 1236.48 (C-N). mp: 221-223 $^{\circ}\text{C}$ (ethyl acetate/ petroleum ether), literature mp: 218-220 $^{\circ}\text{C}$.^[167]

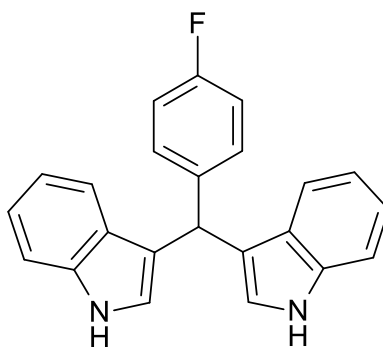
5.5 - 3-[1-(1H-Indol-3-yl)-1-methyl-ethyl]-1H-indole (1-58-2)



65

Synthesised as **19** using an excess of acetone (2 mL) and was heated to 60 °C to yield **65** as white needles (0.214 g, 37%). Chromatography solvent 2:98 ethyl acetate: toluene. ¹H NMR (300 MHz, CDCl₃): δ_H = 7.92 (s, 2H, NH), 7.50 (d, *J* = 8.0, 2H, Ar H), 7.38 (d, *J* = 8.0, 2H, Ar H), 7.15 (t, *J* = 7.5, 2H, Ar H), 7.11 (d, *J* = 2.5, 2H, Ar H), 6.96 (t, *J* = 7.5, 2H, Ar H) 1.99 (s, 6H, CH₃). ¹³C NMR (75 MHz, CDCl₃): δ_C = 137.1 (Ar C), 126.3 (Ar C), 125.4 (Ar C), 121.4 (Ar CH), 121.3 (Ar CH), 120.5 (Ar CH), 118.7 (Ar CH), 111.1 (Ar CH), 34.9 (C), 30.0 (CH₃). MS ESI calculated: 274.36 found: 273.14 *m/z*. IR (neat cm⁻¹) 3393.8 (N-H), 1454.33 (C-H), 1333.74 (C-N). Mp: 171-173 °C (ethyl acetate/ toluene), Literature mp: 168-170 °C.^[168]

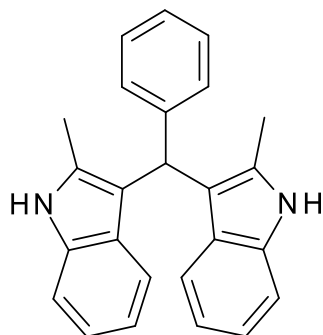
5.6 - 3-[1H-Indol-3-yl-(4-fluorophenyl)methyl]-1H-indole (EJ 1-69-1)



20

Synthesised as **19** using 4-fluorobenzaldehyde (0.225 mL, 2.1 mmol) to yield compound **20** as a yellow solid (0.516 g, 72%). ¹H NMR (300 MHz DMSO-*d*₆): δ_H = 7.78 (s, 2H, NH), 7.33-7.37 (m, 4H, Ar H), 7.18 (d, *J* = 8.0, 2H, Ar H), 7.12 (t, *J* = 7.5, 2H, Ar H), 6.95-7.05 (m, 6H, Ar H), 5.67 (s, 1H, CH). ¹³C NMR (75 MHz, DMSO-*d*₆): δ_C = 140.6 (Ar C), 137.5 (Ar C), 136.9 (Ar C), 130.7 (Ar CH), 125.9 (Ar C), 121.1 (Ar CH), 118.9 (Ar CH), 118.7 (Ar CH), 115.6 (Ar CH), 115.3 (Ar CH), 111.6 (Ar CH), 110.2 (Ar C), 38.9 (CH). MS ESI calculated: 340.39, found: 340.07 *m/z*. IR (neat cm⁻¹) 3462.47 (N-H), 1321.14 (C-N), 1211.72 (C-F). mp: 103-106 °C (ethyl acetate/ petroleum ether), literature mp: 100-102 °C.^[168]

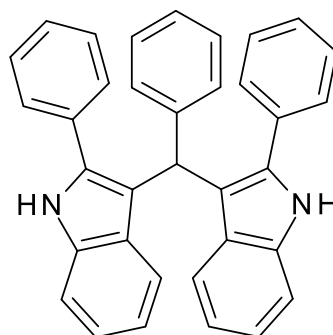
5.7 - 2-Methyl-3-[(2-methyl-1H-indol-3-yl)-phenyl-methyl]-1H-indole
(EJ 1-63-2)



66

To a stirred solution of 2-methylindole (0.55 g, 4.2 mmol) and benzaldehyde (0.226 mL, 2.1 mmol) in DCM (15 mL), concentrated sulfuric acid (0.232 mL, 4.2 mmol) was added. The reaction was left stirring for 24 hours. The desired product precipitated out in reaction mixture, it was filtered by vacuum filtration and washed with 20:80 ethyl acetate: DCM to yield compound **66** as a pink solid. (0.478 g, 65%). ¹H NMR (300 MHz, DMSO-*d*₆): δ_H = 10.79 (s, 2H, NH), 7.16-7.28 (m, 7H, Ar H), 6.88 (t, *J* = 7.5, 2H, Ar H), 6.79 (d, *J* = 8.0, 2H, Ar H), 6.66 (t, *J* = 7.5, 2H, Ar H), 5.92 (s, 1H, CH), 2.06 (s, 6H, CH₃). ¹³C NMR (75 MHz, DMSO-*d*₆): δ_C = 144.6 (Ar C), 135.4 (Ar C), 132.4 (Ar C), 129.1 (Ar CH), 128.6 (Ar C), 128.3 (Ar CH), 126.2 (Ar CH), 119.9 (Ar CH), 118.9 (Ar CH), 118.3 (Ar CH), 112.6 (Ar C), 110.7 (Ar CH), 38.9 (CH), 12.3 (CH₃). MS ESI calculated: 350.46, found: 349.36 *m/z*. IR (neat cm⁻¹) 3392.84 (N-H), 1458.87 (C-H), 1336.85 (C-N). mp: 247-249 °C (ethyl acetate/DCM), literature mp: 246-247 °C.^[166]

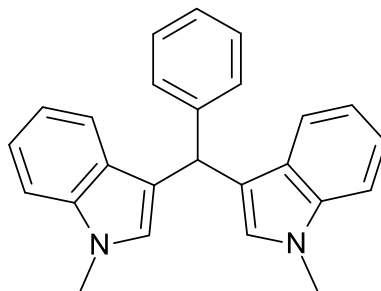
5.8 - 2-Phenyl-3-[phenyl-(2-phenyl-1H-indol-3-yl)methyl]-1H-indole
(EJ 1-64-1)



67

Synthesised as compound **66** using 2-phenylindole (0.8116 g, 4.2 mmol) and benzaldehyde (0.226 mL, 2.1 mmol) to yield compound **67** as a grey solid (0.529 g, 53%). ^1H NMR (300 MHz, DMSO- d_6): δ_{H} = 11.38 (s, 2H, NH), 7.37 (d, J = 8.0, 2H, Ar H), 7.28-7.30 (m, 5H, Ar H), 7.20-7.25 (m, 8H, Ar H), 7.14 (d, J = 7.0, 2H, Ar H), 7.01 (t, J = 7.5, 2H, Ar H), 6.89 (d, J = 8.0, 2H, Ar H), 6.67 (t, J = 7.5, 2H, Ar H) 5.96 (s, 1H, CH). ^{13}C NMR (75 MHz, DMSO- d_6): δ_{C} = 145.9 (Ar C), 136.7 (Ar C), 135.7 (Ar C), 133.2 (Ar C), 129.9 (Ar C), 129.1 (Ar CH), 128.8 (Ar CH), 128.6 (Ar CH), 128.5 (Ar CH), 127.7 (Ar CH), 126.5 (Ar CH), 121.4 (Ar CH), 121.2 (Ar CH), 119.0 (Ar CH), 114.6 (Ar C), 111.8 (Ar CH), 40.3 (CH). MS ESI calculated: 474.59 found: 473.53 m/z . IR (neat cm^{-1}) 3419.99 (N-H), 1307.26 (C-N). mp: 263-265 °C (ethyl acetate/DCM), literature mp: 266-268 °C.^[169]

5.9 - 1-Methyl-3-[(1-methylindol-3-yl)-phenyl-methyl]indole (EJ 1-75-2)



38

THF (20 mL) was dried using 1 Å molecular sieves stirring for 25 minutes. Subsequently, compound **19** (0.322 g, 10 mmol) was added, NaH 60% mineral oil (0.12 g, 30 mmol) was then added and the solution was stirred at room temperature for 20 minutes. Next, MeI (0.426 g, 30 mmol) was added, and the reaction was allowed to stir for 2 hours. Once reaction had reached completion the reaction mixture was extracted with 1 M aqueous HCl (30 mL) and brine (30 mL). The organic layer was dried with magnesium sulfate and the remaining solution was evaporated to dryness *in vacuo*. The crude product was purified by flash column chromatography (30:70) ethyl acetate: petroleum ether) to yield compound **38** as a red solid (0.279 g, 80%) ¹H NMR (300 MHz CDCl₃): δ_H = 7.30-7.41 (m, 8H, Ar H), 7.19-7.24 (m, 3H, Ar H), 7.02 (t, *J* = 7.5, 2H, Ar H), 6.53 (s, 2H, Ar H), 5.88 (s, 1H, CH), 3.70 (s, 6H, CH₃). ¹³C NMR (75 MHz, CDCl₃): δ_C = 144.4 (Ar C), 137.3 (Ar C), 128.6 (Ar CH), 128.2 (Ar CH), 128.2 (Ar CH), 127.4 (Ar C), 126.0 (Ar CH), 121.4 (Ar CH), 120.0 (Ar CH), 118.6 (Ar CH), 118.2 (Ar C), 109.0 (Ar CH), 40.0 (CH), 32.7 (CH₃). MS ESI calculated: 350.46, found: 349.27 *m/z*. IR (neat cm⁻¹) 2850.74 (N-CH₃), 1445.54 (C-H), 1326.55 (C-N). Mp: 193 -196 °C (ethyl acetate/ petroleum ether), literature melting point: 181-183 °C.^[170]

References

1. Louis D, Perry A, Reifenberger G, von Deimling A, Figarella-Branger D, Cavenee W et al. (2016). The 2016 World Health Organization Classification of Tumors of the Central Nervous System: a summary. *Acta Neuropathol Comm*, 131(6);803-820.
2. Quick Brain Tumor Facts [Internet]. National Brain Tumor Society. 2019 [cited 12 August 2019]. Available from: <https://braintumor.org/brain-tumor-information/brain-tumor-facts>
3. Tellingen O.V, Yetkin-Arik B, Gooijer M, Wesseling P, Wurdinger T, de Vries E.T.(2015). Overcoming the blood-brain tumor barrier for effective glioblastoma treatment. *Drug Resist Update*, 19;1-12.
4. Fernandes G, Fernandes B.C, Valente V, Santos J. (2018). Recent advances in the discovery of small molecules targeting glioblastoma. *Eur J Med Chem*, 164;8-26.
5. Almuwaqqat Z, Meisel J, Barac A, Parashar S. (2019). Breast cancer and heart failure. *Heart Fail Clin*, 15(1);65-67.
6. Jian Y, Wang M, Zhang Y, Ou R, Zhu Z, Ou Y, Chen X, Ding Y, Song L, Xu X, Liao W. (2018) Jade family PHD finger 3 (JADE3) increases cancer stem cell-like properties and tumorigenicity in colon cancer. *Cancer Lett*, 428(1);1-11.
7. Vivar I.O, Lin C.L, Firestone G, Bjeldanes L.F. (2009). 3,3'-Diindolylmethane induces a G₁ arrest in human prostate cancer cells irrespective of androgen receptor and p53 status. *Biochem Pharmacol*, 78(5);469-476.
8. El-sayed M, Hamdy N, Osman D, Ahmed, K. (2015). Indoles as anticancer agents. *Adv Mod Oncol Res*, 1(1);20-35.
9. Lee S.O, Li X, Hendrick E. (2014). Diindolylmethane analogs bind NR4A1 and are NR4A1 antagonists in colon cancer cells. *J Clin Mol Endocrinol*, 28(10);1729-1739.
10. Andey T, Patel A, Jackson T, Safe S.H, Singh M. (2013). 1,1-Bis(3'-indolyl)-1-(p-substitutedphenyl)methane compounds inhibit lung cancer cell and tumor growth in a metastatis model. *Eur J Pharm Sci*, 50(2);227-241.
11. Bray F, Ferlay J, Soerjomataram I, Siegel R, Torre L.A, Jemal A. (2018). Global cancer statistics 2018: GLOBOCAN estimates of incidence and mortality worldwide for 36 cancers in 185 countries. *CA-Cancer J Clin*, 68(6);394-424.

12. Macconail L.E, Garraway L.A. (2010). Clinical implications of the cancer genome. *J Clin Oncol*, 28(35);5219–5228.
13. Garraway L.A, Lander E.S. (2013). Lessons from the cancer genome. *Cell*, 153(1);17-37.
14. Wu S, Zhu W, Thompson P, Hannun Y. (2018). Evaluating intrinsic and non-intrinsic cancer risk factors. *Nat Commun*, 9(1);3490.
15. Tarabichi M, Detours V.A. (2015). Variation in cancer risk among tissues can be explained by the number of stem cell divisions. *Sci*, 347(6217);78–81.
16. Magalhaes J.P. (2013). How ageing processes influence cancer. *Nat Rev Cancer*, 5(13);357-365.
17. Tomasetti C, Li L, Vogelstein B. (2017). Stem cell divisions, somatic mutations, cancer etiology, and cancer prevention. *Sci*, 355(6331);1330–1334.
18. Turini M, Redaelli A. (2001). Primary brain tumours: A review of research and management. *Int J Clin Pract*, 55(7);471-475.
19. Jin, B, Kim H.A, Sade B.L, Joung H. (2009). Meningiomas: Diagnosis, Treatment and Outcome. *Am J Neuroradiol*, 10(30);57.
20. Tomasello F, Angileri F, Conti A. (2017). Youmans and Winn Neurological Surgery. *Neurosurg*. 82(2);247-248.
21. Louis D, Ohgaki H, Wiestler O, Cavenee W, Burger P, Jouvett. (2007). The 2007 WHO Classification of Tumours of the Central Nervous System. *Acta Neuropathol Comm*, 114(2);97-109.
22. Patel A, Fisher J, Nichols E, Abd-Allah F, Abdela J, Abdelalim A. (2019). Global, regional and national burden of brain and other CNS cancer, 1990-2016: systematic analysis for the Global Burden of disease study 2016. *Lancet Oncol*, 18(4);376-393.
23. Burnet N.G, Jefferies S.J, Benson R.J. (2005). Years of life lost (YLL) from cancer is an important measure of population burden — and should be considered when allocating research funds. *Br J Cancer*, 92(2);241–245
24. Pineros M, Sierra M.S, Izarzugaza I, Forman D. (2016). Etiology of brain and central nervous system cancer in central and south America. *Cancer Epidem*, 44;141-149.
25. Fisher J.L, Schwartzbaum J.A, Wrensch M, Wiemels J.L. (2007). Epidemiology of brain tumors. *Neurol Clin*, 25(4);867–90
26. Preston-Martin S, Munir R, Chakrabarti I. (2006). The Nervous system. *Cancer Epidem Prev*, 3;1173-1195.

27. Lee W.J, Colt J.S, Heineman E.F. (2005). Agricultural pesticide use and risk of glioma in Nebraska, United States. *Occup Environ Med*, 62;786–792.
28. Provost D, Cantagrel A, Lebailly P. (2007) Brain tumours and exposure to pesticides: a case-control study in southwestern France. *Occup Environ Med*, 64(8);509–514.
29. Ostrom Q.T, Bauchet L, Davis F.G, Deltour I, Fisher J.L, Langer C.E. (2014). The epidemiology of glioma in adults: a ‘state of the science’ review. *Neuro Oncol*, 16(7);896–913.
30. Dorsey J.F, Hollander A.B, Alonso-Basanta M, Macyszyn L, Bohman L.E, Judy KD. (2014). Cancer of the central nervous system. *Clin Oncol*, 5;938–1001.
31. The University of Sydney [Internet]. *Psycho-oncology Co-operative Research Group (PoCoG) (2008). Quality of Life Office*. [Cited 27 July 2019] Available from: http://www.pocog.org.au/content.aspx?page=Brain_tumours
32. Litofsky N, Farace E, Anderson F, Meyers C, Huang W, Laws, E. (2004). Depression in patients with high-grade glioma: Results of the Glioma Outcomes Project. *Neurosurg*, 54(2);358– 366.
33. Gao H, Jiang X. (2013). Progress on the diagnosis and evaluation of brain tumors. *Cancer Imaging*, 13(4);466–481.
34. Bernard F, Romsa J, Hustinx R. (2003). Imaging gliomas with positron emission tomography and single-photon emission computed tomography. *Semin Nucl Med*, 33(2);148-162.
35. Olivero W.C, Dulebohn S.C, Lister J.R. (1995). The use of PET in evaluating patients with primary brain tumours: is it useful?. *J Neurol Neurosurg Psychiatry*, 58;250-252.
36. Haberer T, Habermehl T, Jakel O, Rieken S. (2012). Proton and carbon ion radiotherapy for primary brain tumors delivered with active raster scanning at the Heidelberg Ion Therapy Centre (HIT): Early treatment results and study concepts. *Radiat Oncol*, 7(47).
37. Brodbelt A, Greenberg D, Winters T, Williams M, Von S, Collins V.P. (2015). Glioblastoma in England: 2007-2011. *Eur J Oncol*, 51(4);533-542.
38. Banan R, Hartmann C. (2017). The new WHO 2016 classification of brain tumors—what neurosurgeons need to know. *Acta Neuro Comm*, 159(3);403-418.

39. Nakamura M, Yang F, Fujisawa H, Yonekawa Y, Kleihues P, Ohgaki H. (2000). Loss of Heterozygosity on Chromosome 19 in Secondary Glioblastomas. *J Neuropath Exp Neur*, 59(6);539–543.
40. Ohgaki H, Kleihues P. (2007). Genetic pathways to primary and secondary glioblastoma. *Am J Pathol*, 170(5);1445-1435.
41. Ohgaki H, Wantanabe K, Tachibana O, Sata K, Yonekawa Y, Kleihues P. (2008). Overexpression of the EGF receptor and p53 mutations are mutually exclusive in the evolution of primary and secondary glioblastomas. *Brain Pathol*, 6(3);217-223.
42. Lacroix M, Abi-Said D, Founrey D, Gokaslan Z. (2001). A multivariate analysis of 416 patients with glioblastoma multiforme: prognosis, extent of resection and survival. *J Neurol*, 95(2);190-198.
43. Markert J.M. (2012). The role of Early resection vs biopsy in the management of low-grade gliomas. *JAMA*, 302(18);1918-1919.
44. Levin V.A, Silver P, Hannigan J, Wara W.M, Gutin P.H, Davis R.L, Wilson C.B. (1990). Superiority of post-radiotherapy adjuvant chemotherapy with CCNU, procarbazine, and vincristine (PCV) over BCNU for anaplastic gliomas: NCOG 6G61 final report. *Int J Radiat*, 18(2);321-324.
45. Nguyen Q.T, Tsien R.Y. (2015). Fluorescence-guided surgery with live molecular navigation – a new cutting edge. *Nat Rev Cancer*, 13(9);653-662.
46. Heinemann I.K, Jahn M, Jahn D. (2008). The biochemistry of heme biosynthesis. *Arch Biochem Biophys*, 474(2);238-251.
47. Pogue B.W, Gibbs-Strauss S, Valdés P.A, Samkoe K, Roberts D.W, Paulsen K. D. (2010). Review of Neurosurgical Fluorescence Imaging Methodologies. *J Sel Top Quant*, 16(3);493–505.
48. Craig S, Wright J, Sloan A.E, Brady-Kalnay S.M. (2016). Fluorescent-Guided Surgical Resection of Glioma with Targeted Molecular Imaging Agents: A Literature Review. *World Neurosurg*, 90;154–163.
49. Stummer W, Pichlmeier U, Meinel T, Wiestler O.D, Zanella F, Reulen H.J. (2006). Fluorescence-guided surgery with 5-aminolevulinic acid for resection of malignant glioma: a randomised controlled multicentre phase III trial. *Lancet Oncol*, 7(5);392-401.

50. Senders J.T, Muskens I.S, Schnoor R, Karhade A.V, Cote D.J, Smith T.R, Broekman M.L. (2017). Agents for fluorescence-guided glioma surgery: a systematic review of preclinical and clinical results. *Acta neurochir*, 159(1);151–167.
51. Chung I.W, Eljamel S. (2013). Risk factors for developing oral 5-aminolevulinic acid- induced side effects in patients undergoing fluorescence guided resection. *Photodyn Ther*, 4(10);362-367.
52. Kristiansen K, Hagen S, Kollevold T. (1981). Combined modality therapy of operated astrocytomas grade III and IV. Confirmation of the value of postoperative irradiation and lack of potentiation of bleomycin on survival time: a prospective multicentre trial of the Scandinavian glioblastoma study group. *Cancer*, 47;649-652.
53. Laperriere N, Zuraw L, Gairncross G. (2002). Radiotherapy for newly diagnosed malignant glioma in adults: a systematic review. *Radiat Oncol J*, 64;259-273.
54. Stupp R, Mason W.P, van den Bent M.J, Weller M, Fisher B, Taphoorn M.J, Belanger K, Brandes A.A, Marosi C, Bogdahn U, Curschmann J, Janzer R.C, Ludwin S.K, Gorlia T, Allgeier A, Lacombe D, Cairncross J.G, Eisenhauer E, Mirimanoff R.O. (2005). Radiotherapy plus concomitant and adjuvant temozolomide for glioblastoma. *N Engl J Med*, 354(10);987-996.
55. Walker M, Alexander E, Hunt W, MacCarty C.S, Mahely M. (1978). Evaluation of BCNU and/or radiotherapy in the treatment of anaplastic gliomas. *J Neurosurg*, 49(3);333-343.
56. Walker M, Strike T.A, Sheline G.E. (1979). An analysis of dose-effect relationship in the radiotherapy of malignant gliomas. *Int J Radiat*, 5(10);1725-1731.
57. Parton S, Pearce A. (2012). A review of the necessary planning target volume margins for patients receiving radiation to the brain. *J Med Imaging Radiat Oncol*. 43(2);143.
58. Burnet N.G, Thomas S.J, Burton K.E, Jefferies S.J. (2004). Defining the tumour and target volumes for radiotherapy. *Cancer Imaging*, 4(2);153–161.
59. Rampling R, James A, Papanastassiou V. (2004). The present and future management of malignant brain tumours: Surgery, Radiotherapy and Chemotherapy. *J Neurol Neurosurg Psychiatry*, 7;24-30.

60. Inda M.M, Bonavia R, Seoane J. (2014). Glioblastoma multiforme: A look inside its heterogenous nature. *Cancers*, 6(1); 226-239.
61. Taal W, Bromberg J.E, Bent M.J. (2015). Chemotherapy in glioma. *CNS Oncol*, 4(3);179-192.
62. Bregy A, Shah A, Diaz M, Pierce H, Ames P, Diaz D, Komotar R. (2013). The role of Gliadel wafers in the treatment of high-grade gliomas. *Exp Rev Anticancer Ther*, 13(12);1453-1461.
63. Stupp R, Mason W.P, van den Bent M.J. (2005). Radiotherapy plus concomitant and adjuvant Temozolomide for Glioblastoma. *N Engl J Med*, 352(10);987-996.
64. Lee S.Y. (2016). Temozolomide resistance in glioblastoma multiforme. *Gen Dis*, 3(3);198-210.
65. Agarwala S.S, Kirkwood J.M. (2000). Temozolomide, a novel alkylating agent with activity in the central nervous system, may improve the treatment of metastatic melanoma. *Oncol*, 5(2);144-151.
66. Denny B.J, Wheelhouse R.T, Stevens M, Tsang L, Slack J.A. (1994). NMR and molecular modelling investigation of the mechanism of activation of the antitumour drug temozolomide and its interaction with DNA. *Biochem*, 33;9045-9051.
67. Newlands E.S, Stevens M.G, Wedge S.R. (1997). Temozolomide: a review of its discovery, chemical properties, pre-clinical development and clinical trials. *Cancer Treatment Rev*, 23;35-61.
68. Zambruno G, Alvino E, Castiglia D, Pepponi R, Caporaso P, Lacal P.M, Marra G, Fischer F, Bonmassar E. (2006). A single cycle of treatment with temozolomide, alone or combined with O-6-benzylguanine induces strong chemoresistance in melanoma cell clones in vitro: Role of O-6-methylguanine-DNA, methyltransferase and the mismatch repair system. *Int J Oncol*, 29(4);785-797.
69. Zhang J, Stevens M.F, Laughton C.S, Madhusudan S, Bradshaw T.D. (2010). Acquired resistance to Temozolomide in glioma cell lines: molecular mechanisms and potential translational applications. *Onco*, 78(2);103-114.
70. Thomas A, Tanaka M, Trepel J, Reinhold W. C, Rajapakse V.N, Pommier Y. (2017). Temozolomide in the Era of Precision Medicine. *Cancer Res*, 77(4);823–826.

71. Zhang J, Stevens M, Bradshaw T.D. (2015). Temozolomide: Mechanisms of action, repair and resistance. *Curr Molecular Pharmacol*, 5;102-114.
72. Perazzoli G, Prados J, Ortiz R, Caba O, Cabeza L, Berdasco M, Melguizo C. (2015). Temozolomide Resistance in Glioblastoma Cell Lines: Implication of MGMT, MMR, P-Glycoprotein and CD133 Expression. *PloS One*, 10(10).
73. World Cancer Research Fund. (2007). American Institute for Cancer Research. Food, Nutrition, Physical Activity, and the Prevention of Cancer: A Global Perspective. *Am J Cancer Res*, 1(10);464-469.
74. Soerjomataram I, Vries D.V. (2010). Increased consumption of fruit and vegetables and future cancer incidence in selected European countries. *Eur J Cancer*, 46(14);2563-2580.
75. Gandini S, Merzenich H, Robertson C, Boyle P. (2000). Meta-analysis of studies on breast cancer risk and diet: the role of fruit and vegetable consumption and the intake of associated micronutrients. *Eur J Cancer*, 36;636-646.
76. Voorrips L.E, Goldbohm R.A, van Poppel G, Sturmans F, Hermus R.J, van den Brandt P.A. (2000). Vegetable and fruit consumption and risks of colon and rectal cancer in a prospective cohort study: The Netherlands Cohort Study on Diet and Cancer. *Am J Epidemiol*, 152:1081–1092.
77. Potter JD, Steinmetz KA. (1996). Vegetables, fruit and cancer prevention: A review. *J Am Diet Assoc*, 10;1027-1039.
78. Terry P, Wolk A, Persson I, Magnusson C. (2001). Brassica vegetables and breast cancer risk. *JAMA*, 285(23);2975-2977
79. Voorrips L.E, Goldbohm R.A, van Poppel G. (2000). Vegetable and fruit consumption and risks of colon and rectal cancer in a prospective cohort study: The Netherlands Cohort Study on Diet and Cancer. *Am J of Epidemiol*, 152(11);1081-1092.
80. Chow W.H, Schuman L.M, McLaughlin J.K. (1992). A cohort study of tobacco use, diet, occupation, and lung cancer mortality. *Cancer Cause Control*, 3(3);247-254.
81. Feskanich D, Ziegler R.G, Michaud D.S. (2000). Prospective study of fruit and vegetable consumption and risk of lung cancer among men and women. *J Natl Cancer Inst*, 92(22);1812-1823
82. Bell M.C, Crowley-Nowick P, Bradlow H. (2000). Placebo-controlled trial of indole-3-carbinol in the treatment of CIN. *Gynecologic Oncol*, 78(2):123-129.

83. International agency for research on cancer. Cruciferous vegetables, isothiocyanates and indoles. (2004) *IRAC handbook of cancer prevention*. 9.
84. Navarro S.L, Li F, Lampe J.W. (2011). Mechanisms of action of isothiocyanates in cancer chemoprevention: an update. *Food funct.* 2;579-587.
85. McDanell R, McLean A.E, Hanley A.B, Heaney R.K, Fenwick G.R. (1988). Chemical and biological properties of indole glucosinolates (glucobrassicins): a review. *Food Chem Toxicol*, 26;59–70.
86. Gebicki J, Marcinek A, Michalski R, Sikora A. (2010). Radicals and Radical ions derived from indole, indole-3-carbinol and diindolylmethane. *J Phys Chem*, 25(114);6787-6794.
87. Reed G.A, Arneson D, Putnam W, Smith H, Gray J, Sullivan D, Mayo M, Crowell J, Hurwitz A. (2006). Single-dose and multiple-dose administration of indole-3-carbinol to women: pharmacokinetics based on 3,3'-Diindolylmethane. *Cancer Epidemiol Biomark Prev*, 15(22):2477-2481.
88. Sravanthi T.V, Manju S.L. (2015). A promising scaffold for drug development. *Eur J Pharm Sci*, 91;1-10.
89. Dadashpour S, Emami S. Indole in the target-based design of anticancer agents. (2018). A versatile scaffold with diverse mechanisms. *Eur J Med Chem*, 150;9-29.
90. Nicastro H, Gary L, Firestone L, Leonard F, Bjeldanes L. (2013). 3,3'-Diindolylmethane rapidly and selectively inhibits hepatocyte growth factor/c-Met signalling in breast cancer cells. *J Nutr Biochem*, 24(11);1882-1888.
91. Li X.J, Park E.S, Park M.H, Kim S.M. (2013). 3,3'-Diindolylmethane suppresses the growth of gastric cancer cells via activation of the hippo signalling pathway. *Oncology Rep*, 30(5);2419-2426.
92. Kim S.J, Lee J, Kim S.M. (2012). 3,3'-Diindolylmethane suppresses growth of human esophageal squamous cancer cells by G1 cell cycle arrest. *Oncol. Rep*, 27;1669–1673.
93. Kim E.J, Park S.Y, Shin H.K, Kwon D.Y, Surh Y.J, Park J.H. (2007). Activation of caspase-8 contributes to 3,3'-Diindolylmethane-induced apoptosis in colon cancer cells. *J Nutr*, 137;31–36.
94. Gong Y, Firestone G.L, Bjeldanes L.F. (2006). 3,3'-diindolylmethane is a novel topoisomerase II α catalytic inhibitor that induces S-phase retardation and mitotic delay in human hepatoma HepG2 cells. *Mol Pharmacol*, 69(4);1320-1327.

95. Ali S, Banerjee S, Ahmad A, El-Rayes BF, Phillip PA, Sarkar FH. (2008). Apoptosis-inducing effect of erlotinib is potentiated by 3,3'-diindolylmethane in vitro and in vivo using an orthotopic model of pancreatic cancer. *Mol Cancer Ther*, 7(6);1708-1719.
96. Kim S. M. (2016). Cellular and Molecular Mechanisms of 3,3'-Diindolylmethane in Gastrointestinal Cancer. *Int J Mol Sci*, 17(7);1155.
97. Vanderlaag K, Yunpeng S, Frankel A.E, Burghardt R.C, Barhoumi R. (2010). 1,1-Bis(3'-indolyl)-1-(p-substituted phenyl)methanes induce autophagic cell death in estrogen receptor negative breast cancer. *BMC cancer*, 10(1);669.
98. Wiatrak B.J. (2003) Overview of recurrent respiratory papillomatosis. *Int J Pediatr Otorhinolaryngol*, 11(6);433-441.
99. Derkay C.S, Wiatrak B.J. (2009). Recurrent Respiratory Papillomatosis: A review. *Laryngoscope*, 118(7);1236-1247.
100. Ghosh M.K, Bhowmik A, Das N, Pal U, Mandal M, Bhattacharya S, Sarker M, Jaisankar P, Maiti N.C. (2013). 2,2'-Diphenyl-3,3'-Diindolylmethane: A potent compound induces apoptosis in breast cancer cells by inhibiting EGFR pathway. *PloS One*, 8(3);e59798.
101. Safe S, McDougal A, Gupta M.S, Morrow D, Ramamoorthy K, Lee J.E. (2001). Methyl-substituted diindolylmethanes as inhibition of estrogen-induced growth of T47D cells and mammary tumors in rats. *Breast Cancer Res Tr*, 66(2);147-157.
102. Dai Y, Zhang W, Sun Q, Zhang X, Zhou X, Hu Y, Shi J. (2014). Nuclear receptor Nur77 promotes cerebral cell apoptosis and induces early brain injury after experimental subarachnoid haemorrhage in rats. *J Neurosci Res*. 92(9);1110-1121.
103. Chintharlapalli S, Burghardt R, Papineni S, Ramaiah S, Yoon K, Safe S. (2005). Activation of Nur77 by selected 1,1-Bis(3'indolyl)-1-(p-substituted phenyl)methanes induces apoptosis through nuclear pathways. *J Bio Chem*, 280(26);24903-14.
104. Chintharlapalli S, Cho S.D, Yoon K, Abdelrahim M, Lei P, Hamilton S, Khan S, Safe S. (2007). Nur77 agonists induce proapoptotic genes and responses in colon cancer cells through nuclear receptor-dependent and nuclear receptor-independent pathways. *Cancer Res*, 67(2);674-683.
105. Fajas L, Debril M.B, Auwerx J. (2001). Peroxisome proliferator-activated receptor- γ : from adipogenesis to carcinogenesis. *J Mol Endocrinol*, 27;1–9.

106. Kassouf W, Chintharlapalli S, Abdelrahim M, Nelkin G, Safe S, Kamat A.M. (2006). Inhibition of bladder tumour growth by 1,1-Bis(3'-indolyl)-1-(p-substitutedphenyl)methanes: A new class of peroxisome proliferator-activated receptor γ agonists. *Cancer Res*, 66(1);412-418.
107. Lei P, Abdelrahim M, Cho S.D, Liu S, Chintharlapalli S, Safe S. (2008). 1,1- Bis (3'-indolyl)-1-(p -substituted phenyl)methanes inhibit colon cancer cell and tumor growth through activation of c-jun N-terminal kinase. *Carcinogenesis*, 29(6);1139-1147.
108. Cho H.T, Choi E.S, Cho N.P, Cho S. (2011). Anti-tumorigenic effect of DIM-pPhBr and DIM-pPHF originating from cruciferous vegetables in KB human oral squamous cell carcinoma through apoptotic cell death. *J Food Saf*, 26(4);398-402.
109. Tocco G, Zedda G, Casu M, Simbula G, Begala M. (2017). Solvent-free addition of indole to aldehydes: unexpected synthesis of novel 1-[1-(1H)-Indol-3-yl) Alkyl]-1H-Indoles and preliminary evaluation of their cytotoxicity in hepatocarcinoma cells. *Molecules*, 22(10);1747.
110. Krishnaiah Y.S.R. (2012). Pharmaceutical technologies for enhancing oral bioavailability of poor soluble drugs. *JBB*. 2(2);28-36.
111. Benet L.Z, Hosey C.M, Ursu O, Oprea T.I. (2016). BDDCS, the rule of 5 and drugability. *Adv Drug Deliv Rev*, 101;89-98.
112. Molinspiration Cheminformatics Software. 2019 [cited 16 September 2019]. Available from: <https://www.molinspiration.com/>
113. Jellinck P.H, Forkert P.G, Riddick D.S, Okey A.D, Michnovicz J.J, Bradlow H.L. Ah receptor binding properties of indole carbinols and induction of hepatic estradiol hydroxylation. (1993). *Biochem Pharmacol*, 45(5);1129-1136.
114. Safe S, De Miranda B.R, Miller J.A, Hansen R.J, Lunghofer P.J, Gustafson D.L, Colagiovanni D, Tjalkens R.B. (2013). Neuroprotective efficacy and and pharmacokinetic behaviour of novel anti-inflammatory para-phenyl substituted diindolylmethanes in a mouse model of Parkinson's disease. *J Pharmacol Exp Ther*, 345(1);125-138.
115. Peng J, Lu J, Shen Q, Zheng M. (2013). In silico site of metabolism (SOM) prediction for human UGT-catalyzed reactions. *J Bioinform*. 30(3);398-405.
116. Safe S, Patel A, Spencer S, Chougule M.B, Singh M. (2012). Pharmacokinetic evaluation of in vitro-in vivo correlation (IVIC) of novel

- methylene-substituted 3,3' diindolylmethane (DIM). *Eur J Pharm Sci*, 46(1-2);8-16.
117. Jella R.R, Nagarajan R. (2013). Synthesis of indole alkaloids arsindoline A, arsindole B and their analogues in low melting mixtures. *Tetrahedron*, 69(48);10249-10253.
118. Majik M.S, Parameswaran P.S, Praveen P.J. (2015). Bis(indolyl)methane alkaloids: Isolation, Bioactivity and Syntheses. *Synthesis*, 47(13);1827-1837.
119. Nemallapudi B.R, Zyryanov G.V, Avula B, Guda M, Cirandur S, Venkataramaiah C, Gundala S. (2019). Meglumine as a green, efficient and reusable catalyst for synthesis and molecular docking studies of bis(indolyl)methanes as antioxidant agents. *Bio Chem*. 87;465-473.
120. Shiri M, Zolfigol M.A, Kruger H.G, Tanbakouchian Z. (2010). Bis- and Trisindolylmethanes (BIMs and TIMs). *Chem Rev*, 110;2250-2293.
121. Korolev A.M, Yudina N, Lazhko E.I, Reznikova M.I, Preobrazhenskaya M.N. (1999). Transformations of 3-formylindoles under the action of acids. *Chem Heterocycl*, 35(5);561-569.
122. Fridkin G, Boutard N, Lubell W.D. (2009). β,β -Disubstituted C- and N-Vinylindoles from one-step condensation of aldehydes and indole derivatives. *J Org Chem*, 74(15);5603-5606.
123. Pillaiyar T, Dawood M, Irum H, Muller C.E. (2018). A rapid, efficient and versatile green synthesis of diindolylmethanes. *Arkivoc*, 3;1-19.
124. Kamal A, Khan M.N, Reddy S.K, Ahmed S.K, Kumar K.P. (2007). An efficient synthesis of bis(indolyl)methanes and evaluation of their antimicrobial activities. *J Enzyme Inhib Med*, 24(2);559-565.
125. Wang Y.M, Yin Z, Zhang Z.H. (2005). An efficient and practical process for the synthesis of bis(indolyl)methanes catalyzed by Zirconium Tetrachloride. *Chem Heterocycl*, 36(52);1949-1954.
126. Desai U.V, Mitragotri S.D, Thopate T.S, Pore D.M, Wadgonkar P.P. (2007). Lithium Tetrafluoroborate-catalyzed solventless synthesis of α -aminonitriles. *Chem Monthly*, 138(8);759-762.
127. Vahdat S.M, Khaksar S, Baghery S. (2011). An efficient one-pot synthesis of Bis (indolyl)methanes catalyzed by ionic liquid with multi-SO₃H groups under ambient temperature in water. *World Appl Sci J*, 15(6);877-884.

128. Rajendran A, Raghupathy D, Priyadarshini M. (2011). A domino green synthesis of bis(indolyl)methanes catalyzed by ionic liquid [Et₃NH][H₂SO₄]. *Int J Chemtech Res*, 3(1);298-302.
129. Sandip S, Sonar S, Shelke K.F, Shingare M.S. (2008). Ionic liquid promoted synthesis of Bis(indolyl)methanes. *Cent Eur J Chem*, 6(4);622-626.
130. Zolfigol M.A, Khazaei A, Moosavi-Zare A.R, Zare A. Ionic liquid 3-methyl-1-sulfonic acid imidazolium chloride as a novel and highly efficient catalyst for the very rapid synthesis of bis(indolyl)methanes under solvent-free conditions. (2009). *New J Chem*, 42(1);95-102.
131. Hazarika P, Sharma S.D, Konwar D. (2008). Efficient synthesis of bis- and tris-indolylalkanes catalyzed by a Bronsted acid-surfactant catalyst in water. *Synth Commun*, 38(17);2870-2880.
132. Veisi H, Maleki B, Eshbala F.M, Vesisi H, Masti R, Ashrafi S.S, Baghayeri M. (2014). *In situ* generation of Iron(III) dodecyl sulfate as Lewis acid-surfactant catalyst for synthesis of bis-indolyl, tris-indolyl, Di(bis-indolyl), tetra(bis-indolyl)methanes and 3-alkylated indole compounds in water. *RSC Adv*, 5(4);30683-30688.
133. Reddy V.A, Reddy N.V.L, Ravinder K, Goud V.T. (2003). Zeolite catalyzed synthesis of bis(Indolyl)methanes. *ChemInform*, 33(21);3687-3694.
134. Karthik M, Magesh C.J, Perumal P.T, Palanichamy M, Arabindoo B, Murugesan V. (2005). Zeolite-catalyzed eco-friendly synthesis of Vibrindole A and bis(indolyl)methanes. *App Catal A*, 286(1);137-141.
135. Malik A.K, Pal R, Mandal T. (2007). Facile formation of bis(3-indolyl)methyl-arenes by iodine catalyzed reaction of indole with α,α' -bis(arylmethylene)ketones and α -substituted arylmethylene ketones in dry ethanol. *Ind J Chem*, 46B(12);2056-2059.
136. Zahran M, Abdin Y, Salama H. (2008). Eco-friendly and efficient synthesis of bis(indolyl)methanes under microwave irradiation. *Arkivoc*, 14;256-265.
137. Das P, Das J. (2012). Synthesis of aryl/alkyl(2,2'-bis-3-methylindolyl)methanes and aryl(3,3'-bis indolyl)methanes promoted by secondary amine based ionic liquids and microwave irradiation. *Tetrahedron*, 53(35);4718-4720.
138. Joshi R.S, Mandhane P.G, Diwakar S.D, Gill C.H. (2010). Ultrasound assisted green synthesis of bis(indol-3-yl)methanes catalyzed by 1-hexenesulphonic acid sodium salt. *Ultrason Sonochem*, 17(2);298-300.

139. Li J, Sun M.X, He G, Xu X.Y. (2011). Efficient and green synthesis of bis(indolyl)methanes catalyzed by ABS in aqueous media under ultrasound irradiation. *Ultrason Sonochem.* 18(1);412-414.
140. D'Azuria M. (1991). Photochemical synthesis of Diindolylmethanes. *Tetrahedron*, 47(44);9225-9230.
141. He F, Li P, Gu Y, Li G. (2009). Glycerol as a promoting medium for electrophilic activation of aldehydes: catalyst-free synthesis of di(indolyl)methanes, xantehe-1,8(2H)-diones and 1-oxohexahydroxanthenes. *Green Chem*, 11;1767-1773.
142. Hikawa H, Suzuki H, Yokoyama Y, Isao A. (2013). Mechanistic studies for synthesis of Bis(indolyl)methanes: Pd-Catalyzed C-H Activation of Indole-Carboxylic Acids with Benzyl Alcohols in Water. *Catalysts*, 3(2);486-500.
143. Bandgar B.P, Patil A.V, Kamble V.T. (2007). Fluoroboric acid adsorbed on silica gel catalyzed synthesis of bisindolyl alkanes under mild and solvent-free conditions. *Arkivoc*, 16;252-259.
144. Khosropur A.R, Baltork I.M, Khodaei M.M, Ghanbary P. (2006). Chemoselective One-pot conversion of Primary Alcohols to their Bis(indolyl)methanes promoted by $\text{Bi}(\text{NO}_3)_3 \cdot 5\text{H}_2\text{O}$. *Z.Naturforsch*, 62b;537-539.
145. Nikoofar K, Ghanbari K. (2015). A domino electro-oxidative synthesis of 3,3'-bis(indolyl)methane nanoparticles. *Chem Monthly*, 146(22);2021-2027.
146. Yang J, Wang Z, Pan F, Li Y, Bao W. (2010). CuBr-catalyzed selective oxidation of *N*-azomethine: highly efficient synthesis of methine-bridged bis-indole compounds. *Org Biomol Chem*, 8;2975-2978.
147. Gopalaiah K, Chandrudu S.N. (2015). Iron-catalyzed oxidative coupling of benzylamines and indoles: Novel approach for synthesis of Bis(indolyl)methanes. *Synthesis*, 47(12);1766-1774.
148. Xie Z.F, Hui Y.H, Chen Y.C, Gong H.W. (2014). Convenient synthesis of bis(indolyl)alkanes by dithiocarbohydrazone Schiff base/ $\text{Zn}(\text{ClO}_4)_2 \cdot 6\text{H}_2\text{O}$ catalyzed Friedel-Crafts reaction of indoles with imines. *Chin Chem Lett*, 25(1);163-165.
149. Ballini R, Palmieri A, Petrini M, Torregiani E. (2006). Solventless Clay-promoted Friedel-crafts reaction of indoles with α -amido sulfones: unexpected synthesis of 3-(1-Arylsulfonylalkyl) indoles. *Org Lett*, 8(18);4093-4096.
150. Vallee Y, Mauger H.C, Denis J.N, Pouchot M.T. (2000). The reaction of Nitrones with indoles. *Tetrahedron*, 56(5);791-804.

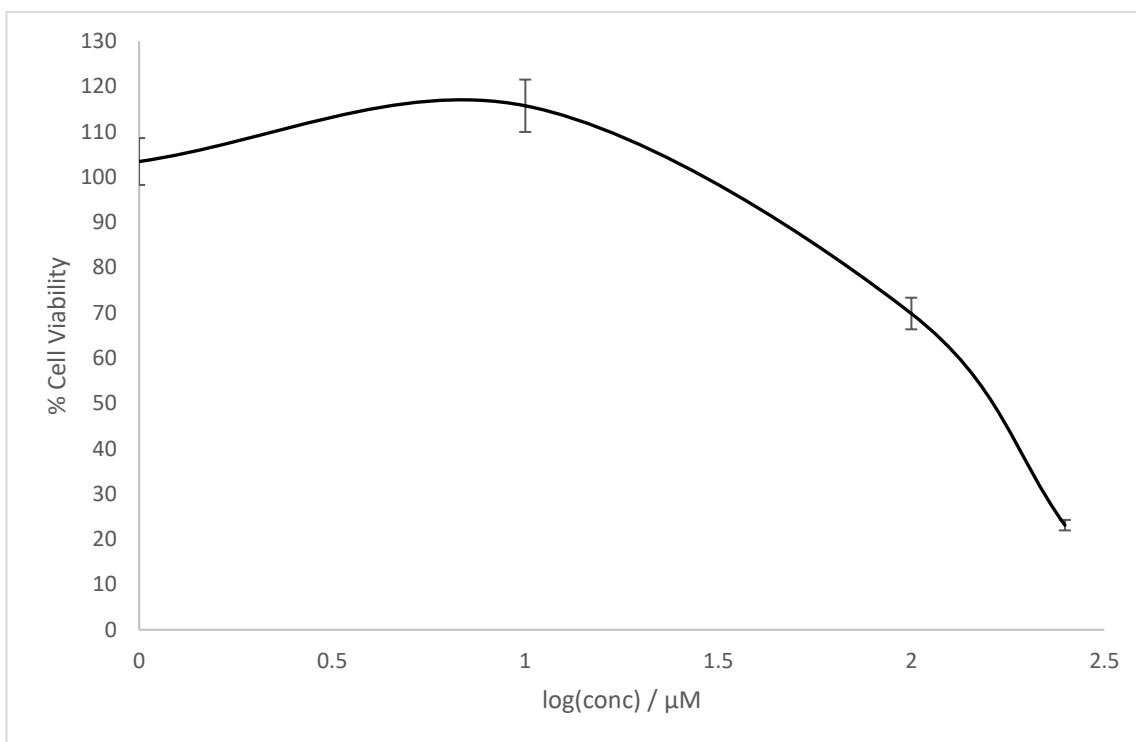
151. Vallee Y, Mauger H.C, Denis J.N. (1997). The reaction of Nitrones with indoles. Synthesis of asymmetrical diindolylalcanes. *Tetrahedron*, 38(49);8515-8518.
152. Promega. *CellTitre 96 AQueous One Solution Cell Proliferation Assay*. (2012). Madison, United States of America: Promega Technical Bulletin (1st ed.).
153. Bradlow H.L. (2008). Indole-3-carbinol as a Chemoprotective Agent in Breast and Prostate Cancer. *In Vivo*, 22;441-448.
154. Chen D.Z, Qi M, Auburn K.J, Carter T.H. (2001). Indole-3-carbinol and Diindolylmethane Induce Apoptosis of Human Cervical Cancer Cells and in Murine HPV16-Transgenic Preneoplastic Cervical Epithelium. *Nutr J*, 131(12);3294-3302.
155. Moiseeva E.P, Almedia G.M, Jones G.D.D. (2007). Extended treatment with physiologic concentrations of dietary phytochemicals results in altered gene expression, reduced growth, and apoptosis of cancer cells. *Mol Cancer Ther*, 6;3071-3079.
156. Garikapaty V, Ashok B.T, Tadi K, Mittelman A, Tiwari R.K. (2005). Synthetic dimer of indole-3-carbinol: Second generation diet derived anti-cancer agent in hormone sensitive prostate cancer. *Prostate*, 66(9);453-462.
157. Snape T.J, Prabhu S, Akbar Z, Harris F, Karakoula K, Lea R, Rowther F, Warr T. (2013). Preliminary biological evaluation and mechanism of action studies of selected 2-arylindoles against glioblastoma. *Bioorgan Med Chem*, 21(7);1918-1924.
158. Sherer C. (2017). A multidisciplinary investigation into the design, synthesis and evaluation of a novel class of anti-glioblastoma drug fragments. Doctoral thesis. University of Central Lancashire.
159. Snape T.J, Sherer C, Prabhu S, Adams D, Hayes J, Rowther F, Tolaymat I, Warr T. (2018). Towards identifying potent new hits for glioblastoma. *Med Chem Comm*, 9;1850-1861.
160. Escobedo-González R, Vargas-Requena C.L, Moyers-Montoya E, Aceves-Hernández J.M, Nicolás-Vázquez M.I, Miranda-Ruvalcaba R. (2017). In silico Study of the Pharmacologic Properties and Cytotoxicity Pathways in Cancer Cells of Various Indolylquinone Analogues of Perezone. *Molecules*, 22(7);1060.
161. Spaczyńska E, Mrozek-Wilczkiewicz A, Malarz K, Kos J, Gonec T, Oravec M, Gawecki R, Bak A, Dohanosova, Kapustikova I, Liptaj T. (2019). Design and

- synthesis of anticancer 1-hydroxynaphthalene-2-carboxanilides with a p53 independent mechanism of action. *Sci Rep*, 9;6387.
162. Khazaei M, Pazhouhi M, Khazaei S. (2019). Temozolomide and tranilast synergistic antiproliferative affect on human glioblastoma multiforme cell line (U87MG). *Med J Islam Repub Iran*, 33;39.
163. Lan F, Yang Y, Han J, Wu Q, Yu H, Yue X. (2016). Sulforaphane reverses chemo-resistance to temozolomide in glioblastoma cells by NF-kB-dependent pathway downregulating MGMT expression. *Int J Oncol*, 48(2);559-568.
164. Pandey V, Ranjan N, Narne P, Babu P.P. (2019). Roscovitine effectively enhances antitumour activity of temozolomide in vitro and in vivo mediated by increased autophagy and Caspase-3 dependent apoptosis. *Sci Rep*, 9(1);5012.
165. Lee S.Y. (2016). Temozolomide resistance in glioblastoma multiforme. *Genes Dis*, 3(3);198-210.
166. Honarmand M, Esmaeili E. (2017). Tris(hydroxymethyl)methane ammonium hydrogensulfate as a nano ionic liquid and its catalytic activity in the synthesis of bis(indolyl)methanes. *J Mol Liq*, 225;741-749.
167. Nemallapudi B, Zyryanov G, Avula B, Guda M.R, Cirandur S, Venkataramaiah C, Rajendra W, Gundala S. (2019). Meglumine as a green, efficient and reusable catalyst for synthesis and molecular docking studies of bis(indolyl)methanes as antioxidant agents. *J Biorgan Chem*, 87;465-473.
168. Cheng Y, Ou X, Ma J, Sun L, Ma Z.H. (2019). A new amphiphilic Bronsted acid as catalyst for the Friedel-Crafts reactions of indoles in water. *Eur J Organ Chem*, 2019(1);66-72.
169. Srinivasa A, Varma P.P, Hulikal V, Mahadevan K.M. (2008). Antimony (III) Sulfate catalysed condensation reaction o indoles with carbonyl compounds. *Chem Monthly*, 139(2);111-115.
170. Wang X, Aldrich C.C. (2019). Development of an imidazole salt catalytic system for the preparation of bis(indolyl)methanes and bis(naphthyl)methane. *PLoS One*, 14(4);e0216008.

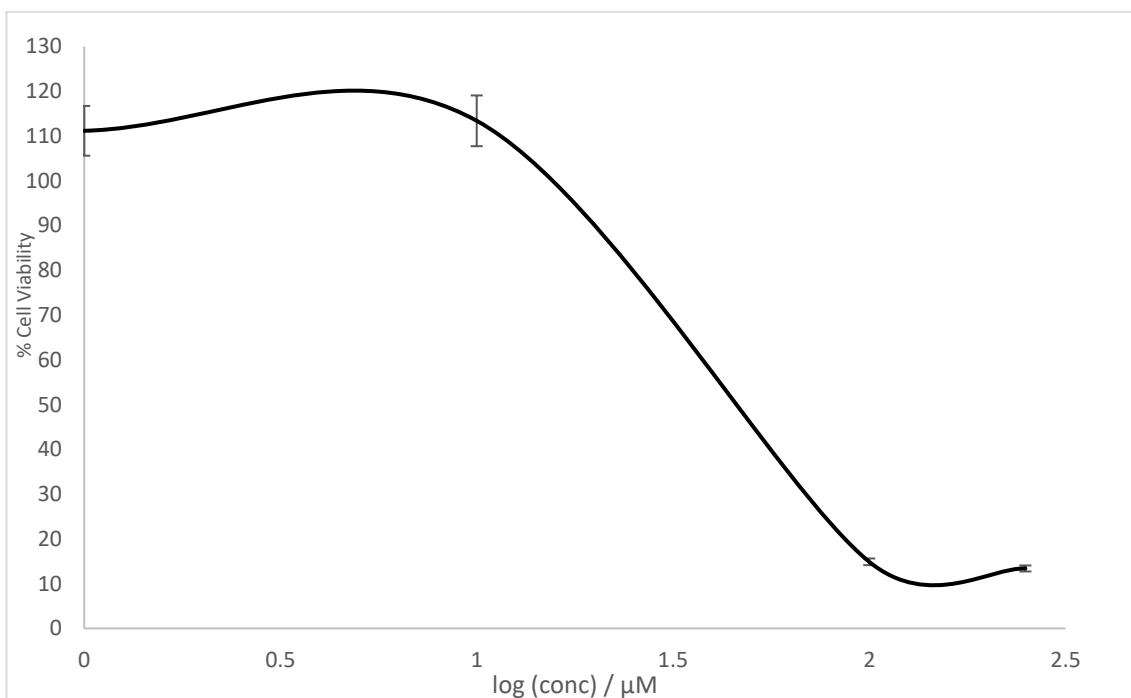
Appendix

Cell viability graphs

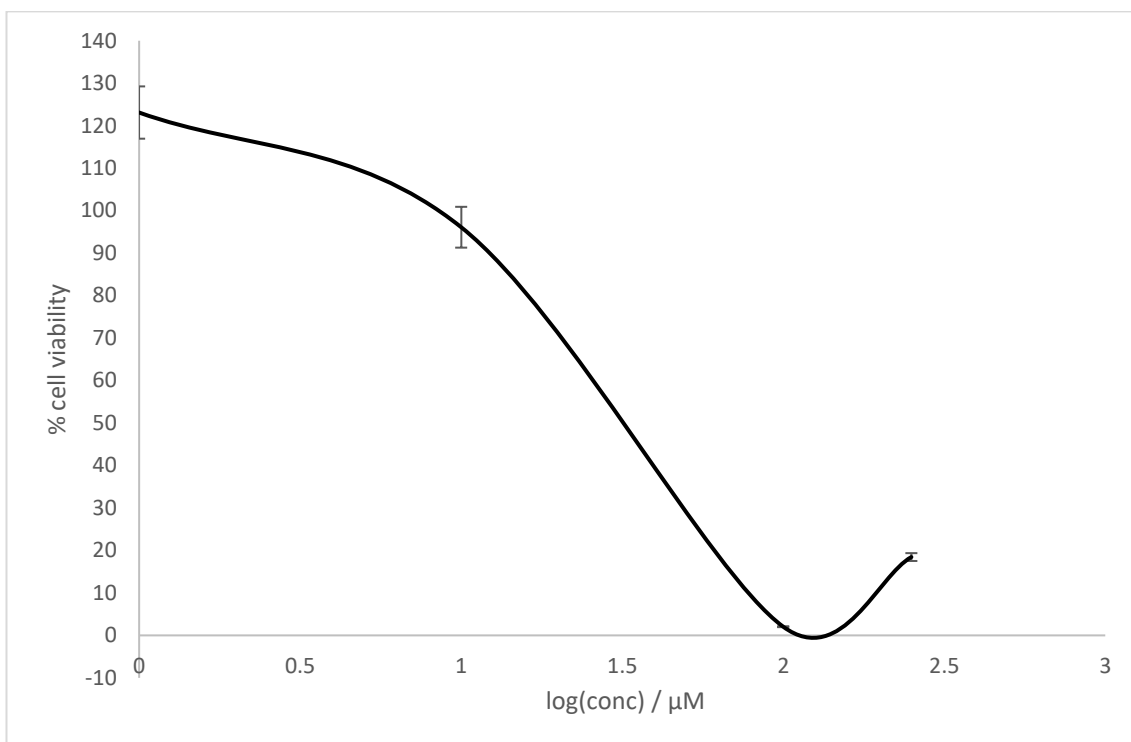
I3C



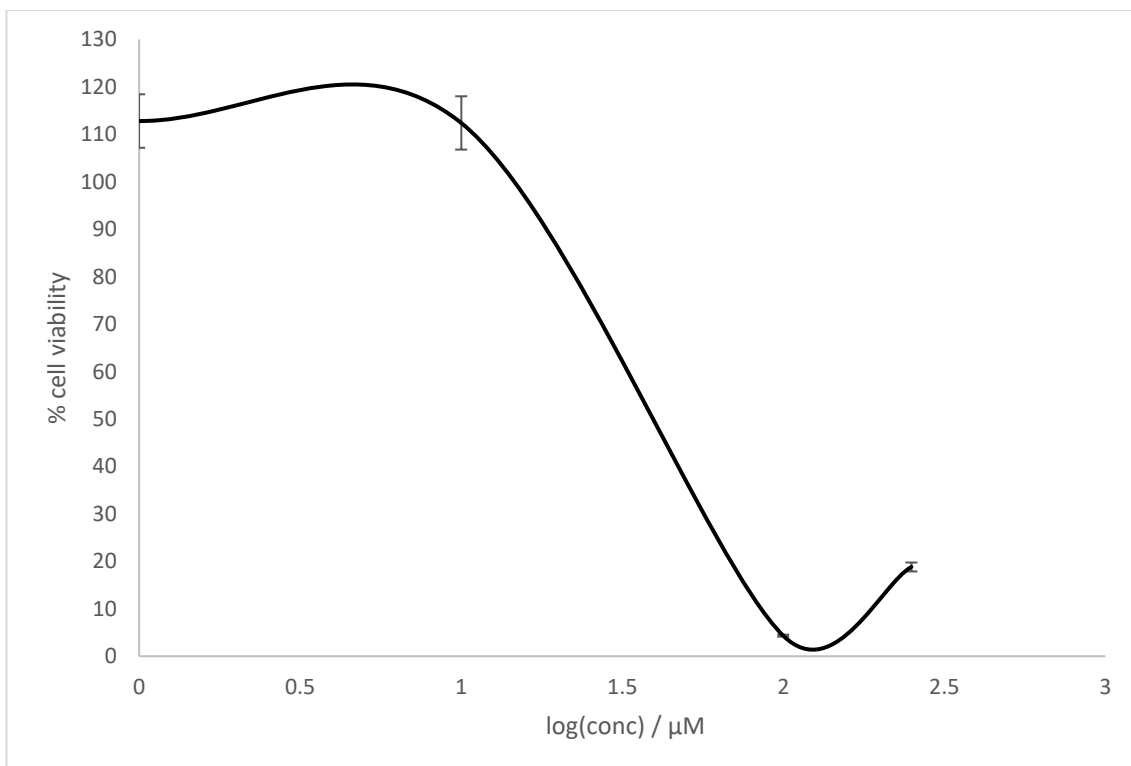
DIM



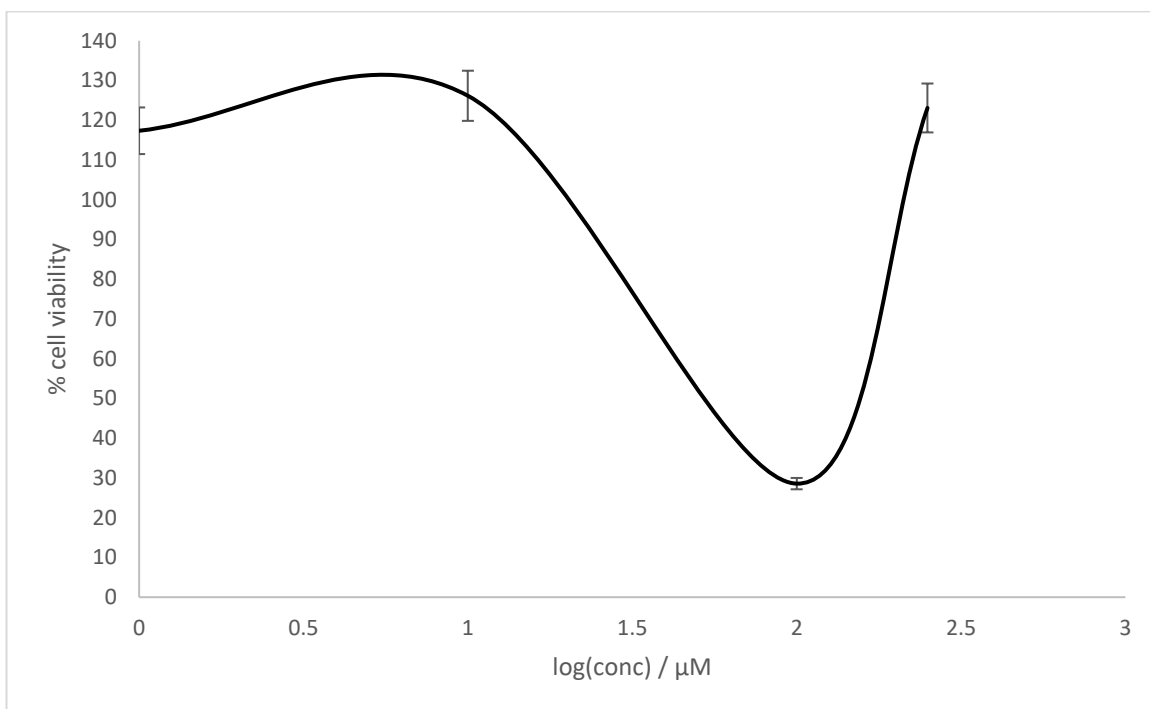
Compound 19



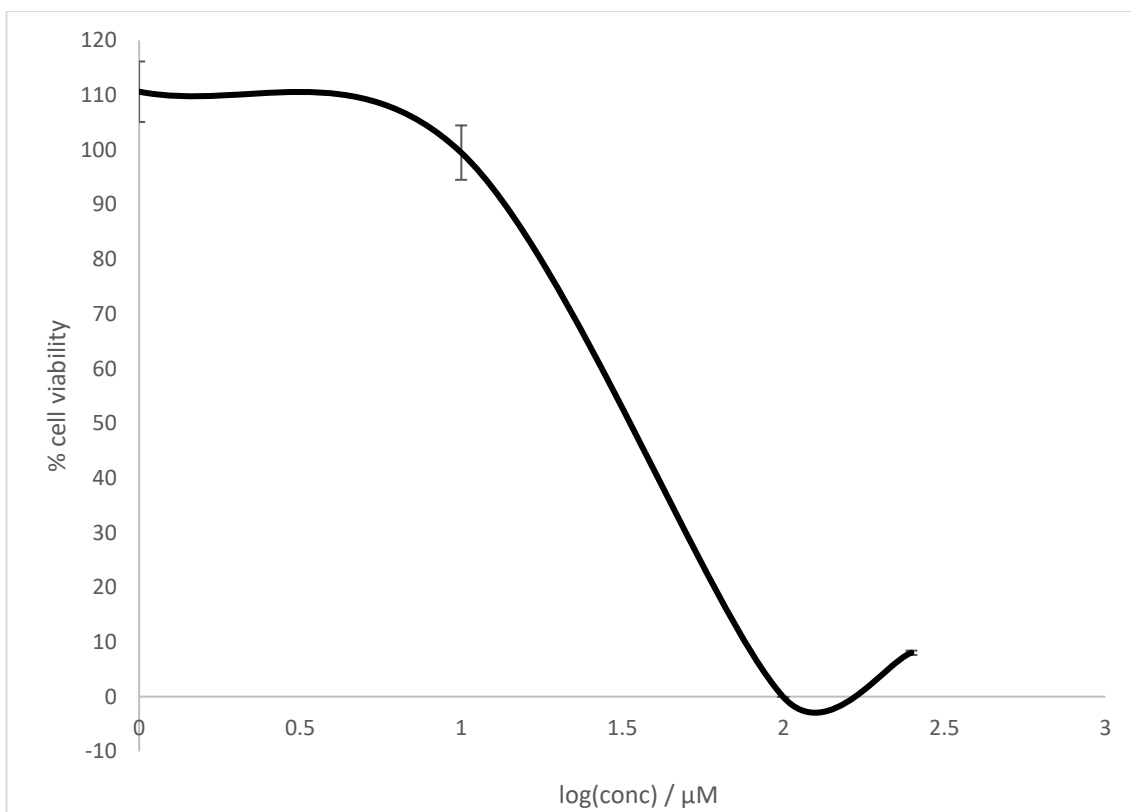
Compound 17



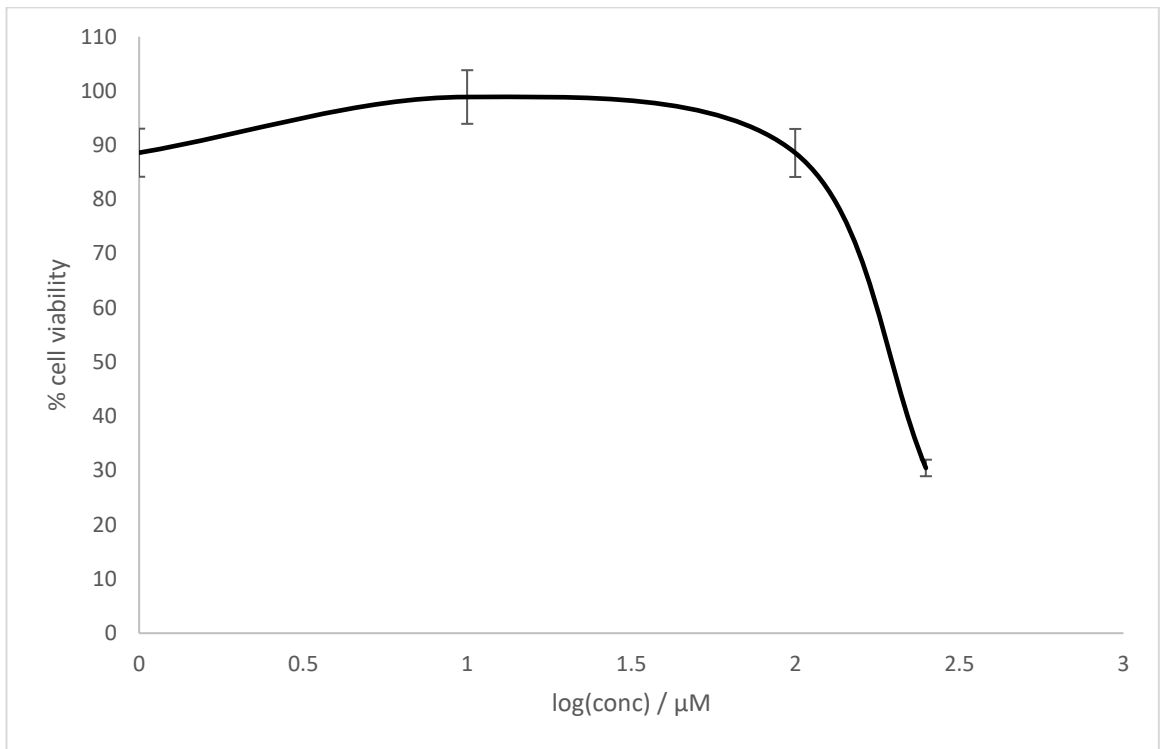
Compound 64



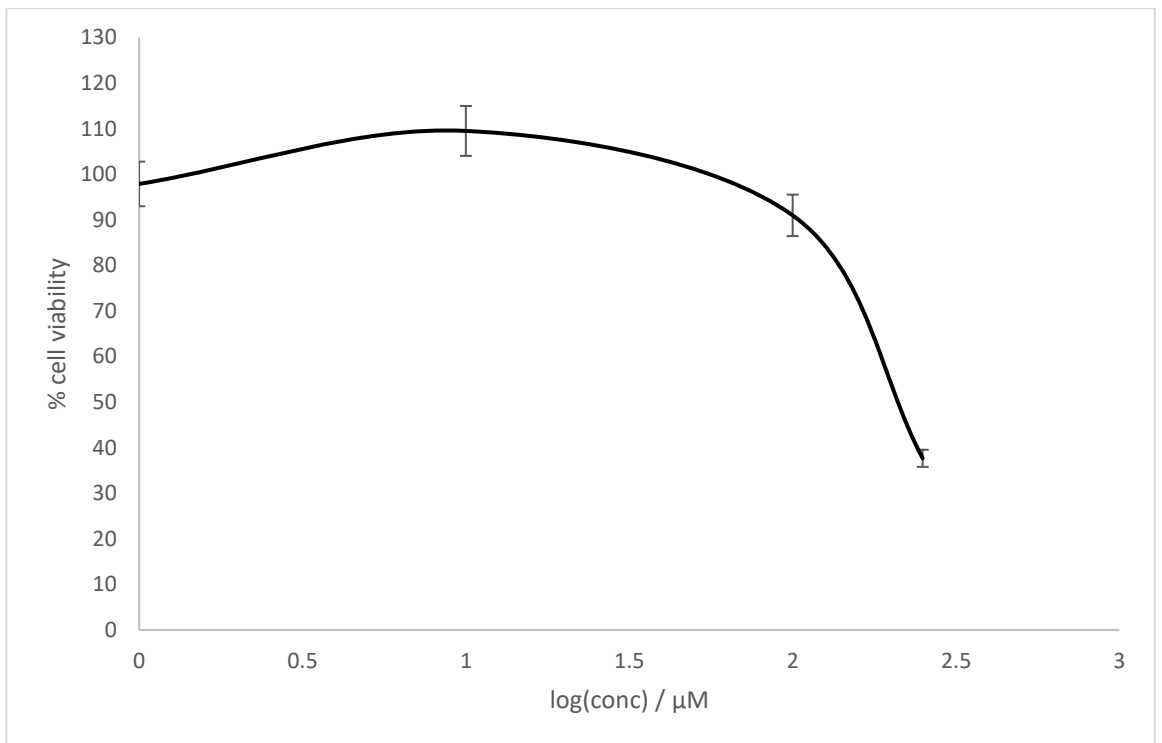
Compound 65



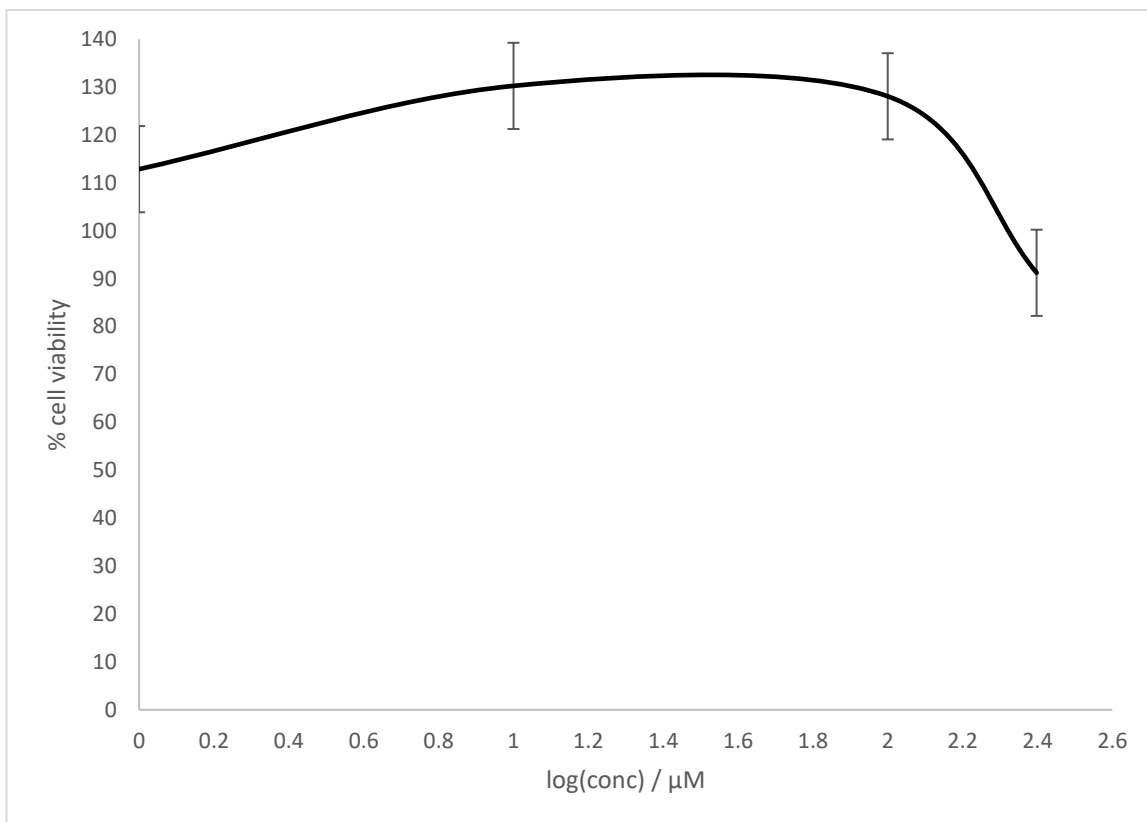
Compound 20



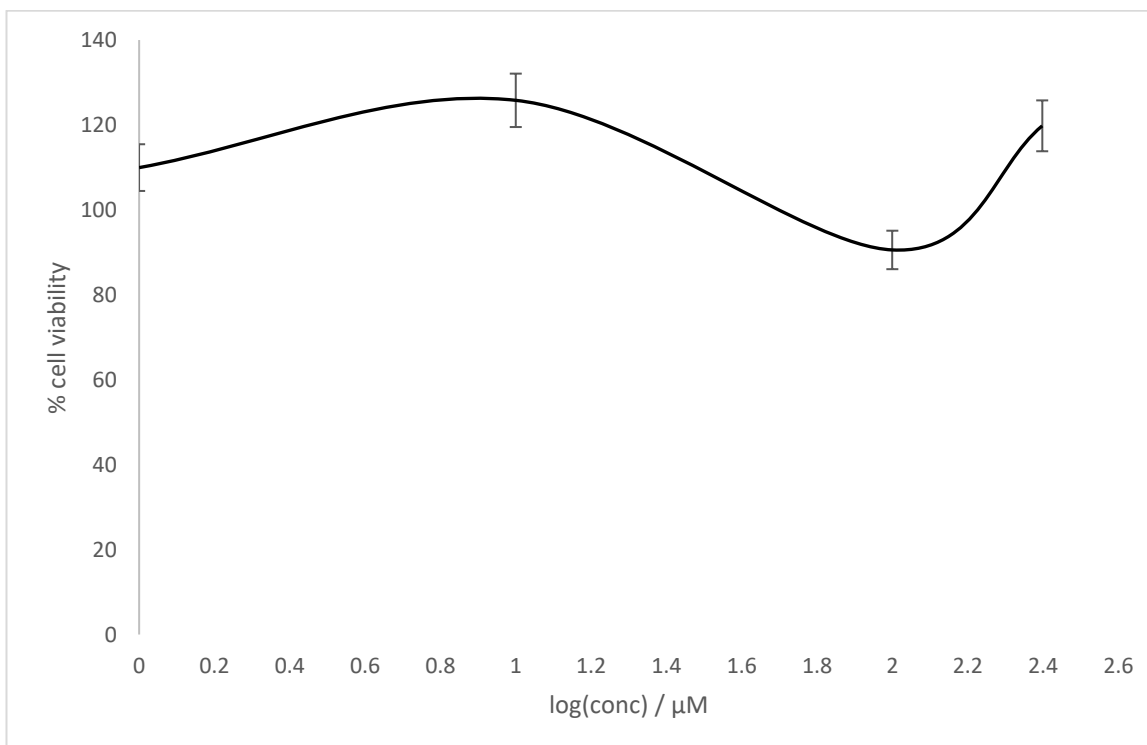
Compound 66



Compound 67

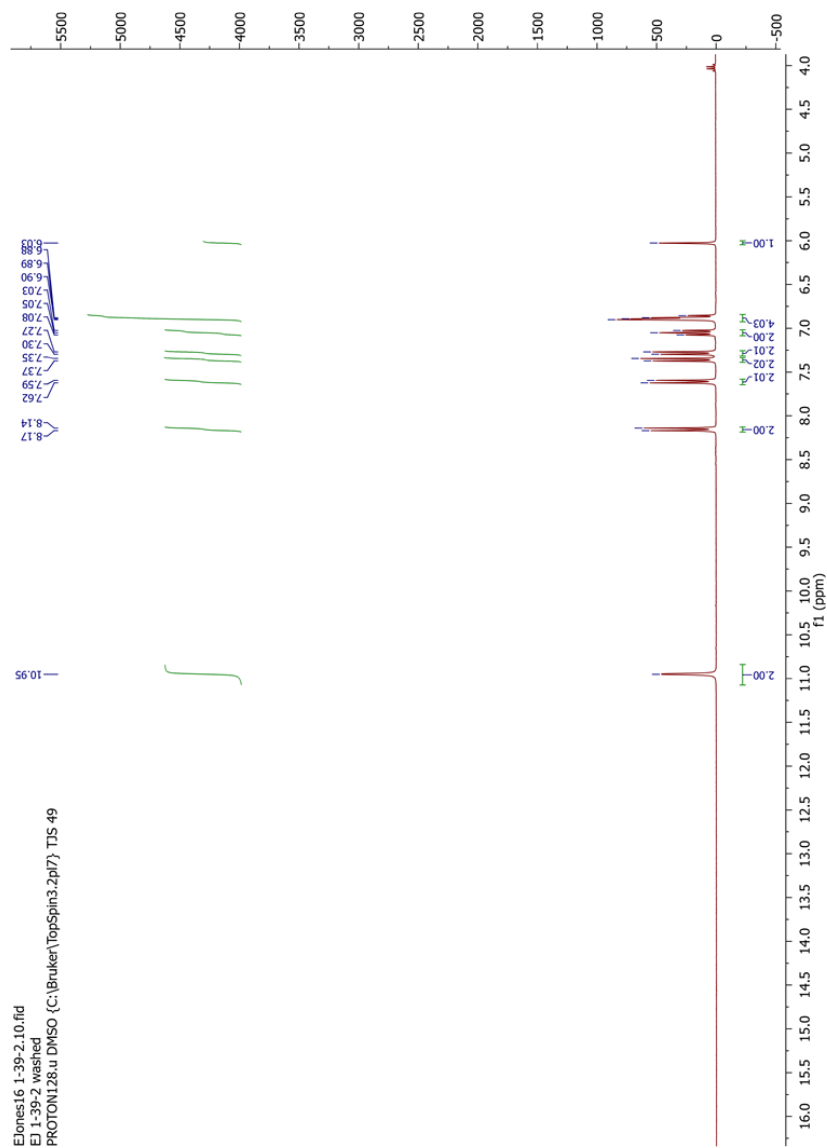


Compound 38

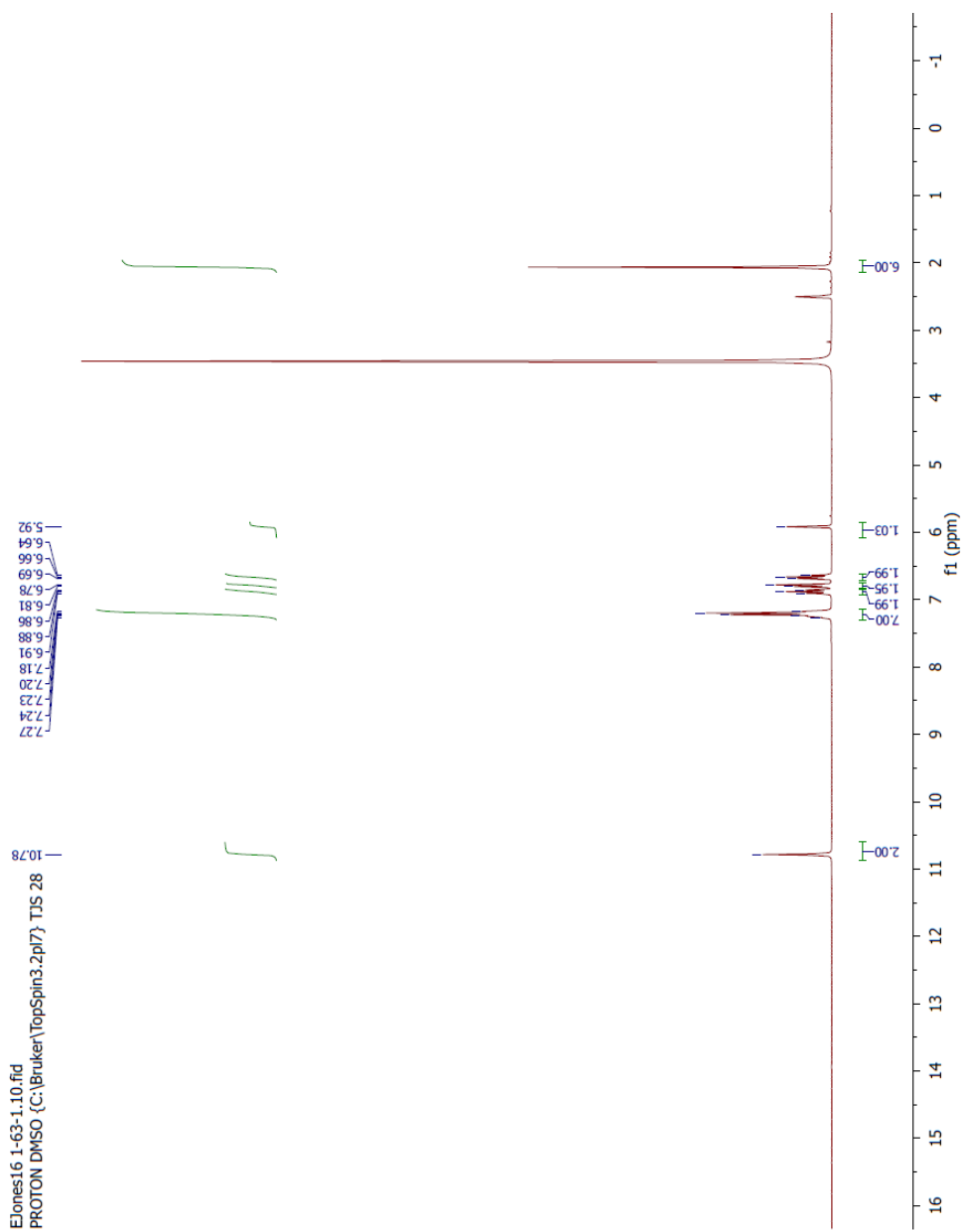


Analysis of selected compounds

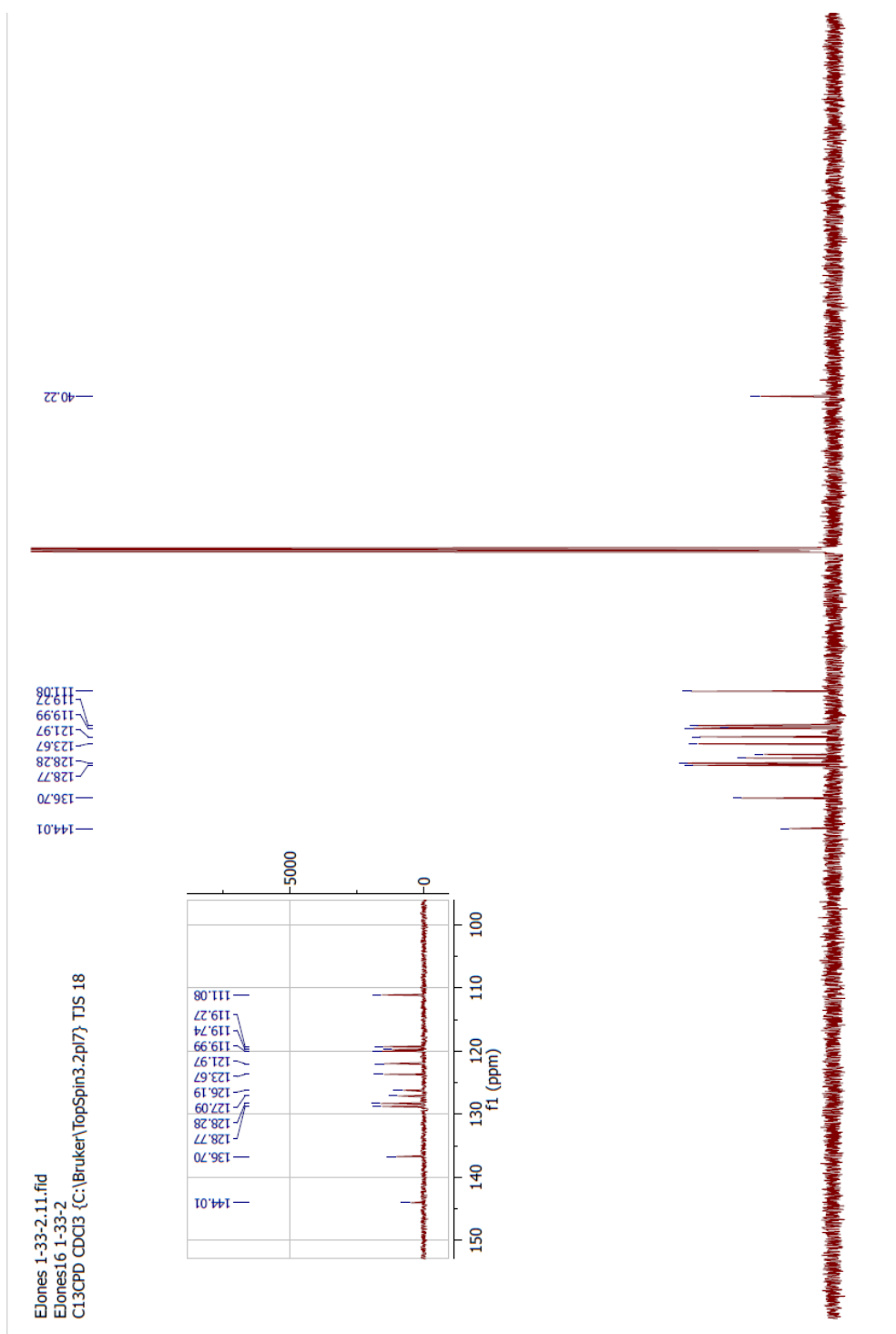
¹H NMR of compound 64



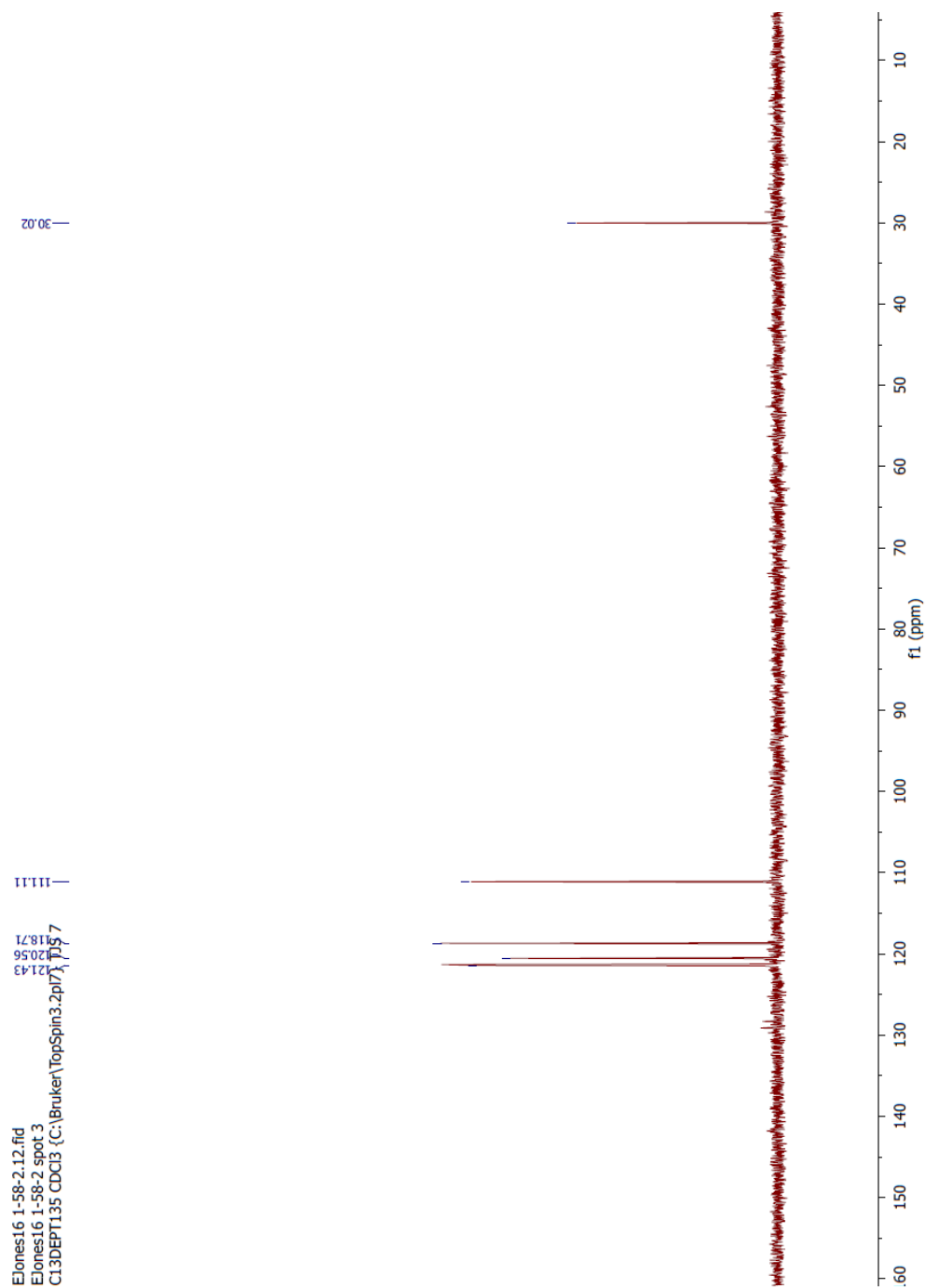
¹H NMR of compound **66**



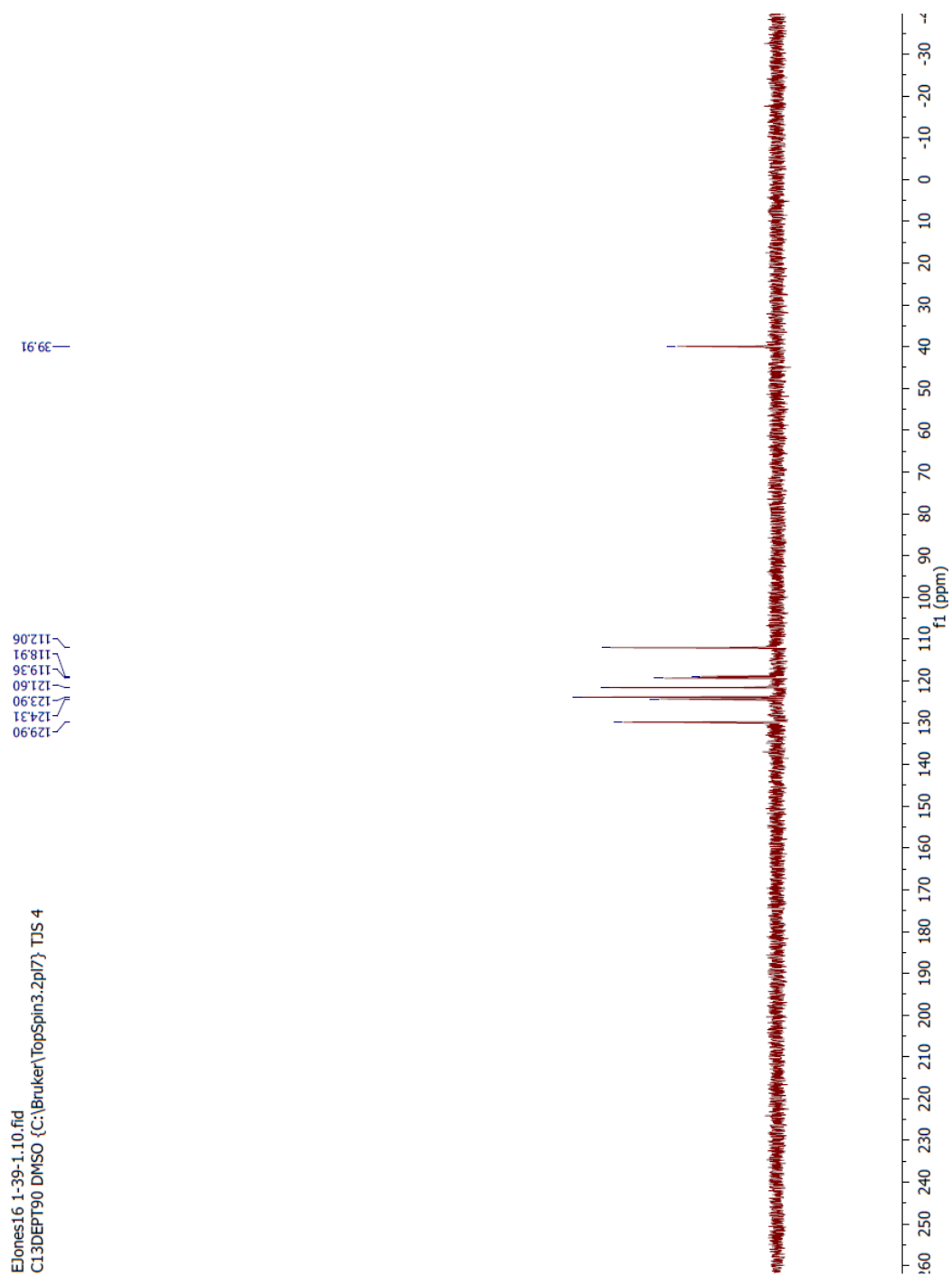
¹³C NMR of compound 19



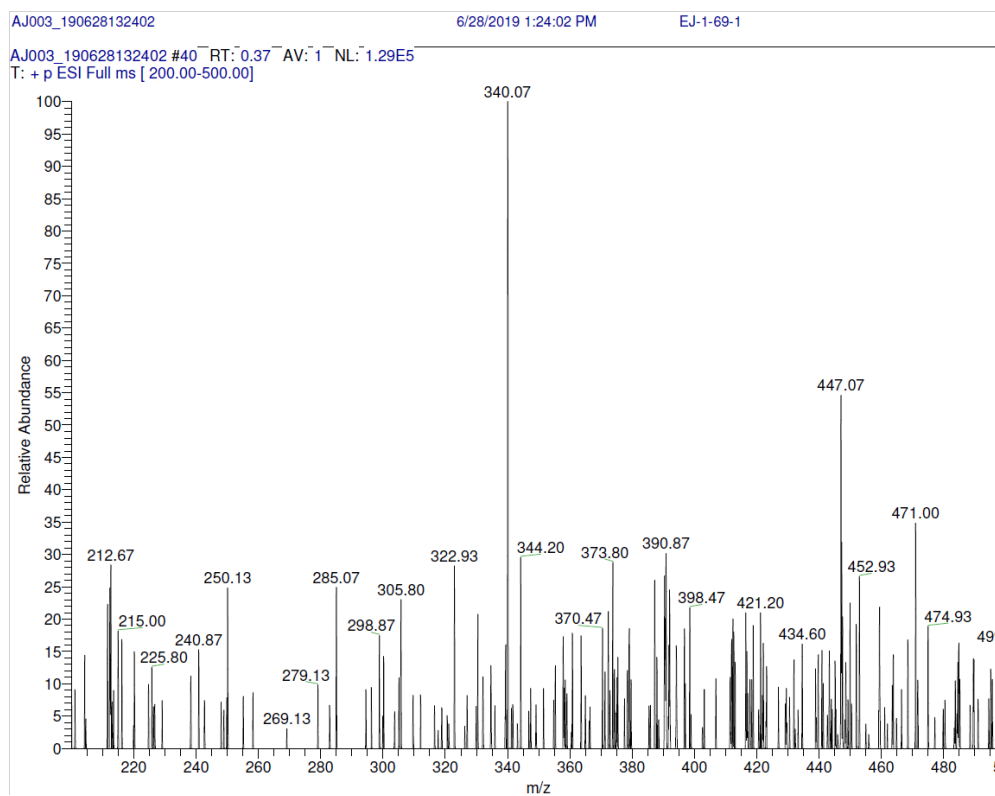
DEPT-135 NMR of compound 65



DEPT-90 NMR of compound **64**

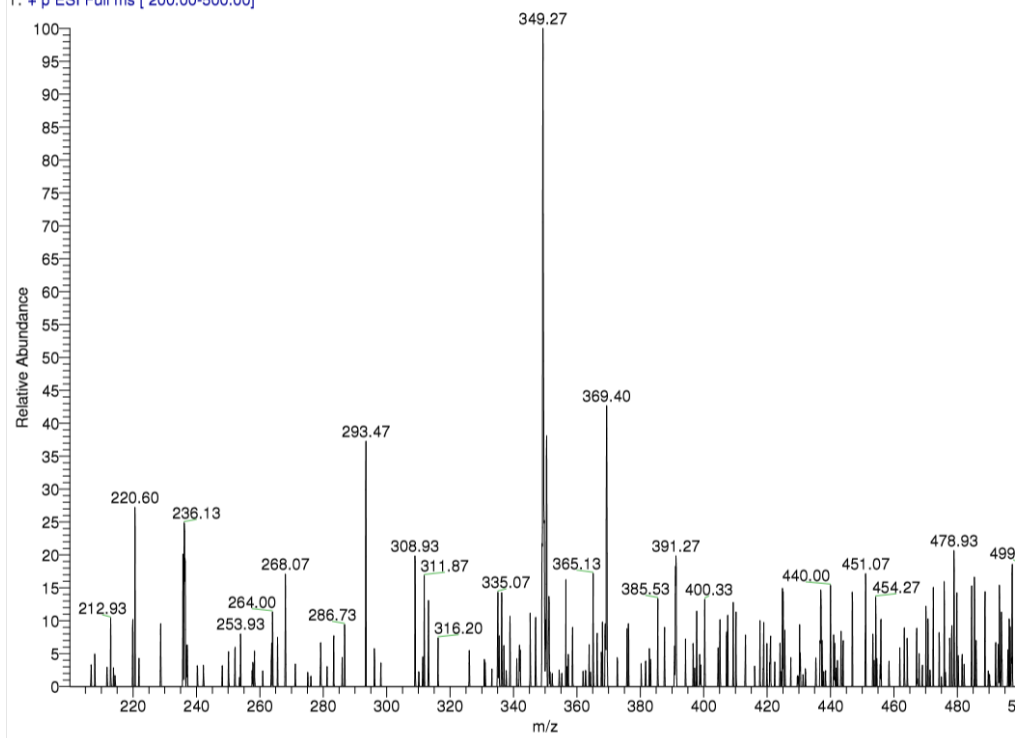


LC-MS of compound **20**

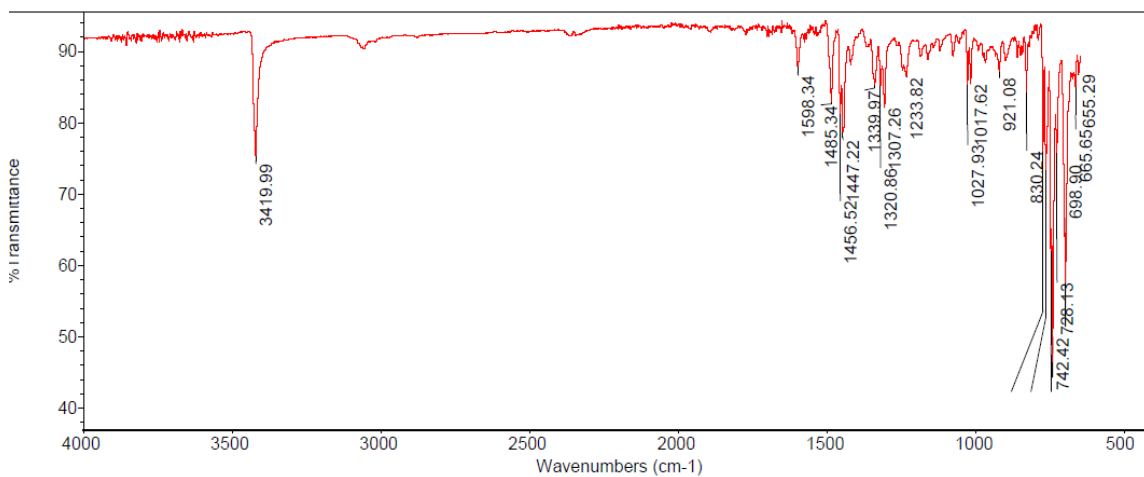


LC-MS of compound **38**

AJ003_190628133922 #85 RT: 0.74 AV: 1 NL: 7.63E5
T: + p ESI Full ms [200.00-500.00]



IR Spectra of compound 66



IR spectra of compound 67

